AN INVESTIGATION

OF

OBLIQUE INCIDENCE PROPAGATION

OF

RADIO PULSES

BETWEEN GRAHAMSTOWN AND DURBAN

A Thesis submitted in fulfilment

of the requirements of RHODES

UNIVERSITY for the degree of

MASTER OF SCIENCE.

by

ARUNAJALLAM NADASEN, B.Sc.(Hons.)

1967

A C K N O W L E D G E M E N T S

Sincere thanks are due to the following:-

The South African Council for Scientific and Industrial Research for a research grant.

Professor J.A. Gledhill, M.Sc., Ph.D.(S.A.), Ph.D.(Yale), F. Inst.P. for his able supervision and his invaluable advice, criticism and encouragement throughout the period of this research.

Professor J.T. Davidson for his never waning encouragement and interest.

Mr. H. Helm for the design and construction of the transmitter.

Dr. H.S. Govinden for his constant interest and valuable discussions.

Mr. A.R. Scanlan for the modification of the camera motor.

The University College of Fort Hare for help in various ways.

The University College, Durban, for kindly allowing the erection of the antennae on the campus.

Mr. A.J. Fletcher for making available scaled values of Grahamstown ionograms.

Mr. M.H. Williams for obtaining N-H profiles from ionograms.

Mr. Dennis A. Govender for the photographs of apparatus and recordings.

Miss S. Singh for the typing of this thesis.

A portion of this work was financed from an Antarctic Research Grant (to the Physics Department of Rhodes University) administered by the Department of Transport of the South African Government. This support is gratefully acknowledged.

C O N T E N T S

ABBREVIATIONS, SYMBOLS AND UNITS

The following are used throughout the text:

kc/s	=	kilocycles per second
c/s	=	cycles per second
Mc/s	=	megacycles per second
µsec	=	microseconds
KV	=	kilovolts
mV	=	millivolts
mm	=	millimeters
mH	=	millihenries
w.r.t.	=	with respect to
R.F.	=	radio frequency
I.F.	=	intermediate frequency
A.F.	=	audio frequency
dbs	=	decibels
mu	=	amplification factor
pF	=	picofarads
A.V.C.	=	automatic volume control
D.C.	=	direct current
S.W.G.	=	standard wire gauge
H.T.	=	high tension
K	=	kilohoms
M	=	megohms
kW	=	Kilowatts
L.M.T.	=	Local Mean Time
km	=	kilometres
MUF	=	maximum usable frequency i.e. the highest frequency that could be propagated between any two places for a particular electron distribution on the ionosphere.

S U M M A R Y

This thesis describes the investigation carried out on the propagation of radio pulses of frequency 4.73 Mc/s between Grahamstown and Durban.

The thesis is divided into two sections - A and B. Section A consists of two chapters. The introductory chapter gives a brief account of how the existence of the ionosphere came to be known. Then follows a description of the different layers of ionization and a review of the theories that have been propounded on the formation of these layers.

Chapter 2 deals with the apparatus which includes the transmitter in Grahamstown and the receiving apparatus in Durban. The receiving apparatus comprises:-

(i) a superheterodyne receiver whose gain was high (between 130 and 140 dbs);

(ii) a time delay calibrator which could measure time differences of 100 μsec fairly accurately;

(iii) a 310 A Tektronix oscilloscope;

(iv) a continuously running 35 mm recording camera.

Section B is made up of three chapters and is concerned with the actual analysis of the data recorded. The theory of propagation of radio waves in the ionosphere is discussed in Chapter 3. The effects of the magnetic field are neglected since it is found that the error introduced would not make the results unacceptable.

Chapter 4 contains the analysis of the data recorded. One summer day and one winter day are discussed in detail in order to obtain the pattern of the diurnal variations for both summer and winter. Some interesting phenomena are also dealt with. An attempt to do ray tracing was successful and the paths followed by a Pedersen and a lower ray from Grahamstown to Durban have been drawn.

New topics for further research are discussed in Chapter 5.

There are two appendices. Appendix I gives the time delays of all the pulses recorded and their possible identifications. An overall picture of the propagation via the various layers throughout the day (both for summer and for winter) is presented in Appendix II.

S E C T I O N A

1. I N T R O D U C T I O N

1.1. DISCOVERY OF THE IONOSPHERE

"The existence of the ionosphere, as an electrically conducting region, was first glimpsed in 1883 by Balfour Stewart. He inferred it from a study of the small daily geomagnetic variation observed at the earth's surface." (1). Nevertheless no direct evidence was obtained. When in 1901 Marconi (2) was able to send signals across the Atlantic, a puzzling situation arose, for it had previously been proved by mathematical physicists that it was impossible to receive ground wave signals at very great distances. It was known that radio waves travelling through the atmosphere - a medium then supposed to possess constant electrical properties - must travel in straight lines (except for diffraction). Hertz (3) had shown that they could be made to diverge from a straight line only by interposing a reflecting material in their path.

How these signals reached a point which necessitated their curving round an obstacle 200 miles high required an explanation. In 1902 Kennelly (4) and Heaviside (5) suggested independently that the earth was surrounded by a conducting region which acted as a reflector of radio waves. Appleton and Barnett (6) in 1925 obtained direct evidence for the existence of an ionized region by detecting the "sky wave."

The pulse-sounding method devised by Breit and Tuve (7) in 1925 was used to investigate these ionized regions and it was found that there were several well-defined layers in the upper atmosphere. On the suggestion by R.A. Watson-Watt (8) the name "Ionosphere" was given to the entire domain of regions of ionization.

The ionosphere may be defined as, "the part of the earth's outer atmosphere where ions and electrons are present in quantities sufficient to affect the propagation of radio waves." (9)

1.2 DESCRIPTION OF LAYERS

For short distance studies, the ionosphere may be assumed to be horizontally stratified, consisting of several ionized layers. For long distances, however, it may be regarded to a first approximation as spherically stratified.

The lowest layer is the D-region at a height of about 70-90 km. This high collision-frequency region is responsible for a great deal of absorption of high frequency signals. Above the D-region is the E-region which stretches from 90 km to 140 km. The ion density in this region, which is believed to be due to ultra violet radiations and X-rays (see Section 1.32), is controlled very closely by the solar zenith angle and solar activity. At night the ionization decreases markedly. Sometimes the E-region may be stratified into many layers, namely E_1, E_2, etc.

The F-region lies above 140 km. This region is often stratified into F_1 and F_2. The bifurcation is not very marked and is sometimes seen only as an inflection in the F-region electron density distribution. The ionization in the F-region is mainly due to solar ultra-violet radiation.

The abnormal or sporadic-E layer is found quite often at heights between 100 and 150 km. It is a thin layer with a large electron density gradient, which is superimposed on the normal ionosphere profile. The thickness of the layer varies from 500 to 2,000 metres and the electron density gradients approach values up to 10^5 or 10^6 electrons/cm^3/km. This has been verified by rockets flown over New Mexico and Manitoba (10). The horizontal extent is generally large enough for it to be regarded as a definite layer capable of producing reflections.

There are three major zones in which the temporal variation of the occurrence of sporadic-E is markedly different:-

(i) The Auroral Zone

Here the E_s appears mainly at night and shows little seasonal variation.

(ii) The Middle Latitude Zone

Here it is predominantly a summer time phenomenon occurring more intensely by day.

(iii) The Equatorial Zone

In this zone, the sporadic-E layer is a day time phenomenon with little seasonal variation.

1.3 REVIEW OF THEORIES OF THE FORMATION OF THE IONOSPHERE

1.31 CHAPMAN'S THEORY AND SUBSEQUENT DEVELOPMENT

As an ionizing radiation from outside penetrates deeper and deeper into the atmosphere, it encounters an ever-increasing density of gas. Hence the rate of production of electrons per unit volume rises with decreasing height. Since the radiation is being absorbed in the process its intensity decreases. Consequently the rate of production of electrons drops as well. Accordingly a level is found at which the rate of production of electrons is a maximum.

The general problem of calculating the rate of production for different heights, for an atmosphere containing many gases and for a solar spectrum spread over a wide range of wavelengths, is quite complicated. Further, the rate of loss of electrons must also be calculated in order to obtain the electron density at different levels.

Many theories on the formation of the ionosphere were propounded. The first substantial theory, which still forms the basis for more refined calculations, was proposed in 1930 by Chapman (11). Here he made the following simplifying assumptions:-

(i) a single absorption cross-section;

(ii) an isothermal atmosphere of uniform composition in gravitational equilibrium in which the density varies exponentially with height;

(iii) a flat earth.

He then derived a law for the variation of N (electron density) with height which is now known as the Chapman Law (12). He considered the ionizing radiation entering the atmosphere at an angle χ from the zenith and showed that the rate of production, q, of electrons at a height Z above the ground is given by

$$q = q_0 \exp.\left[1 - \frac{Z - Z_0}{H} - \sec\chi \exp\left\{\frac{Z - Z_0}{H}\right\}\right] \qquad .....(1.1)$$

where q_0 is the maximum rate of electron production when $\chi = 0$, Z_0 is the height of maximum rate of production when $\chi = 0$, and $H = \frac{RT}{Mg}$ is the scale height (R is gas constant, T is absolute temperature, M is mean molecular weight and g is acceleration due to gravity.)

If the electrons are assumed to be lost by recombination with positive ions, then the rate of removal of electrons is given by

$$\alpha N^2$$

where α is a constant called the recombination coefficient and N is the electron density.

Therefore the variation of N with time is given by

$$\frac{dN}{dt} = q - \alpha N^2 \qquad .....(1.2)$$

If α is large, the processes of formation and removal of electrons come into equilibrium in a very short time. Then $\frac{dN}{dt}$ may be neglected and equation (1.2) becomes

$$q = \alpha N^2 \qquad .....(1.3)$$

Combining equations (1.1) and (1.3) and assuming N_o is the peak electron density,

$$N = N_o \exp \tfrac{1}{2} \left[1 - \frac{Z - Z_o}{H} - \sec \chi \exp \left\{ \frac{Z - Z_o}{H} \right\} \right] \quad \ldots.(1.4)$$

This is called the Chapman Law and gives a characteristically shaped layer of ionization. It assumes that the recombination coefficient is independent of height.

Chapman himself soon modified his basic theory by extending the case of the flat earth to a spherical one (13). This changed the expected distribution and variation of ion density for large solar zenith angles such as occurred at sunrise and sunset.

Bradbury (14) suggested that the E- and F_1-regions were formed as a result of the absorption of special bands of solar radiation and that negative-ion formation was the predominant loss process in these regions. The F_2-region is probably not due to the absorption of any particular band of solar radiation, but owes its formation to the preponderance at this level of electron-positive-ion recombination over the negative-ion formation during the day. Hence the variation of loss with height could be regarded as playing a major role in modifying the F-region electron density distribution. Mohler (15) used the observational data for the ionosphere at Washington and supported Bradbury's hypothesis by showing that the F_2 level was far above the height where the rate of production is a maximum.

In 1939 Chapman (16) stated that the principal radiations are not monochromatic nor are all the absorbing constituents distributed exponentially. Nicolet (17) extended the theory to deal with gases which were not at the same temperature at all heights.

Chapman's original idea was to account for discrete layers of ionization. However, direct measurements by rockets (18) have verified that the ionosphere is more nearly a continuum of ionization from the D-region to the peak of the F-region. The various regions represent banks of ionization without a pronounced minima between them.

Shimazaki (19) extended Chapman's theory to include variable scale height, non-uniform recombination coefficient and ionospheric movements. By analysing the observational material from all over the world, he showed that the Chapman model was inadequate to explain experimental data. The Bradbury model was found to be superior in every respect.

If the ionizing radiation were in the X-ray region of wavelengths, ionization would be accompanied by secondary electrons and photons which could themselves ionize. If these were easily absorbed, Chapman's expression for the rate of production would not change. If these travelled appreciable distances before producing ionization, the resulting rate of production would be different from the Chapman function (20).

1.32 THEORIES OF IONIZING PROCESSES

It is generally agreed that most of the observed electron density of the F-region is attributable to the ionization of atomic oxygen by the entire broad spectral range from about 200 to 900Å .

A large number of hypotheses were put forward for the lower ionosphere. In 1923, Vegard (21) noted an heavily ionized layer at a height of 100 km and attributed the charging of the particles to X-rays and γ-rays. Assuming solar ultra-violet radiation as a source, Hulburt (22) calculated ionization equilibrium for various gases from the Saha theory. This gave a region of ionization at 200 km which explained the F-region as observed in winter. Since the E-region could not be explained on the basis of this theory, he stated that it might be due to the omission of wave-lengths shorter than the ultra-violet series (viz. X-rays). In the same year Vegard suggested independently that X-rays were a source of ionization in the E-region (23).

In trying to seek for an ultra-violet explanation, Penndorf (24) assumed photochemical equilibrium. However, his theory placed the ionization in the D-region. Further the theoretical work of Nicolet and Mange (25) on oxygen distribution in the high atmosphere showed that O_2 distribution departed completely from photo-chemical equilibrium. This was also verified by rocket measurements (26).

In 1948, Hoyle and Bates (20) revived the X-ray hypothesis. They derived the spectrum of X-rays

necessary to produce the observed E-layer, and found that best agreement with altitude distribution of the E-layer ionization was obtained with an X-ray spectrum having a maximum in the neighbourhood of 38Å. A V-2 rocket fired on 29th September, 1949 (27) telemetered data which showed the presence of solar X-rays above 87 km and hence supported the idea that E-layer ionization is directly related to the absorption of X-rays emitted by the sun. Havens et al. (28) ascribed the entire E-region and an appreciable portion of the F-region to X-rays.

The work of Watanabe et al. (29) on the absorption of O_2 and N_2 in the range 850Å to 1100Å renewed support for the ultra-violet theory. As a result of newer data, Houston (30) proposed a theory of the lower ionosphere that included contributions of X-rays and ultra-violet radiations.

The photo-ionization of nitric oxide by Lyman-α (i.e. a strong flux of solar radiation of wavelength 1215.7Å) as a process of ionization of the D-region was originally proposed by Nicolet (31) in 1945. Subsequently Nicolet and Aiken (32) made a very thorough study of the D-region ionization and verified that it involves photons in the spectral range 1100-1340Å and below 10Å.

Hinteregger and Watanabe (33) showed that the spectral range 800-1027Å that ionizes O_2 contributes a greater (or comparable) photoionization rate than X-rays towards the formation of the E-region. They suggested

that the base of the E-layer could be controlled by Lyman -β(1025.7Å) and C III (977 Å). In a later paper (34), they re-examined the photoionization rates and propounded the most acceptable theory on the process of ionization of the upper atmosphere. They attributed the lowest part of the E-region to the ultra-violet spectrum 911-1027 Å, while Lyman-β (1025.7Å) shaped the base of the E-layer. Above 120 km. soft X-rays (10 - 170Å) made an appreciable contribution. 280 - 370Å dominated the region from 130 to 150 km. The F-region absorbed the broad spectral range from about 280Å to 911Å. Above 200 km the range 465 - 630 Å was of particular importance.

1.33 FORMATION OF SPORADIC-E

The narrowness of the layer, the absence of diurnal and seasonal variations in its preferred heights of occurrence and the lack of correlation with solar activity seem to rule out the possibility that the sporadic-E layer is formed in the same way as the normal ionospheric layers (i.e. ultra-violet and X-ray ionization).

The two possible ways in which the sporadic-E layer is formed are:-

(i) redistribution of existing electrons;

(ii) changes in the rates of production or loss of electrons.

(a) The Auroral Zone

Auroral activity and the incidence of E_s in the auroral zone show a strong positive correlation (35). This leads one to believe that in high latitudes the predominant types of E_s are due to charged particles penetrating into the lower ionosphere from outside the earth's atmosphere.

(b) The Equatorial Zone

The fact that the equatorial sporadic-E layer coincides approximately with the zone of the equatorial electrojet (i.e. the daytime current stream which flows along the magnetic equator at 100 km level) suggests that the current in the electrojet might be directly responsible for the E_s ionization. Matsushita (36) states that the equatorial E_s might be a kind of irregularity in the equatorial electrojet.

(c) The Middle Latitude Zone

It was first noted by Helliwell and later by Pfister (37) that there was a strong tendency for the sporadic -E layer in the temperate zone to occur at certain specific altitudes which were separated by 6 km. Millman, Bedinger and others (38, 39) observed strong wind shears with the same altitude separation. Hence suspicion arose that the high electron density gradients were associated with wind shears.

A horizontal movement of neutral air in the presence of ions and electrons causes them to move in varying degrees, thus polarizing the medium and producing electric fields inside it. Further, ions

and electrons moving in a magnetic field are acted on by forces at right angles to both the velocity and the field. Thus the existence of the horizontal component of the earth's magnetic field gives rise to vertical drift motions of charged particles.

If the wind shear is high, the velocity of the horizontal wind varies rapidly with height, which in turn results in a corresponding variation in the vertical velocity of the charged particles. At a level where the wind velocity approaches zero, the vertical drift speed of the ions and electrons also becomes zero. Hence there would be an accumulation of charged particles at this level, resulting in the formation of a sporadic-E layer in which the electron density is 3 to 10 times that in the normal E.

1.4 DIURNAL VARIATION OF ELECTRON DENSITY IN THE IONOSPHERE

It is fairly well established that the major part of the ionization in the upper atmosphere is due to the sun's radiations (see sections 1.31 and 1.32). The loss processes are mainly recombination and attachment of electrons to neutral particles (i.e. negative-ion formation). So while electrons are being formed by the ionizing radiations, they are being lost continuously as well.

If the loss process is not delayed considerably, the electron density would vary with the intensity of the rays emitted by the sun. For any point in the

upper atmosphere, the sun's radiations have diurnal variations, which are governed by the zenith angle of the sun. Except for certain departures, the electron density in the normal layers of the ionosphere conforms to this variation in a general way. A brief discussion of the different regions follows.

(i) F-region

Here, contrary to expectations, the electron density does not reduce to zero shortly after sunset, but persists throughout the night. The peak of the nighttime electron density in the F-region has been obtained by Hinteregger and Watanabe (33) as 10^5 el/cm^3 occurring approximately around 320 km.

During an hour period around sunrise there is a comparatively high build up of electron density at this altitude due to the combined effect of the low recombination rate (because of the low density of particles) and the relatively high ionization rate (since the radiations do not have to pass through a dense atmosphere before reaching this level).

As the sun rises, its rays reach lower altitudes with the result that the location of the maximum descends. However, at lower altitudes the recombination rates are higher. Hence the F-region electron density peak (i.e. the F_2-layer) does not correspondingly shift downwards. Only a ledge is developed, which descends to about 180 km (i.e. the F_1-layer). Thus the F-region splits into two layers, viz., F_1 and F_2.

The F_1-layer electron density increases as the sun rises further and reaches a maximum just after noon. Thereafter it falls again until the F_1-layer merges into the F_2-layer around sunset. The F_2-layer electron density is characterised by:-

(i) A very rapid increase at sunrise;

(ii) the maximum occurring late in the afternoon, particularly in summer;

(iii) a rather gradual decline throughout the night.

Some of these irregularities could be explained by the low rate of recombination at this altitude.

(ii) The E-region

The electron density in the E-region is very low before dawn (generally about 3000 el/cm^3). It increases steadily from sunrise until it attains a maximum value just after noon and then falls in a regular manner to a small value shortly after sunset. Some vestige of the E-layer appears to continue throughout the night. The diurnal variation is much the same at all latitudes and the peak of the electron density during daylight hours could generally be taken as being in the region of 2.8×10^5 el/cm^3. The mid-day maximum of ion density occurs at a height which depends directly upon the zenith angle of the sun at noon.

(iii) The D-region

The regular diurnal variation in the D-region is substantially similar to that of the E-region.

1.5 PURPOSE OF CARRYING OUT THE RESEARCH PROJECT

Research on the oblique incidence propagation of radio waves has been carried out in many parts of the world. Besides Marconi in 1901 (2) and Eccles in 1912 (40), Appleton and Barnett (6) were among the first to attempt this project. They worked on the interference between the sky wave and the ground wave, and determined the angles of the downcoming rays and the height of the reflecting layer. However, the first organized experiment in England was conducted by Farmer and Ratcliffe (41) between Cambridge and Edinburgh in May, 1935.

Oblique incidence propagation was investigated by Martyn et al. (42) in Australia as early as 1932, while such experiments were carried out in 1936 in Germany (43). Pierce (44) of the Cruft Laboratory was able to obtain records over distances of 1,300 km and 6,000 km.

In South Africa, however, research on oblique incidence propagation of radio pulses is very rare. The only work of which we are aware was between Salisbury and Johannesburg in 1957-8 by R.W. Vice and M.W. McElhinny but this has never been published.

Work on oblique incidence propagation seems to require more attention in South Africa. For instance, recordings of pulses transmitted from Sanae, Antarctica and picked up in Grahamstown have been obtained since July, 1962. However, these recordings have not been

utilised, basically because of lack of experience in the analysis of oblique incidence records. This immediately requires workers to get familiar with oblique incidence records and the techniques of deriving information from them. If one could interpret records for short distances, then one would find it easier to develop a method to analyse records for long distance propagation.

The author was particularly suited to carry out this project because he was originally stationed at Fort Hare, 65 kilometres from Grahamstown. It was agreed then that research on oblique incidence propagation be carried between Grahamstown and Alice, as a first step in obtaining experience with the techniques for later use in the Antarctic project. Subsequently the author had to move to Durban and oblique incidence propagation was in fact carried out between Grahamstown and Durban.

The purpose was to analyse in detail some records and to gain experience in identifying the kinds of propagation which occur.

2. THE APPARATUS

The research project consisted essentially of transmitting pulses at Grahamstown and receiving them in Durban. This involved the transmission of pulses of short duration with steep leading edges and accurate determination of the time delay between different pulses at the receiving end. Thus the times of propagation of different pulses could be determined to enable the identification of different modes of propagation. These facts were borne in mind in the construction of the apparatus.

2.1 THE TRANSMITTER

The transmitter used for this project was constructed by H. Helm of the Physics Department of Rhodes University. It was designed to transmit pulses of radio-frequency waves, subject to the following requirements:-

(i) the output power during pulses should be of the order at least 1 kilowatt;

(ii) the frequency should lie in the range 4.0 to 5.0 Mc/s, but should be adjustable to any value within this range;

(iii) the pulse length should be of the order of 100 μsec;

(iv) the pulse repetition rate should be of the order of 10 per second.

The block diagram shown in Fig. 1 illustrates the mode of operation of the transmitter. The circuit

diagram of its essential parts is given in Fig. 2.

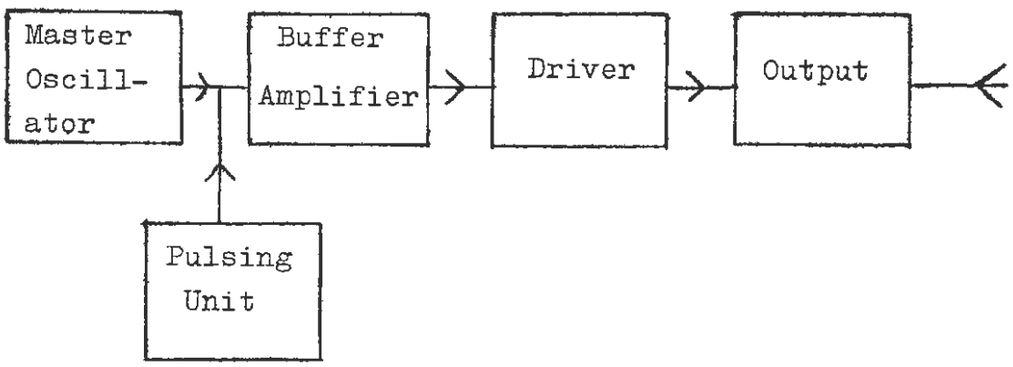

FIG. 1 - BLOCK DIAGRAM OF TRANSMITTER

Fundamentally, the transmitter consists of a continuously-running master oscillator followed by three amplifying stages, viz. a buffer amplifier, a push-pull driver stage and a push-pull output stage. All three amplifying stages were operated under "Class C" conditions, the buffer stage being self-biased and the others having fixed bias.

Pulsing the transmitter on and off was achieved by controlling the grid voltage of the buffer amplifier by means of the pulsing unit. The buffer amplifier thus functioned as both gate and amplifier; when its grid voltage was made strongly negative, the signal from the osoillator would not be passed on to the rest of the transmitter, whereas when this voltage was brought up to a quiescent value of zero, the buffer amplifier would function in the normal way and the transmitter would transmit.

Some details of the various units depicted in the block diagram are given below:-

(a) MASTER OSCILLATOR

This was an ex - R.A.F. model electron-coupled Colpitts oscillator, capable of covering a frequency range from 1 to 20 Mc/s. Its output was fed to the grid of the buffer amplifier via a coupling capaciter (C_{23} in Fig. 2).

(b) PULSING UNIT (see Fig. 2)

A stepped-down version of the mains voltage was applied to the input valve; this signal was then squared by means of the first two amplifying stages and differentiated with the aid of C_2 and R_5. T_2 amplified the "pips" applied to it; the double diode T_3 ensured that only positive-going pips from the output of T_2 were passed on to T_4, which formed part of a blocking oscillator. These positive-going pips charged up the capacitor combination C_4 and C_5 in a sequence of steps, this process continuing until the voltage on the grid of T_4 was sufficiently high for the blocking oscillator to operate. The blocking oscillator would then "fire", producing an output pulse of very short duration; this would discharge C_4 and C_5, and the process of step-wise charging of these capacitors would then begin all over again. Thus it will be seen that this circuit provided a means of "dividing down" the main frequency, by producing

an output pulse after an integral number of cycles of the mains voltage had elapsed. The number of charging steps was adjusted by varying the cathode voltage of the blocking oscillator tube with the aid of R_{10}.

The output pulse from the blocking oscillator was used to trigger a cathode-coupled multivibrator (T_5 and T_6) which produced a gating pulse of the order of 10 millisec. in length; The positive pulse from this multivibrator was differentiated by C_{12} and R_{20} and used to trigger another cathode-coupled multivibrator (T_7 and T_8), which with the aid of the differentiating combination C_{14} and R_{27} provided an output "pip". This "pip" triggered yet another cathode-coupled multivibrator (T_9 and T_{10}) which generated the gating pulse responsible for controlling the operation of the buffer amplifier. The grid of the latter was connected to earth via the resistor R_{34} which was also the load resistor of T_{17}, whose cathode was made 400 volts negative with respect to earth. In the absence of the gating pulse, T_{17} was conducting, so that the grid of the buffer amplifier tube T_{12} was strongly negative and T_{12} was consequently cut-off. On the other hand, when the negative-going gating pulse arrived at the grid of T_{17}, T_{17} was cut-off and the combination R_{34} and C_{17} functioned as an ordinary self-biasing circuit for a class C

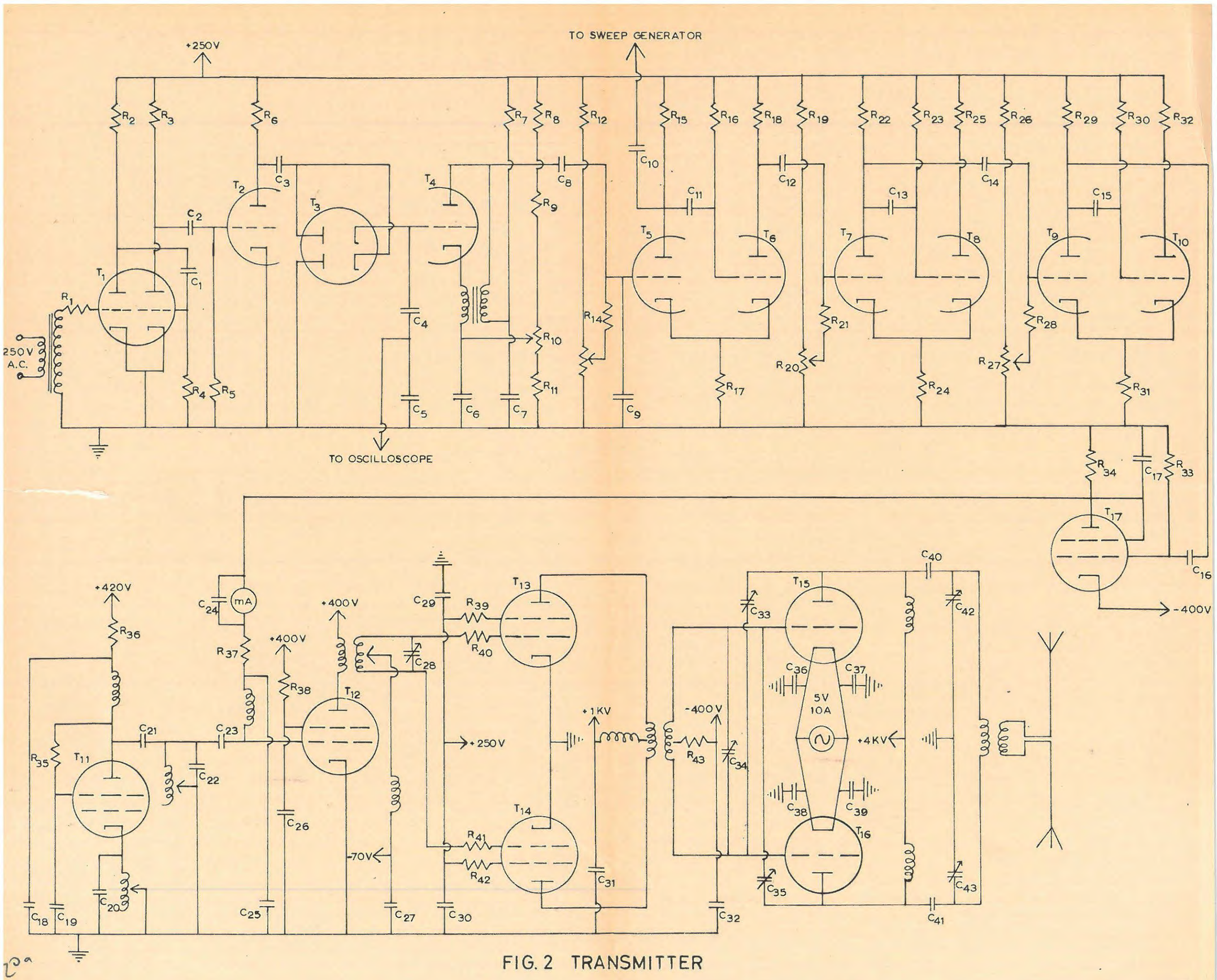

FIG. 2 TRANSMITTER

FIG 2 - CIRCUIT OF TRANSMITTER

R_1	=	47K	R_{31}	=	10K
R_2	=	500K	R_{32}	=	10K
R_3	=	220K	R_{33}	=	1.0M
R_4	=	220K	R_{34}	=	30K
R_5	=	10K	R_{35}	=	100K
R_6	=	10K	R_{36}	=	5.0K
R_7	=	10K	R_{37}	=	33K
R_8	=	100K	R_{38}	=	820 ohms
R_9	=	33K	R_{39}	=	47 ohms
R_{10}	=	25K	R_{40}	=	47 ohms
R_{11}	=	270K	R_{41}	=	47 ohms
R_{12}	=	2M	R_{42}	=	47 ohms
R_{13}	=	1M	R_{43}	=	100 ohms
R_{14}	=	22K			
R_{15}	=	22K	T_1	=	6SN7
R_{16}	=	2.2M	T_2	=	½6SN7
R_{17}	=	10K	T_3	=	6H6
R_{18}	=	10K	T_4	=	½6SN7
R_{19}	=	470K	T_5	=	½6SN7
R_{20}	=	250K	T_6	=	½6SN7
R_{21}	=	22K	T_7	=	½6SN7
R_{22}	=	22K	T_8	=	½6SN7
R_{23}	=	2.2M	T_9	=	½6SN7
R_{24}	=	10K	T_{10}	=	½6SN7
R_{25}	=	10K	T_{11}	=	807
R_{26}	=	220K	T_{12}	=	6L6G
R_{27}	=	100K	T_{13}	=	807
R_{28}	=	22K	T_{14}	=	807
R_{29}	=	22K	T_{15}	=	354-E 53
R_{30}	=	2.2M	T_{16}	=	354-E 53
			T_{17}	=	6L6G

FIG. 2 (CONTD.)

C_1 = 0.1 μF
C_2 = 0.001 μF
C_3 = 0.01 μF
C_4 = 0.01 μF
C_5 = 0.05 μF
C_6 = 8 μF
C_7 = 0.5 μF
C_8 = 0.1 μF
C_9 = 540 pF
C_{10} = 1.0 μF
C_{11} = 0.01 μF
C_{12} = 1000 pF
C_{13} = 0.001 μF
C_{14} = 100 pF
C_{15} = 200 pF
C_{16} = 0.1 μF
C_{17} = 100 pF

C_{25} = 0.01 μF
C_{26} = 0.022 μF
C_{27} = 0.001 μF
C_{28} = maximum 350 pF
C_{29} = 0.001 μF
C_{30} = 0.001 μF
C_{31} = 0.001 μF
C_{32} = 0.001 μF
C_{33} = maximum 20 pF
C_{34} = maximum 150 pF
C_{35} = maximum 20 pF
C_{36} = 0.001 μF
C_{37} = 0.001 μF
C_{38} = 0.001 μF
C_{39} = 0.001 μF
C_{40} = 400 pF
C_{41} = 400 pF
C_{42} = maximum 100 pF
C_{43} = maximum 100 pF

C_{18}, C_{19}, C_{20}, C_{21}, C_{22}, C_{23}, and C_{24} were components of a piece of commercial equipment used as part of the transmitter and as such there was no necessity to measure their capacitances.

amplifier. The value of C_{17} was so chosen that the time constant of R_{34} and C_{17} was not such as to produce excessive distortion of the pulse shape.

(c) BUFFER AMPLIFIER, DRIVER AND OUTPUT STAGES

These were conventionally designed Class C amplifying stages. Since the output tubes were triodes, it was necessary to use the neutralizing capacitors C_{33} and C_{35}.

The output stages fed a half-wave dipole aerial, as can be seen in Fig. 2. The R.F. output voltage on the antenna of the transmitter was estimated to be in the region of 2 - 3 KV. However, it was not possible to calculate the actual power radiated since this would require a knowledge of the effective radiation resistance. Therefore a conservative figure of 1 KW as the output power was assumed.

2.2 THE RECEIVING APPARATUS

The receiving apparatus comprised:

(i) A superheterodyne receiver;

(ii) A time delay calibrator;

(iii) An oscilloscope; and

(iv) A recording camera.

Fig. 3 shows the layout of the receiving apparatus, excluding the camera. A block diagram of the apparatus is given in Fig. 4.

The pulses received in Durban were detected and

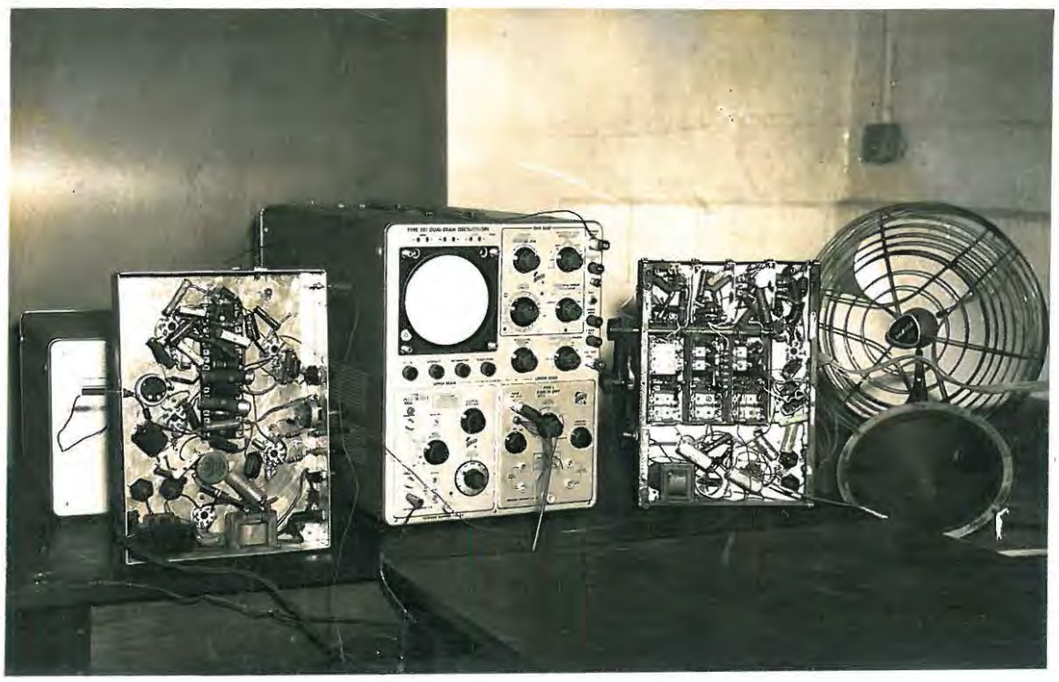

Fig. 3 - RECEIVING APPARATUS.

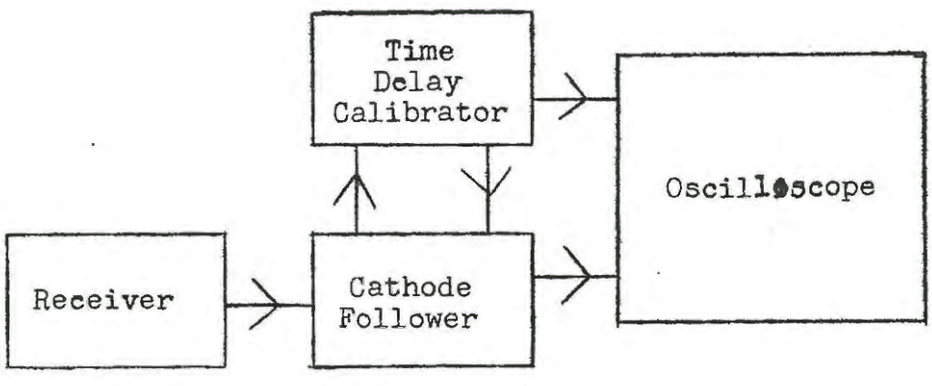

Fig. 4 - BLOCK DIAGRAM OF RECEIVING APPARATUS.

amplified; and thereafter used to trigger the multivibrator of the time delay calibrator. Subsequently the output of the multivibrator triggered the oscilloscope time base and also the ringing oscillator of the time delay calibrator. The time delay calibrator markers and the received pulses were displayed on the oscilloscope screen. They were photographed on continuously running 35 mm. film.

2.21 THE ANTENNAE (see Fig. 5)

As the pulses arrive in Durban at different angles to the horizontal in the vertical plane that passes through Grahamstown and Durban, a half-wave dipole aerial at right angles to this plane is expected to provide the best reception (neglecting ground reflections). Grahamstown lies 48° west of south w.r.t. Durban. Therefore the half-wave dipole aerial (a in Fig. 5) constructed was directed at an angle 42° east of south. However, the sensitivity of the aerial was found to be too low and the output of the receiver was insufficient to trigger the multivibrator.

As an alternative, a long wire antenna of length 240 feet (b in Fig. 5) was resorted to and set up along the Durban-Grahamstown line. For a wire of this length, the optimum orientation with the incoming rays, which have a wavelength of 63 metres, is in the region of 47° or 48° (45, 46) (again neglecting ground reflections). Taking into account the distance between

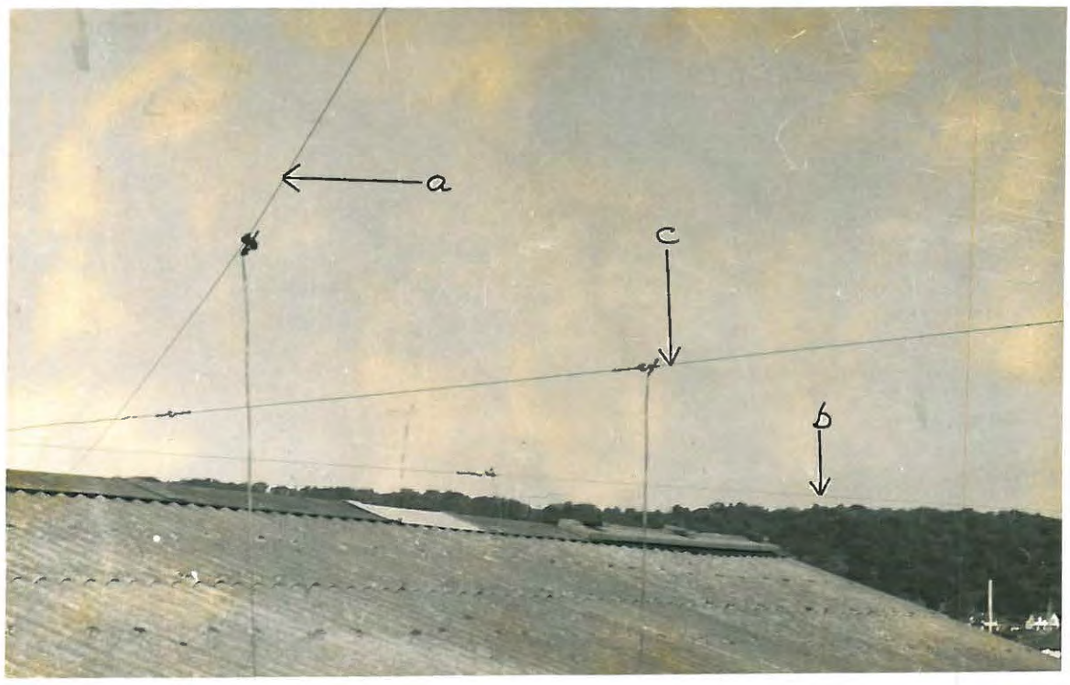

Fig. 5 - ANTENNAE

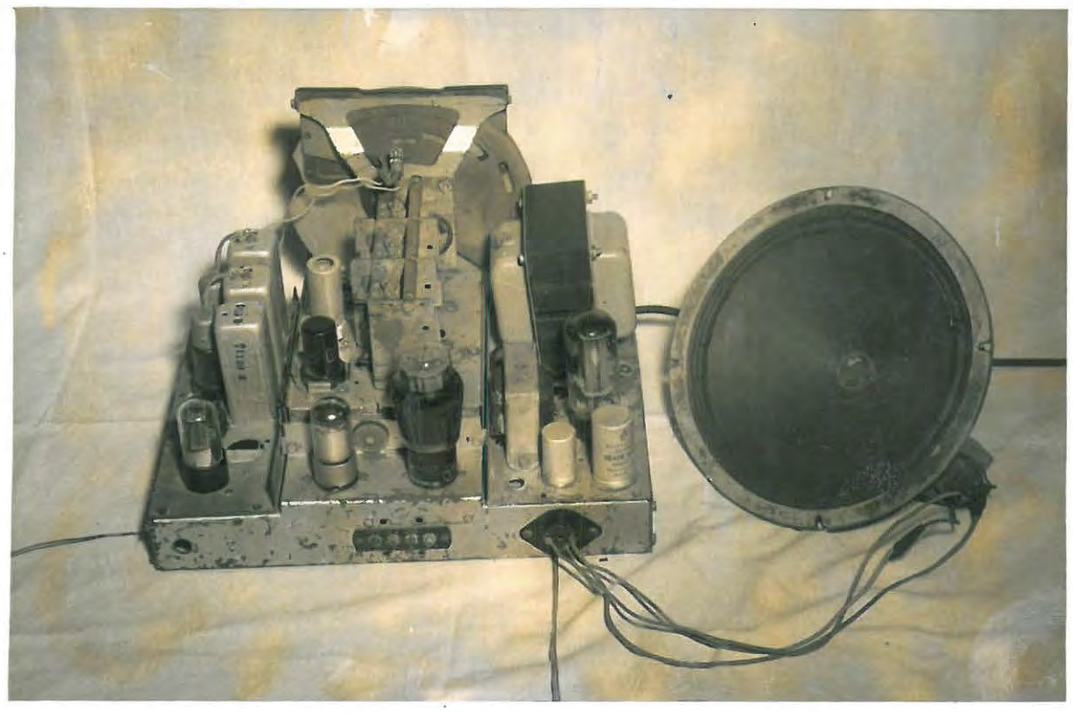

Fig. 6 - RECEIVER

Grahamstown and Durban and the expected heights of reflection of the transmitted pulses, it would appear that the down-coming rays would be at angles varying between 30° and 60° with the horizontal. Accordingly a wire of this length pointing in the direction of Grahamstown would receive well on the upper lobe. This aerial was found to give better results.

It was soon realised that the ground pulse was not being received. Since this might be attributed to the poor orientation of the antenna for the ground pulse, another straight wire antenna of about 210 feet length (c in Fig. 5) was set up at 50° to the Durban-Grahamstown line. Although this did not help in picking up the ground wave, it nevertheless improved the reception of the other pulses when used together with the other long wire antenna. Both aerials were used in parallel throughout the experiment.

2.22 THE SUPERHETERODYNE RECEIVER (Fig. 7)

This is an old commercial receiver on which the following modifications were made:-

(i) The voltages, time constants and bandwidth were so adjusted as to make the receiver suitable for the reception of narrow pulses.

(ii) The overall gain was increased above that of a normal receiver in order that even the weakest pulses from the ionosphere could be detected.

Figs. 6 and 8 show the two views of the receiver.

2.221 THE R.F. AMPLIFIER

The purpose of this amplifier is to increase the selectivity between the antenna and the frequency converter (see section 2.222). This reduces the intermediate frequency response and cross modulation. It also increases the signal-to-noise ratio at the converter.

The circuit of this amplifier is included in Fig. 7. It is a conventional single-tuned transformer - coupled potential amplifier (47) employing a 6SK7 remote-cut-off pentode. The coils of the tank circuit (in the grid) were of fixed values and the condensers (C_1) were of the variable type. The gain of the amplifier was measured and found to be 22 dbs at 4.73 Mc/s.

2.222 THE FREQUENCY CONVERTER

The conversion of the signal from the radio frequency to the I.F. value was originally achieved by mixing the output of a local oscillator employing a 6L5 medium-mu triode with the R.F. signal in a 6L7 pentagrid mixer. This combination proved satisfactory except that the noise from the mixer was very high. Consequently weak signals from the ionosphere could not be detected.

Since no improvement could be brought about by altering the circuit components, the frequency changer section was modified to include an ECH 81 triode heptode converter, which is a low noise tube. Additional advantages of the tube are that it has a very high conversion transconductance and its frequency drift is very small. To overcome the

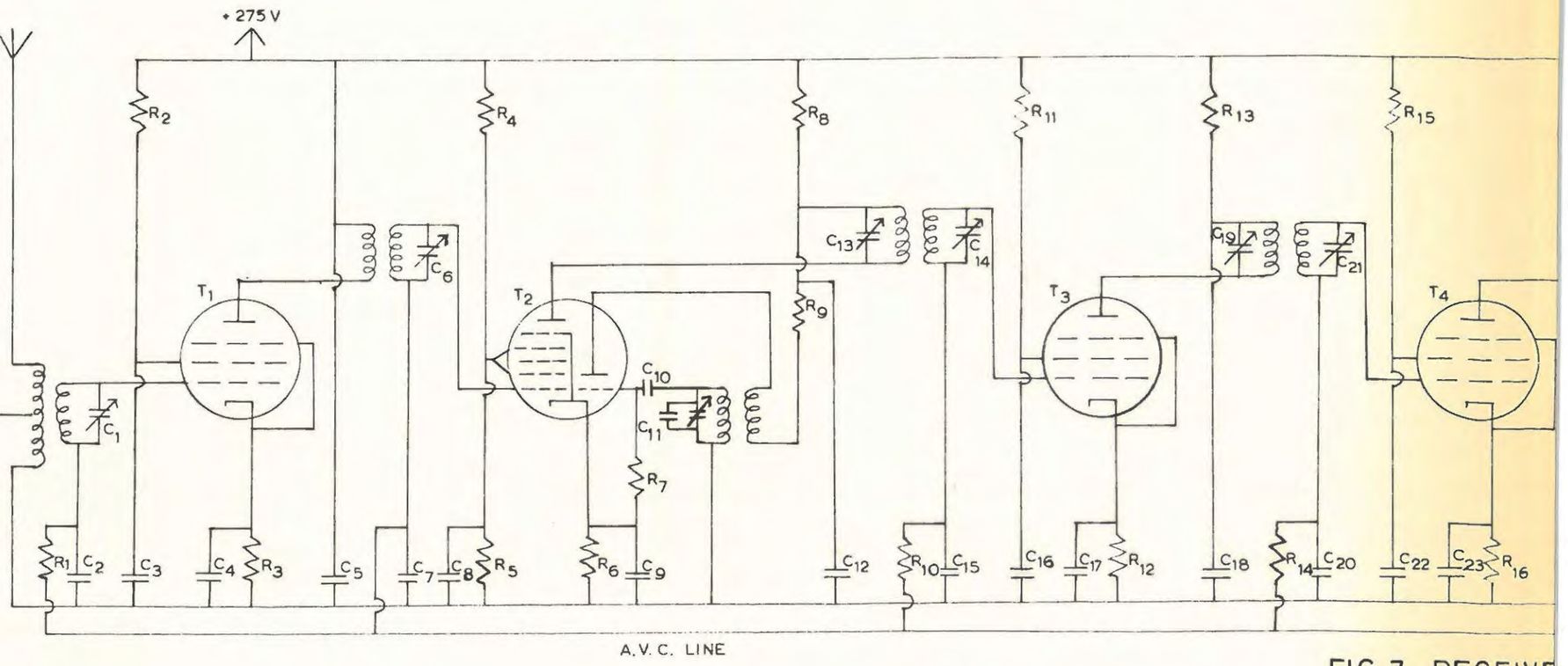

FIG. 7 RECEIVE

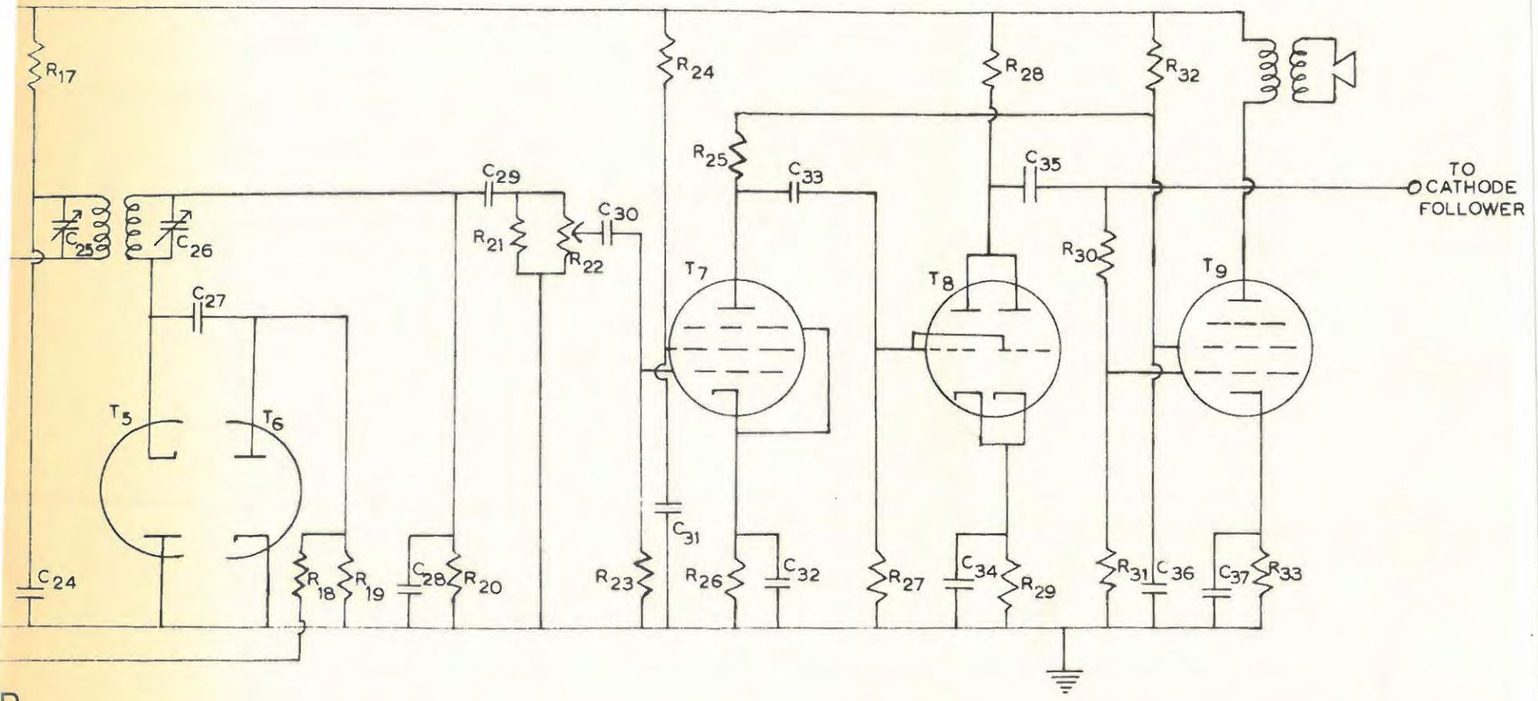
R17
R24
R28
R32
R25
C33
C35
TO
CATHODE
FOLLOWER
C29
C30
R21
R22
C25
C26
C27
T7
T8
T9
R30
T5
T6
C31
C24
R18
R19
C28
R20
R23
R26
C32
R27
C34
R29
R31
C36
C37
R33

R

FIG 7 CIRCUIT DIAGRAM OF RECEIVER

R_1 = 51K
R_2 = 100K
R_3 = 400 ohms
R_4 = 43K
R_5 = 100K
R_6 = 330 ohms
R_7 = 47K
R_8 = 15K
R_9 = 22K
R_{10} = 47K
R_{11} = 200K
R_{12} = 680 ohms
R_{13} = 10K
R_{14} = 47K
R_{15} = 250K
R_{16} = 1.0K
R_{17} = 25K
R_{18} = 1.0M
R_{19} = 1.0M
R_{20} = 100K
R_{21} = 150K
R_{22} = 2.0M
R_{23} = 100K
R_{24} = 270K
R_{25} = 100K
R_{26} = 1.0K
R_{27} = 100K
R_{28} = 22K
R_{29} = 6.8K
R_{30} = 3.9M
R_{31} = 470K
R_{32} = 1.6K
R_{33} = 820 ohms

T_1 = 6SK7
T_2 = ECH81
T_3 = 6K7
T_4 = 6K7
T_5 = ½6H6
T_6 = ½6H6
T_7 = 6SJ7
T_8 = 6SN7
T_9 = 6L6

FIG. 7 (CONTINUED)

C_2 = 0.05 μF
C_3 = 0.5 μF
C_4 = 10.0 μF
C_5 = 0.1 μF
C_7 = 0.05 μF
C_8 = 0.1 μF
C_9 = 0.05 μF
C_{10} = 50 pF
C_{12} = 0.01 μF
C_{15} = 0.01 μF
C_{16} = 0.01 μF
C_{17} = 5.0 μF
C_{18} = 0.01 μF
C_{20} = 0.01 μF
C_{22} = 0.01 μF
C_{23} = 0.47 μF
C_{24} = 0.01 μF
C_{27} = 1000 pF
C_{28} = 220 pF
C_{29} = 0.1 μF
C_{30} = 0.1 μF
C_{31} = 0.1 μF
C_{32} = 10 μF
C_{33} = 0.04 μF
C_{34} = 25 μF
C_{35} = 0.05 μF
C_{36} = 8.0 μF
C_{37} = 50 μF

C_1, C_6, C_{11}, C_{13}, C_{14}, C_{19}, C_{21}, C_{25} and C_{26} were variable capacitors (trimmers, tuning condensers and padding capacitors) of the original receiver and as such there was no need to measure their values.

undesirable reduction of internal resistance, a potential divider arrangement was employed to provide the screen voltage for the heptode. Here again the coils of the tank circuits were of fixed values and the condensers (C_6 and C_{11}) were of the variable type, consisting of padded mica capacitors, air-mica trimmers and parallel plate tuning condensers. The mixer provided a gain of 16 dbs.

2.223 THE I.F. AMPLIFIERS

The object of conversion is to allow convenient amplification at constant bandwidth. This was achieved by a two stage amplifier as shown in Fig. 7. In order to reduce the broadening of the pulse, double-tuned transformer-coupled amplifiers were used by means of which a large bandwidth could be obtained. A constant amplification over the bandwidth was effected by stagger-tuning of the primary and secondary tank circuits.

The bandwidth was adjusted to 23 kc/s and the overall gain obtained was 42 dbs.

2.224 THE DETECTOR AND A.V.C.

(see circuit diagram in Fig. 7)

The detector is of the "envelope detection" type (48) employing one-half of a 6H6 double-diode tube. A proper choice of the values of R_{28} and C_{28} ensures that the intermediate carrier frequency is wiped out and only the signal appears in the output.

The other half of the 6H6 was used for the A.V.C. Thus the amplitude of the modulated input to the detector was maintained at a constant level, despite the varying amplitude of the pulses from the ionosphere.

2.225 A.F. AMPLIFIERS

The output of the detector must be amplified to atleast 40 volts in order to trigger the multivibrator of the time delay calibrator. To meet this requirement, an R-C coupled amplifier was constructed, consisting of two stages.

Initially the two halves of a 6SL7 tube were used. However, it was found that this gave rise to oscillations due probably to feedback between the electrodes.

The following tubes were therefore incorporated in the circuit:-

(a) A 6SJ7 pentode in the first stage which gave a gain of 41 dbs and

(b) A 6SN7 triode in the second stage - both halves of the tube being connected together. This gave a gain of 23 dbs.

Pulses were found to come in very strongly when propagation conditions were good. At these times the noise level was also very high. With full gain, it was found that while the pulses triggered the apparatus every tenth of the second, the noise triggered the apparatus in between. Therefore the

output of the receiver had to be reduced to an extent such that the noise level dropped to below the value required to trigger the apparatus. This was done with the aid of a volume control (R_{22}).

2.226 POWER AMPLIFIERS

It was necessary to obtain an audible output from the receiver for the following reasons:-

(i) to detect the presence of pulses,

(ii) for rapid tuning of receiver to the transmitter frequency, and

(iii) to provide an easy method of "trouble-shooting" during times of servicing.

Such an output was provided by the power amplifier employing the 6L6 tube and the speaker, as shown in circuit diagram of Fig. 7. Since the output of the voltage amplifier was too high for the input of the 6L6 tube, a potential divider consisting of R_{30} and R_{31} was included to select the correct voltage.

2.227 RECEIVER POWER SUPPLY

The input of the power supply was obtained from a 400-0-400 mains transformer. A 5U4 full-wave rectifier tube was employed. Initially the smoothing was done by two pi-section filters connected in series. However, hot-switching was regularly required. Now, it is recommended that a choke-input filter be used since it limits the hot-switching current to a value

no higher than the peak plate current (49).

Therefore the first pi-section filter had to be converted to a L- section filter. This combination provided the necessary smoothing. An output D.C. voltage of 280 volts with a reasonably low ripple factor was obtained when the required current was drawn by the receiver.

2.228 ADJUSTMENT AND CALIBRATION

2.2281 Adjustment of Voltages and Circuit Components

Voltages were checked throughout the receiver to ascertain whether the tubes were working within the ratings specified and adjustments made accordingly. It was also ensured that all resistors were of the correct wattage.

2.2282 Determination of Optimum I.F.

The correct I.F. of a receiver depends on the design of the I.F. transformers and the tracking of the oscillator tank circuit. For this particular receiver it was determined by trial and error according to the following method:-

A certain I.F. was chosen, say 430 kc/s. After disconnecting the oscillator, a modulated signal of the chosen frequency was injected onto the control grid of the mixer tube (ECH 81). The I.F. transformers were aligned to this frequency and adjusted for maximum gain.

The oscillator was then reconnected, the dial of the receiver set at a certain frequency and a modulated

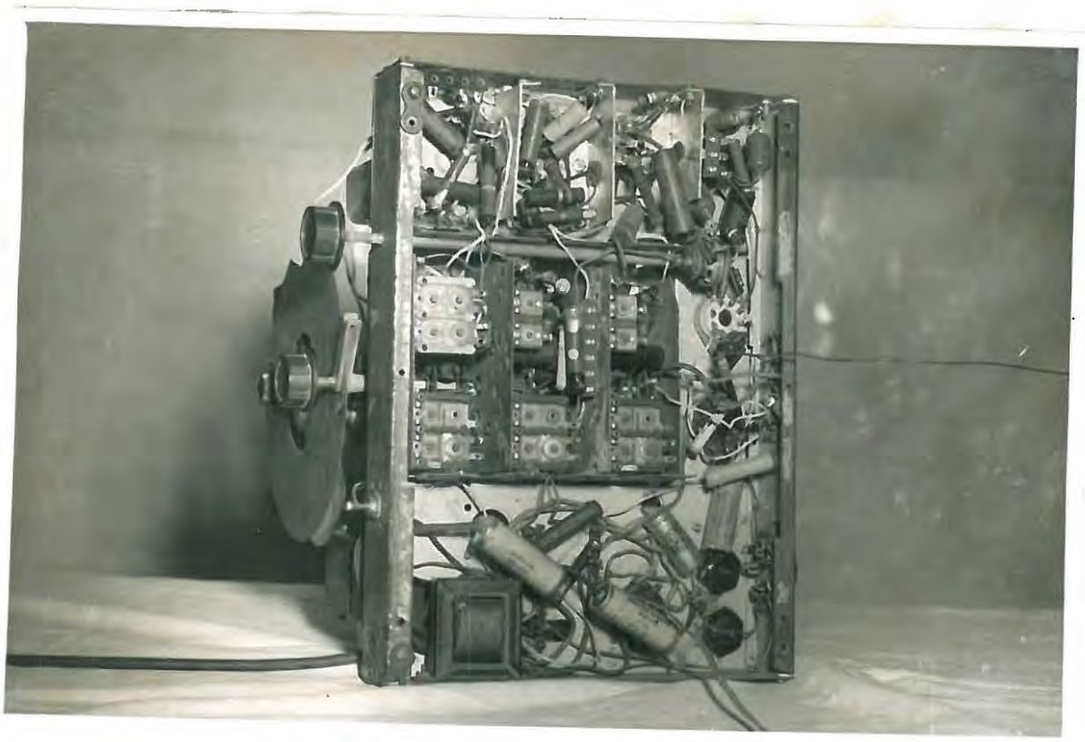

Fig. 8 - RECEIVER

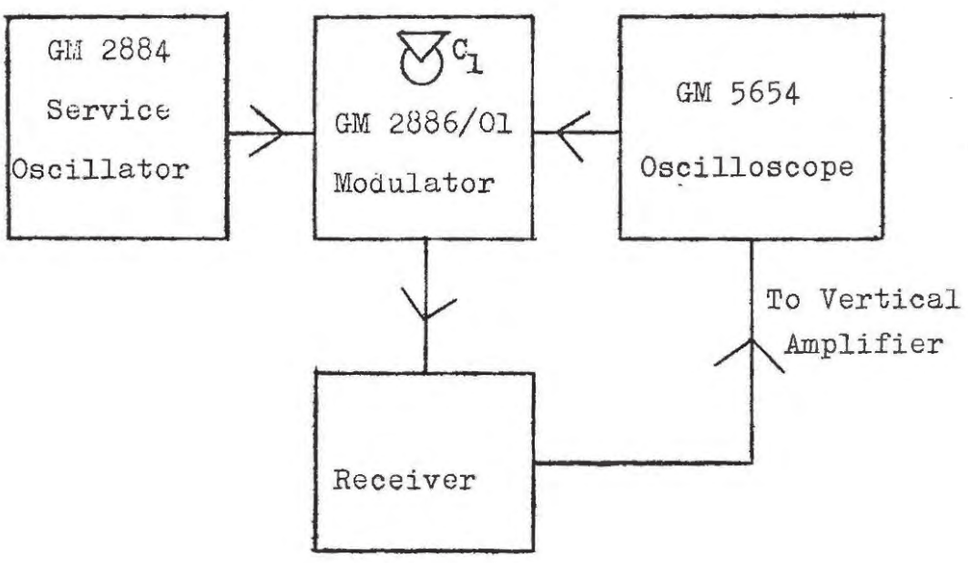

Fig. 9 - TUNING APPARATUS

signal of this frequency applied to the antenna. Subsequently the R.F. trimmers were tuned for maximum output.

The trimmers were then tuned to other R.F. frequencies (the dial being set at the corresponding values) until the frequency range from 500 kc/s to 18 Mc/s was covered. Next, the gain of the receiver for the I.F. of 430 kc/s was measured and noted.

The entire procedure was repeated for another I.F. and the gain was once again noted. By repeating this process, it was found that maximum gain was obtained when the I.F. was between 460 and 470 kc/s. By restricting the gain measurements to I.F. values between 460 and 470 kc/s, the optimum I.F. was found to be 467 kc/s. Hence the I.F. amplifiers were tuned to this value.

2.2283 Alignment Of I.F. Stages

The reproduction quality of a receiver depends on its selectivity characteristics. A high fidelity and broad bandwidth was ensured by careful alignment of the I.F. stages.

The method adopted here resulted in fairly accurate tuning and permitted a quick review of the selectivity characteristics. The block diagram of the apparatus used for the alignment is shown in Fig. 9. It consists of:

(i) The Philips GM 5654 Oscilloscope

This is a conventional linear sweep oscilloscope with a variable time base frequency. It also

incorporates a standard vertical amplifier. An interesting feature of the oscilloscope is that it has an output terminal for the saw-tooth voltage of its time base on the rear panel.

(ii) The Philips GM 2884 Service Oscillator

This is a standard oscillator providing unmodulated high-frequency sinusoidal signals, variable over a wide range of frequencies.

(iii) The Philips GM 2886/01 Frequency Modulator

It includes an oscillator of a fixed frequency (4 Mc/s), which is frequency modulated by means of a reactance tube controlled by the voltage supplied by the time base of the oscilloscope. The maximum degree of frequency modulation is 50 kc/s.

The alignment was carried out according to the manufacturers' instructions.

Initially it was found that the bandwidth was too low. It was readjusted by staggered-tuning of the primary and secondary of each I.F. transformer. Thus the bandwidth was increased to 23 kc/s.

The Fourier analysis of a pulse shows that zeros occur at $\frac{1}{T}$, $\frac{2}{T}$, $\frac{3}{T}$, etc., where T is the pulse duration. Good reproduction of pulses requires side bands to pass the higher harmonics of the pulse repetition frequency. The recommended bandwidth is $\frac{3}{T}$. For $T = 100\ \mu sec$, the bandwidth required is 30 kc/s. A bandwidth of 23 kc/s causes a slight distortion to the pulse (resulting in two peaks with a trough in between). This did not unduly affect the leading edge of the

pulse, which is of importance in the experiment. Therefore the bandwidth was not increased further.

2.2284 Adjustment of R.F. Circuits

The receiver dial was set at a frequency at the end of one of the wave bands. A modulated R.F. signal of this frequency was applied to the antenna of the receiver. Then the R.F. trimmers (C_1, C_6, and C_{11} in Fig. 7) of this waveband were adjusted for maximum gain. This process was repeated for frequencies at the middle of the waveband and at the other end of the waveband. The other wavebands were also similarly aligned.

2.2285 Observation on Width of Pulses received

When the first tests were carried out, undesirable broadening of the pulses was observed despite the fact that the bandwidth of the I.F. amplifiers was large enough. After careful examination of all the circuits, the broadening was attributed to the low time constants of the screen and cathode circuits throughout the receiver. Therefore the values of the decoupling capacitors were increased to obtain reasonably high time constants for the circuits in question. This reduced the broadening appreciably. However, it was found that generally the pulsewidth obtained in the output of the receiver was in the region of 200 μsec. No amount of modification of the circuit components could reduce the pulsewidth to a value less than this.

It might be mentioned that pulses received in

Grahamstown from the Antarctica indicate that it is not easily possible to get narrower pulses. The ionosphere is also responsible for some broadening of pulses. Hence no further attempt was made to reduce the pulse-width.

2.2286 Gain Characteristics

Initially it was not envisaged that transmissions would be carried out at 4.73 Mc/s only. Therefore the entire frequency band of the receiver was tuned for optimum operation and a frequency response curve was determined (see Fig. 10). As can be seen the gain is reasonably constant - varying between 130 and 140 dbs over a range of 18 Mc/s.

2.229 MECHANICAL CONSTRUCTION OF THE RECEIVER (refer to Figs. 6 and 8)

The entire receiver was constructed on a galvanized iron chassis. In designing the layout, maximum care was taken to prevent undesirable coupling between different sections.

Certain desirable features in the structural arrangement of the original receiver were retained:-

(i) The R.F. amplifier and frequency changer were in a separate unit screwed onto the middle of the chassis. There was adequate shielding between them.

(ii) The I.F. tank circuits were covered with aluminium cans.

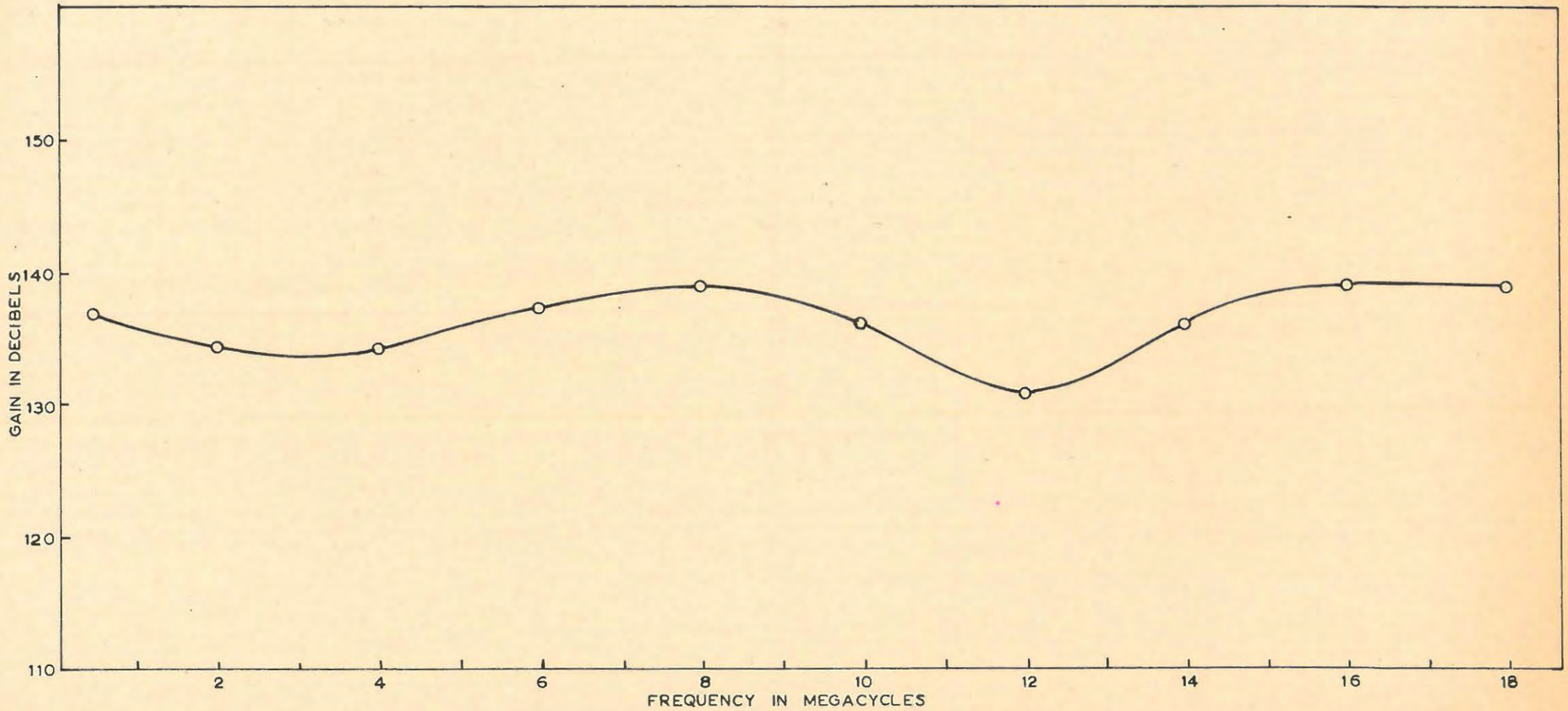

FIG. 10 FREQUENCY RESPONSE OF RECEIVER

(iii) The power supply was located at one end of the chassis to permit free circulation of air and thus to prevent undesirable heating of the receiver.

The following modifications were made to improve the performance of the receiver:-

(i) Aluminium strips were used to separate the different I.F. stages from one another.

(ii) Aluminium cans served to shield:
   (a) the ECH 81 tube which is a glass type,
   (b) the grid terminals of the 6K7 tubes.

(iii) Short shielded cables were used for the leads from the I.F. transformers to the grids of the 6K7 tubes. This can be noticed on the top left-hand corner of Fig. 6.

(iv) The leads from the antenna terminal to the grid of the R.F. amplifier had to pass over the A.F. stages. These leads picked up undesirable effects and the use of shielded cables here improved the reception considerably.

2.23 THE TIME DELAY CALIBRATOR

The main function of the time delay calibrator is to generate pulses with accurately known time separation. When these time-markers are displayed on the screen of the oscilloscope, they provide a simple method of determining the time delays between the various pulses. The circuit diagram of the time delay calibrator is

given in Fig. 11 and a view of the apparatus is shown in Fig. 12.

2.231 THE CATHODE-COUPLED GATE

This is essentially the cathode-coupled multivibrator which is so arranged that only one of the tubes (T_2) is normally conducting while the other (T_1) is biased beyond cut-off. When the positive pulse from the receiver is fed to the grid of T_1, it triggers off the gate.

When the grid of T_1 is returned to a positive potential rather than to ground, it is found that the pulse-width of the gate is directly proportional to the D.C. voltage on the grid (50). Hence a variable potentiometer (R_2) was included in order to vary the pulse-width as required. Since the anode load of T_1 was found to affect the waveform of the output pulses markedly, a variable potentiometer (R_4) in series with the load resistor proved useful for rapid adjustment of the load.

The grid of T_2 was returned to the plate supply through a large resistor (R_7) and a potentiometer (R_6). This served to reduce the jitter in the trailing edge of the pulse. It also permitted greater control of the pulse-width with the D.C. bias potential of T_1.

As a negative gate was required, the output was taken from the plate of T_1. This output was used for:

(i) triggering the oscilloscope;

(ii) activating the RLC ringing circuit.

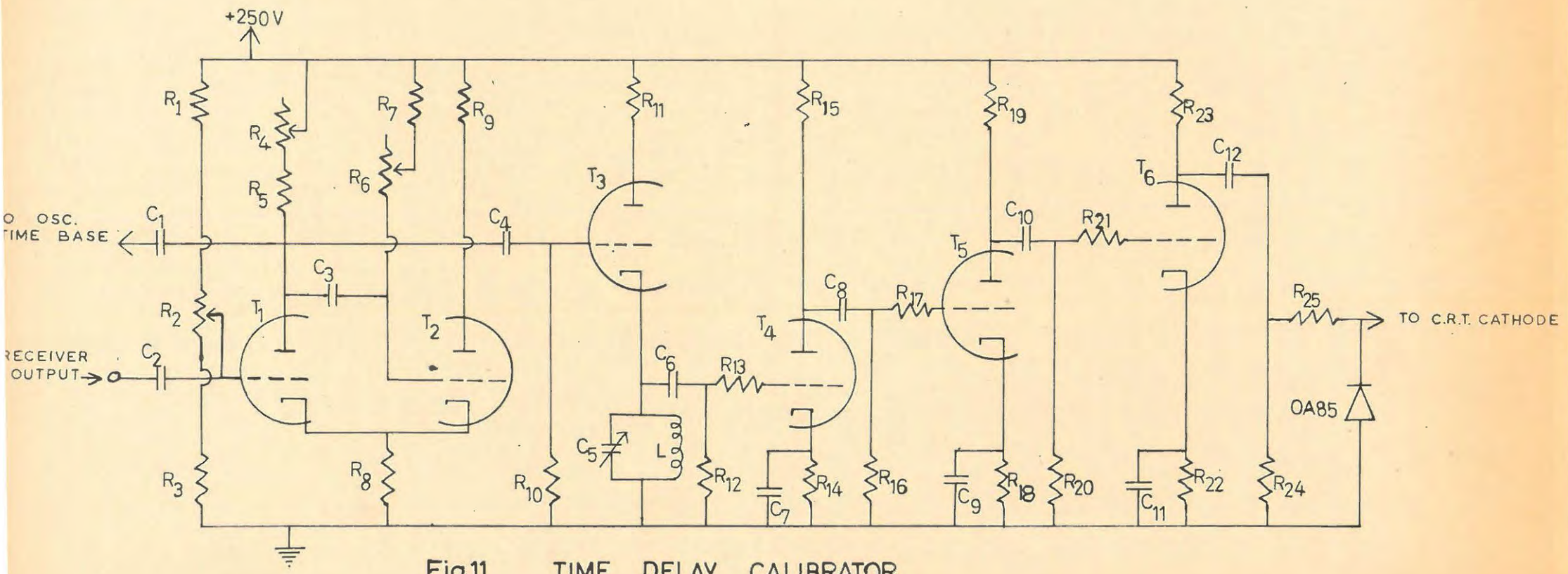

Fig.11 TIME DELAY CALIBRATOR.

FIG. 11 TIME DELAY CALIBRATOR

R_1 = 100K
R_2 = maximum 20K
R_3 = 4.7K
R_4 = maximum 20K
R_5 = 33K
R_6 = maximum 200K
R_7 = 100K
R_8 = 10K
R_9 = 27K
R_{10} = 3.3M
R_{11} = 27K
R_{12} = 1.0M
R_{13} = 220K
R_{14} = 2.5K
R_{15} = 47K
R_{16} = 1.0M
R_{17} = 220K
R_{18} = 1.0K
R_{19} = 47K
R_{20} = 1.0M
R_{21} = 200K
R_{22} = 330 ohms
R_{23} = 47K
R_{24} = 100K
R_{25} = 100K

C_1 = 1.0 μF
C_2 = 0.02 μF
C_3 = 0.02 μF
C_4 = 0.05 μF
C_5 = Maximum 5250pF
C_6 = 0.05 μF
C_7 = 0.1 μF
C_8 = 0.05 μF
C_9 = 0.1 μF
C_{10} = 0.2 μF
C_{11} = 0.1 μF
C_{12} = 56 pF

L = 50 mH

T_1 = $\frac{1}{2}$ 6SN7
T_2 = $\frac{1}{2}$ 6SN7
T_3 = $\frac{1}{2}$ 6SN7
T_4 = $\frac{1}{2}$ 6SN7
T_5 = $\frac{1}{2}$ 6SN7
T_6 = $\frac{1}{2}$ 6SN7

2.232 THE RLC RINGING CIRCUIT

Here the circuit comprises a triode (T_3) with a tank circuit in the cathode. When the negative gate is applied to the grid of T_3, the grid voltage falls and the tube is cut off. The output taken across the tank circuit is a train of damped oscillations.

The tank circuit consists of:-

(i) padded mica capacitors and an air-mica trimmer,

(ii) a coil of 800 turns of 24 S.W.G. enamelled wire wound on a perspex core of length 0.75 cm and diameter 1.8 cm.
(For the coil, L = 50 mH., $C_{self} \approx 200$ pF, R = 17 ohms and Q $\approx$ 200).

The tank circuit was tuned accurately to 10 kc/s with the aid of a 100 kc/s crystal oscillator and a double beam oscilloscope.

It was found that at least 25 oscillations had sufficient amplitude to serve as time-markers, which were, at this stage, sinusoidal in shape.

2.233 THE CLIPPING AMPLIFIERS

It was then necessary to convert the sinusoidal output of the ringing circuit into square waves. Three stages of clipping amplifiers were designed to effect this.

These are essentially triode amplifiers with resistive loads and large resistors in series with the grids.

The three amplifiers functioned as follows:-

(i) the first merely amplified the signal;

(ii) the second clipped off a portion of the peaks;

(iii) the final amplifier gave an output approximating to a square wave.

2.234 THE PEAKING CIRCUIT

The peaking circuit differentiates the square wave pulses. By careful choice of the capacitance (C_{12}) and the resistance (R_{24}), the time constant was made small enough so that the output pulses would have short durations and steep leading edges. (The time constant was 5.6 μsec, which was small compared with 100 μsec, the separation of the pulses.)

2.235 THE CLIPPING DIODE

The negative portion of the pulses were then clipped off by the germanium diode OA 85.

This provided a series of positive pulses lasting for about 2.5 milliseconds. The separation between any two pulses was 100 μsec, and the amplitude of the pulses was about 50 volts, which was sufficient to modulate the trace on the oscilloscope screen.

2.236 POWER SUPPLY FOR THE TIME DELAY CALIBRATOR

The power supply for the time delay calibrator was the conventional full-wave rectifier employing a 5U4

vacuum tube followed by two pi-section filters in series. The input to the rectifier tube was obtained from a 360-0-360 mains transformer.

2.237 SYNCHRONIZATION OF THE TIME DELAY CALIBRATOR WITH THE RECEIVED PULSES

In order that the time markers be displayed on the oscilloscope screen simultaneously with the received pulses, it is essential that the time delay calibrator be synchronized in some way with the receiver. The first time marker should coincide with the leading edge of the first pulse received. Thus the pulses that follow would be spread over a calibrated scale.

This was effected by arranging the cathode-coupled gate such that it was triggered by the first pulse received. Accordingly, the positive output from the A.F. stage of the receiver was fed to the grid of T_1 in Fig. 11 via the cathode follower. To prevent the ensuing pulses from re-triggering the gate, the duration of the gate pulse was made sufficiently large.

2.24 THE OSCILLOSCOPE

The pulses and time markers were displayed on a Tektronix 310 A oscilloscope with a P 11 blue screen.

The following procedure was adopted for setting up the oscilloscope for the reception of pulses:-

(i) The vertical amplifier gain was reduced to zero.

(ii) The trigger of the time base was set at "external negative" for "A.C. triggering" so that it could be triggered by the negative pulses from the cathode-coupled gate.

(iii) The time base frequency control was adjusted for a sweep duration of 2.5 milliseconds. (see 2.235).

(iv) The sweep was then centralized on the screen.

(v) The time-markers and the pulses received were applied to the "C.R.T. cathode" terminal located on the rear panel of the oscilloscope. (This terminal is connected to the cathode of the cathode ray tube via a blocking condenser.) Hence the applied signals modulated the intensity of the beam on the screen.

Note: During the latter part of the experiment the 310A oscilloscope developed a fault. It was then replaced by a 551, whose operational instructions are very similar to those of the 310A.

Fig. 12 - TIME DELAY CALIBRATOR

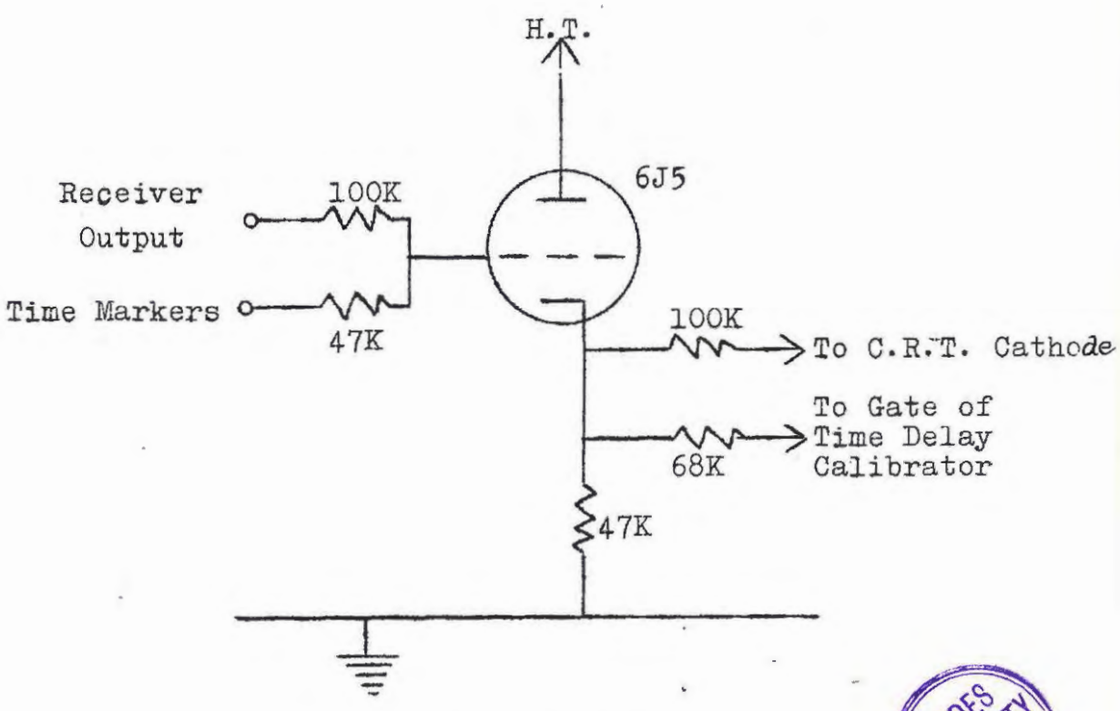

Fig. 13 - CATHODE FOLLOWER

RHODES UNIVERSITY LIBRARY

2.25 THE CATHODE FOLLOWER (Fig. 13)

The low input impedance of the cathode-coupled gate caused a marked decrease in the amplitude of the pulses when the receiver output was applied directly to it. Similar effects were observed when the outputs from the receiver and the time delay calibrator were fed to the oscilloscope.

This was remedied by including a cathode follower (as shown in the block diagram of Fig. 4), which served to match impedances in both cases.

It might appear from Fig. 13 that, if the time markers are re-applied to the grid of the cathode follower which feeds pulses to the cathode-coupled gate, a feedback loop is formed between the time delay calibrator and the cathode follower. It must be remembered, however, that after the gate is triggered off by the first pulse it remains quiescent until the tube T_1 (Fig. 11) stops conducting. During this period the cathode-coupled gate cannot be triggered by the time markers and the ensuing pulses. The gate circuit is adjusted such that all these pulses pass through before it recovers.

2.26 THE RECORDING CAMERA

The recording camera, shown in Fig. 14, was originally constructed for Gledhill and Szendrei (51). It was a continuously running 35 mm. camera. A four lens combination which could be moved forward and backward focussed the CRT trace onto the film. A

Fig.14 - CAMERA

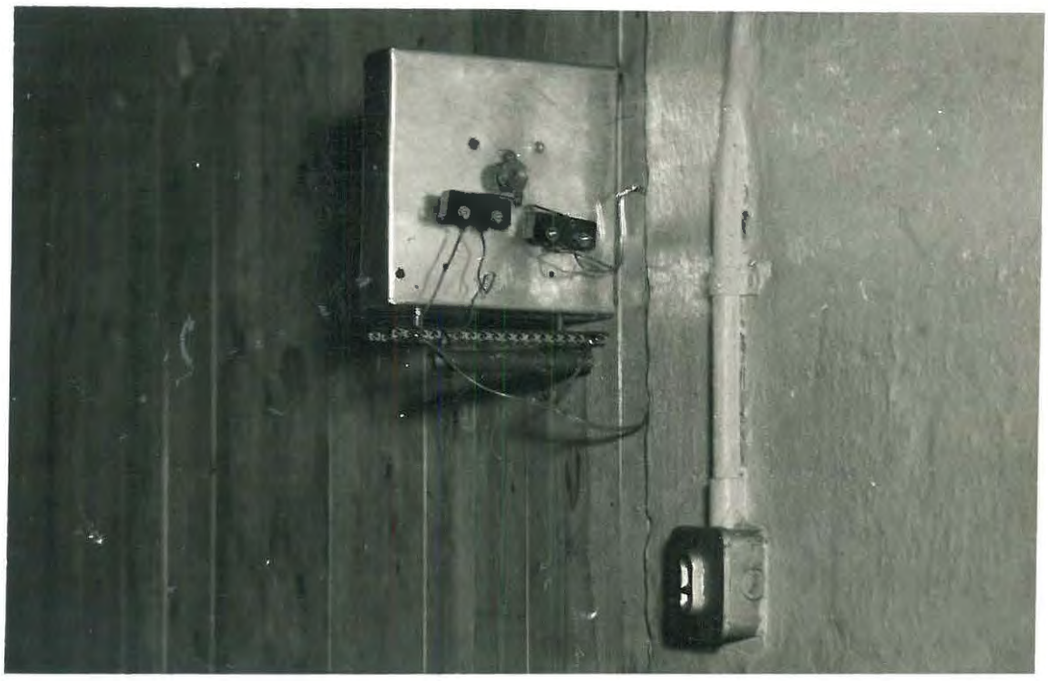

Fig.14(a) - TIME SWITCH

small opening on the upper end of the box was used for viewing. Since the original speed of 25 feet of film per hour was too high, the gears of the motor were modified to reduce the speed to $\frac{3}{4}$ feet per hour which was within the limits required.

2.27 THE TIME SWITCH

In order to derive diurnal variations a clear picture of the oblique incidence propagation throughout the day had to be obtained. This necessitated continuous recordings.

However, it was also essential to obtain day to day variations for longer periods. To take continuous records for these periods would have involved running the transmitter continuously. In order to minimise interference with other radio communication users, a method was devised whereby recordings could be taken for only 15 minutes of every hour. This involved the use of a clock. The minute hand was replaced by a cam cut so that it acted on a microswitch for $\frac{1}{4}$ of its revolution. Since the microswitch was connected in series with the camera motor, the latter was switched on for $\frac{1}{4}$ of every hour.

Another microswitch was set such that it was acted on by the cam for the same period of time. This switch was connected in series with the H.T. of the receiver. Therefore during those times that recordings were not taken, the H.T. of the receiver and the camera motor were switched off. To minimize drift due to warming up, the rest of the apparatus was left switched on continuously. A view of the time switch showing the cam and the micro-switches is shown in Fig. 14(a).

S E C T I O N B

3. FUNDAMENTAL THEORY OF PROPAGATION OF RADIO WAVES IN THE IONOSPHERE

3.1 WAVE GROUP (PULSE)

A wave of a single frequency is not realised in practice, for it would need to have been generated an infinite time in the past and continue to an infinite time in the future. Any wave of shorter duration is a pulse, and in generating a pulse, other frequencies (harmonics, sidebands) are produced. A pulse may be regarded as an integral over a continuous distribution of frequencies and may be represented by a Fourier integral thus:

$$E(t) = \int_{-\infty}^{+\infty} F(f) \cdot e^{2\pi i f t} df \quad \ldots\ldots (3.1)$$

The form of the function F(f) depends upon the shape of the pulse, which is usually a signal of constant frequency f_1 and practically constant amplitude, lasting for a time T, called the duration of the pulse.

3.2 PHASE VELOCITY AND GROUP VELOCITY

When a pulse travels in free space, it does so with a velocity c. All the component frequencies have the same speed. However, when it travels in a dispersive medium, the phase velocity, V, depends upon

the wave frequency. The component frequencies now have different velocities.

The true velocity of the wave packet, i.e. the velocity with which energy is transferred in the direction of propagation, is called the group velocity, U. The latter differs from the phase velocity of any component frequency. The ratio c/U is generally called the "group refractive index" and is denoted by μ', by analogy with the "wave refractive index", $\mu = c/V$, where V is the wave (phase) velocity.

It is obviously important to calculate the group velocity of a pulse travelling through the ionosphere (see section 3.3). The calculation is simplified if a relationship is obtained between the group velocity and the phase velocity, which may be derived as follows:

It is well known that a wave represented by

$$E = E_o \exp \left\{ i (wt - kx) \right\} \quad .....(3.2)$$

has a group velocity

$$U = \frac{dw}{dk} \quad .....(3.3)$$

where k is called the wave number and is given by

$$k = \frac{w}{V}, \quad .....(3.4)$$

(V is the wave velocity).

$$\therefore \frac{1}{U} = \frac{d\frac{w}{V}}{dw} = \frac{1}{V} - \frac{w}{V^2} \cdot \frac{dV}{dw} \quad .....(3.5)$$

Substituting $V = \frac{c}{\mu}$, we have

$$\frac{1}{U} = \frac{\mu}{c} + \frac{w}{c} \cdot \frac{d\mu}{dw}$$

i.e. $$\frac{c}{U} = \mu + w \frac{d\mu}{dw}$$

or $$\mu' = \mu + w \frac{d\mu}{dw} \quad \ldots\ldots\ldots \quad (3.6)$$

But for a medium containing free electrons (in the absence of a magnetic field), the wave refractive index is given by

$$\mu = \left(1 - \frac{f_n^2}{f^2} \right)^{\frac{1}{2}} \quad \ldots\ldots\ldots (3.7)$$

where f is the wave frequency and $f_n = \frac{1}{2\pi} \sqrt{\frac{Ne^2}{\epsilon_o m}}$ is called the plasma frequency corresponding to an electron density N. (e = electronic charge, m = mass of electron and ϵ_o = permittivity of free space) (52).

Combining equations (3.6) and (3.7)

$$\mu' = \left(1 - \frac{f_n^2}{f^2} \right)^{\frac{1}{2}} + w \frac{d}{dw} \left(1 - \frac{f_n^2}{f^2} \right)^{\frac{1}{2}}$$

$$= \left(1 - \frac{f_n^2}{f^2} \right)^{\frac{1}{2}} + \left(1 - \frac{f_n^2}{f^2} \right)^{-\frac{1}{2}} \cdot \frac{f_n^2}{f^2}$$

$$= \left(1 - \frac{f_n^2}{f^2} \right)^{-\frac{1}{2}} \quad \ldots\ldots\ldots\ldots (3.8)$$

Therefore $$\mu' \mu = 1 \quad \ldots\ldots\ldots (3.9)$$

Thus it is seen that the product of the group refractive index and the wave refractive index is unity for a medium containing free electrons (with zero magnetic field).

Writing μ and μ' in terms of c, V and U, we get

$$UV = c^2, \quad \ldots\ldots\ldots(3.10)$$

which shows that the product of the group and phase velocities is equal to the square of the velocity of light in free space.

3.3 VERTICAL INCIDENCE

In the commonest method of using radio waves to investigate the ionosphere, pulses of radio energy are generated by a transmitter on the ground. Each pulse travels upwards and is reflected from the ionosphere. It then returns to a receiver on the ground, and the time of travel is measured in order to derive information about the ionosphere.

When the pulse is travelling vertically up from the ground, it moves in air until it reaches the ionosphere. The refractive index (group and phase) of air is very close to unity. Therefore the velocity of radio waves in air may be taken as the same as in free space. Since air is an insulator, the radio wave only generates a displacement current on account of its changing electric field.

Once the pulse is in the ionosphere, the electric

field sets free electrons into motion, thus setting up a convection current. Part of the displacement current is cancelled out as the convection current is in antiphase with it. Hence the rate of change of electric and magnetic fields is altered. The phase of the wave is shifted - the wave behaving as if it had been speeded up. Consequently the phase velocity increases. According to equation (3.10) it may be inferred that as the phase velocity increases, the group velocity decreases, or in other words the group refractive index increases.

This continues until:-

(i) the pulse reaches the point where the group refractive index is a maximum;

or (ii) the pulse velocity is reduced to zero.

In the former case, the pulse is retarded up to the point of maximum group refractive index. Thereafter it is accelerated until it emerges out of the topside of the ionosphere and disappears into space.

In the latter case, the group velocity decreasing to zero in the ionosphere indicates that the group refractive index reaches infinity. This is said to be the point of reflection of the pulse.

The condition for reflection, therefore, is

$$\mu' = \infty \quad \ldots\ldots\ldots (3.11)$$

$$\text{i.e.} \quad \left(1 - \frac{f_n^2}{f^2}\right)^{-\frac{1}{2}} = \infty$$

$$\text{or} \quad f = f_n \quad \ldots\ldots\ldots\ldots (3.12)$$

Thus the pulse is reflected when the plasma frequency equals the frequency of the radio wave.

But $f_m = \frac{1}{2\pi}\sqrt{\frac{Ne^2}{\epsilon_o m}}$ (see section 3.2)

$\therefore$ 3.12 may be rewritten

$$f = \frac{1}{2\pi}\sqrt{\frac{Ne^2}{\epsilon_o m}}$$

or $$N = \frac{4\pi^2 m f^2 \epsilon_o}{e^2} \quad \text{.....(3.13)}$$

$$= 1.24 \times 10^4 f^2 \text{ electrons per cc. .....(3.14)}$$

where f is in Megacycles/sec.

So for a radio pulse travelling vertically up in the ionosphere, the phase velocity increases and the group velocity decreases depending on the ratio of N to f^2. If there is sufficient ionization for a particular value of f (i.e. $N = 1.24 \times 10^4 f^2$), the group velocity reduces to zero, and the pulse is reflected. The wave group then proceeds to travel vertically downwards with increasing velocity until it emerges out of the ionosphere. Thereafter it travels with the velocity of light in free space until it reaches the ground.

From equation (3.14) it may be deduced that the electron density required to return a pulse increases with the frequency, and the higher the frequency the deeper the penetration into the ionosphere. Pulses

with frequencies higher than that corresponding to the maximum value of N (i.e. the critical frequency) are not returned to ground.

3.4 OBLIQUE INCIDENCE

When a pulse is obliquely incident on the ionosphere, the presence of electrons also retards the wave group. However, the group is not returned to the point of transmission because the direction of the ray changes while it is in the ionosphere. The decrease in phase refractive index as the pulse penetrates deeper into the ionosphere also bends the ray away from the normal. This continues until the group travels horizontally. Thereafter it bends towards the ground and arrives at a point some distance away from the transmitter.

In order to derive information about the ionosphere with the aid of oblique incidence propagation of radio waves, it is necessary to analyse the propagation from the time the pulse leaves the transmitter to the time it reaches the receiver. The path of the ray should be followed all the way and all information obtained from the motion of the pulse carefully noted. An accurate method of doing this would be to use the Booker quartic equation, a comprehensive discussion of which is given by Budden (53).

However, this equation is very complicated and requires laborious calculations to obtain the solution.

A computer program on the Booker quartic for this project would have reduced the calculations considerably, thereby making it possible for all the records taken to be analysed. Since a computer was not available, this method could not be used.

The method developed by Martyn et al. (54) was therefore resorted to, whereby oblique incidence propagation is related to vertical incidence propagation.

Consider a pulse leaving the earth at a point T (in Fig. 15) and striking the ionosphere at the point A at an angle ϕ_o with the vertical. Since the phase refractive index decreases in the ionosphere, the ray will be bent away from the vertical and if the ionization is sufficient, it will be diverted back to earth along the path ABCR. To a receiver at R, the apparent point of reflection would be E. Hence ED appears to be the height of reflection, whereas the true height of reflection is BD.

The problem now is to find the relationship between the frequency of this pulse which follows the path TABCR and the vertical incidence frequency that has an apparent reflection at E. This is easily achieved by considering three theorems (54), namely,

(i) The Secant Law,

(ii) Breit and Tuve's Theorem, and

(iii) Martyn's Theorem,

which are true for flat earth and flat ionosphere and no magnetic field. Since the distance from

Grahamstown to Durban is only 590 km (see section 4.12), the error introduced by assuming flat earth and flat ionosphere is negligible. By drawing a scale diagram of the curvature of the earth between Grahamstown and Durban, it was determined that the error involved would not be in excess of 10 km.

The neglect of the magnetic field seems to introduce a relatively bigger error. This is mainly due to the lateral deviation of the pulses. Calculations from ionograms for Grahamstown have shown that an error of the order of 25 km is introduced if the earth's magnetic field is neglected for vertical incidence propagation. One would expect that the

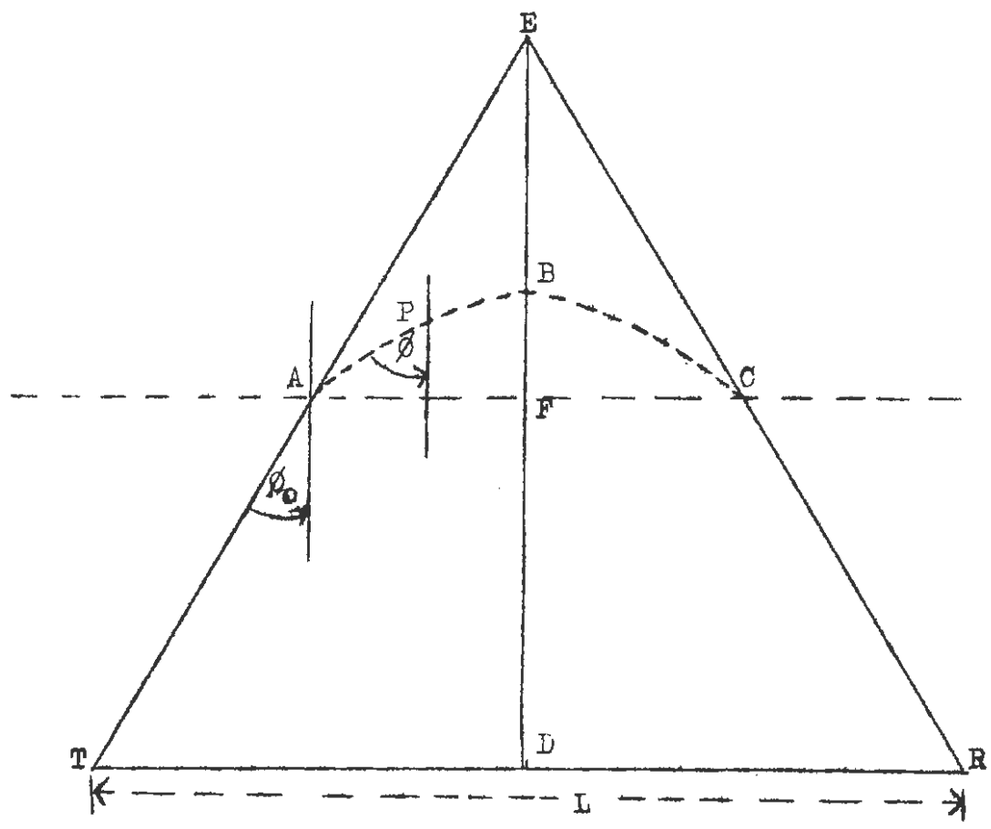

Fig. 15

error for oblique incidence propagation between Grahamstown and Durban to be about twice this. A figure of 50 km, therefore, seems to be a fairly good approximation. Since the errors involved in the recordings were of the same order of magnitude, neglecting the magnetic field in the analysis would not affect the results to an unacceptable extent.

3.41 THE SECANT LAW

Let the electron density at point B (Fig. 15) be N_B. Then the group refractive index for any wave at B is given by equation (3.8) as

$$\mu'_B = \left(1 - \frac{N_B e^2}{4\pi^2 \epsilon_o m f^2}\right)^{-\frac{1}{2}} \qquad \ldots\ldots\ldots(3.15)$$

where f is the wave frequency. If an obliquely propagated ray of frequency f_{ob} follows the path TABCR, the group refractive index at its maximum point B, therefore, is

$$\mu'_{ob} = \left(1 - \frac{N_B e^2}{4\pi^2 \epsilon_o m f_{ob}^2}\right)^{-\frac{1}{2}} \qquad \ldots\ldots(3.16)$$

Now assuming that an ionosonde is placed on the ground vertically below B and the pulses transmitted are of frequency f_v, the group refractive index for these pulses at B is

$$\mu'_v = \left(1 - \frac{N_B e^2}{4\pi^2 \epsilon_o m f_v^2}\right)^{-\frac{1}{2}} \qquad \ldots\ldots\ldots(3.17)$$

If the point B is the true height of reflection for this frequency then

$$\left(1 - \frac{N_B e^2}{4\pi^2 \epsilon_o m f_v^2} \right)^{-\frac{1}{2}} = \infty$$

$$\therefore \quad N_B = \frac{4\pi^2 \epsilon_o m f_v^2}{e^2} \quad \ldots\ldots\ldots (3.18)$$

Substituting for N_B in equation (3.16) gives

$$\mu'_{ob} = \left(1 - \frac{f_v^2}{f_{ob}^2} \right)^{-\frac{1}{2}} \quad \ldots\ldots\ldots (3.19)$$

Therefore the phase refractive index for the obliquely propagated ray at the point B is given by combining equations (3.9) and 3.19)

$$\mu_{ob} = \left(1 - \frac{f_v^2}{f_{ob}^2} \right)^{\frac{1}{2}} \quad \ldots\ldots\ldots (3.20)$$

Next consider any point P(Fig. 15) on the path, where the ray makes an angle ϕ with the vertical. If the phase refractive index at this point is μ_p, then according to Snell's Law.

$$\mu_p = \frac{\sin \phi_o}{\sin \phi} \quad \ldots\ldots\ldots (3.21)$$

where ϕ_o is the angle of incidence of the ray on the ionosphere. On the other hand if the point B is considered it is found that ϕ is 90° and

$$\mu_{ob} = \frac{\sin \phi_o}{\sin 90^o} = \sin \phi_o \quad \ldots\ldots\ldots (3.22)$$

Combining equations (3.20) and (3.22),

$$\sin^2 \phi_o = 1 - \frac{f_v^2}{f_{ob}^2}$$

$$\therefore \quad \cos^2 \phi_o = \frac{f_v^2}{f_{ob}^2}$$

$$\text{i.e. } \cos \phi_o = \frac{f_v}{f_{ob}}$$

$$\text{Hence } f_{ob} = f_v \sec \phi_o \quad \ldots\ldots\ldots (3.23)$$

This is the relationship between the oblique incidence and vertical incidence frequencies reflected from the same true height. If any two quantities in equation (3.23) are known, the third can easily be determined.

3.42 BREIT AND TUVE'S THEOREM

Here the time taken by the curved path TABCR (Fig. 15) at the group speed is stated to be equal to that necessary to travel over the triangular path TER at the velocity of free space.

Consider a small element of the path ds in the ionosphere at a point, say P (Fig. 15). This distance is covered in time $\frac{ds}{U}$, where U is the group velocity at the point. Therefore the time taken to travel the path TABCR is

$$t = \int_{TABCR} \frac{ds}{U} \quad \ldots\ldots\ldots (3.24)$$

But $U = c\mu$ where μ is the phase refractive index.

$$\therefore \quad t = \frac{1}{c} \int_{TABCR} \frac{ds}{\mu} \qquad \ldots\ldots\ldots(3.25)$$

Now dx, the horizontal component of ds, is given by $dx = ds \sin \phi$

$$\text{i.e.} \quad ds = \frac{dx}{\sin \phi} \qquad \ldots\ldots\ldots(3.26)$$

Substituting for ds into equation (3.25) yields

$$t = \frac{1}{c} \int_{TABCR} \frac{dx}{\mu \sin \phi} \qquad \ldots\ldots\ldots(3.27)$$

Snell's Law states that for any point on the path

$$\mu \sin \phi = \sin \phi_o$$

$$\therefore \quad t = \frac{1}{c} \int_{TABCR} \frac{dx}{\sin \phi_o} \qquad \ldots\ldots\ldots(3.28)$$

$$= \frac{1}{c \sin \phi_o} \int_{TABCR} dx$$

$$= \frac{L}{c \sin \phi_o} \qquad \ldots\ldots\ldots(3.29)$$

where L is the distance of transmission.

From Fig. 15 it can be seen that

$$\sin \phi_o = \frac{L/2}{TE} = \frac{L/2}{ER} \qquad \ldots\ldots(3.30)$$

Combining equations (3.29) and (3.30)

$$t = \frac{2TE}{c} = \frac{TE + ER}{c} \qquad \ldots\ldots\ldots(3.31)$$

This is the time which a wave would take to travel the path TER with a velocity c, which proves the theorem.

3.43 MARTYN'S THEOREM

This theorem states that if f_v and f_{ob} are the vertical and oblique incidence frequencies, respectively, reflected from the same true height, then the virtual (apparent) height of reflection for the frequency f_v is equal to the height of the equivalent triangular path for the frequency f_{ob}.

Consider the oblique incidence frequency f_{ob} and the vertical incidence frequency f_v which are reflected from the same true height. For some point P (Fig. 15) on the oblique path which makes an angle ϕ with the vertical, the phase refractive index for the frequency f_{ob} is given by equation (3.7) as

$$\mu_{ob} = \sqrt{1 - \frac{N_p e^2}{4\pi^2 \epsilon_o m f_{ob}^2}} \quad \ldots\ldots\ldots(3.32)$$

where N_p is the electron density at the point P. At this level the phase refractive for the frequency f_v is

$$\mu_v = \sqrt{1 - \frac{N_p e^2}{4\pi^2 \epsilon_o m f_v^2}} \quad \ldots\ldots(3.33)$$

Applying the Secant Law to equation (3.33), we get

$$\mu_v = \sqrt{1 - \frac{N_p e^2 \sec^2\phi_o}{4\pi^2 \epsilon_o m f_{ob}^2}}$$

$$\text{i.e. } \mu_v^2 = 1 - \frac{N_p e^2 \sec^2\phi_o}{4\pi^2 \epsilon_o m f_{ob}^2} \quad \ldots\ldots\ldots(3.34)$$

Equation (3.32) rewritten is

$$\mu_{ob}^2 = 1 - \frac{N_p e^2}{4\pi^2 \epsilon_o m f_{ob}^2} \quad \ldots\ldots\ldots\ldots (3.35)$$

Eliminating $\frac{N_p e^2}{4\pi^2 \epsilon_o m f_{ob}^2}$ between (3.34) and (3.35),

$$\mu_v^2 = 1 - (1 - \mu_{ob}^2) \sec^2 \phi_o$$

or $\underline{\mu_v^2 \cos^2 \phi_o} = \cos^2 \phi_o - 1 + \mu_{ob}^2$

i.e. $$\mu_v^2 \cos^2 \phi_o = \mu_{ob}^2 - \sin^2 \phi_o \quad \ldots\ldots\ldots (3.36)$$

But Snell's law states (see equation (3.21).)

$$\mu_{ob} = \frac{\sin \phi_o}{\sin \phi}$$

Hence equation (3.36) becomes

$$\mu_v^2 \cos^2 \phi_o = \mu_{ob}^2 - \mu_{ob}^2 \sin^2 \phi$$

or $$\mu_v^2 \cos^2 \phi_o = \mu_{ob}^2 \cos^2 \phi$$

i.e. $$\mu_v \cos \phi_o = \mu_{ob} \cos \phi \quad \ldots\ldots\ldots\ldots (3.37)$$

By Breit and Tuve's theorem, the equivalent path for the oblique incidence frequency is

$$P'_{ob} = 2 \left[\int_{AB} \frac{ds}{\mu_{ob}} + TA \right]$$

$$= 2TE \quad \ldots\ldots\ldots\ldots (3.38)$$

Similarly the equivalent path at vertical incidence for the frequency f_v is

$$P'_v = 2\left[\int_{FB}\frac{dh}{\mu_v} + DF\right] \quad \ldots\ldots\ldots(3.39)$$

where dh is the vertical component of ds.

$$\therefore \quad dh = ds \cos \phi \quad \ldots\ldots\ldots(3.40)$$

Substituting for μ_v from equation (3.37) and for dh from equation (3.40) into equation (3.39), we obtain

$$P'_v = 2\left[\int_{AB}\frac{ds\ \cos\phi\ \cos\phi_o}{\mu_{ob}\ \cos\phi} + DF\right]$$

$$= 2\left[\int_{AB}\frac{ds\ \cos\phi_o}{\mu_{ob}} + DF\right] \quad \ldots\ldots\ldots(3.41)$$

From Fig. 15 we see that

$$DF = TA \cos\phi_o$$

$$\therefore \quad P'_v = 2\left[\int_{AB}\frac{ds\ \cos\phi_o}{\mu_{ob}} + TA\cos\phi_o\right]$$

$$= 2\cos\phi_o\left[\int_{AB}\frac{ds}{\mu_{ob}} + TA\right] \quad \ldots\ldots\ldots(3.42)$$

Using equation (3.38), we get

$$P'_v = 2\cos\phi_o\ TE$$

$$= 2DE \quad \ldots\ldots\ldots(3.43)$$

i.e. The virtual height of reflection is equal to DE in Fig. 15.

It may be inferred from the above discussions that Martyn's theorem may be written

$$h'_{ob} = h'_v$$

where h'_v is the virtual height of reflection of the vertical incidence frequency f_v, and h'_{ob} is the height of the equivalent triangular path for the oblique incidence frequency f_{ob} which is reflected from the same true height.

Applying these three theorems, records on oblique incidence propagation could be approximately analysed and the vertical incidence equivalents could be worked out for such quantities as height of reflection, propagation time, electron density, path length and critical frequency.

4. ANALYSIS

4.1 INTRODUCTION

4.11 MODES OF PROPAGATION

When a radio pulse is transmitted from Grahamstown, it is expected to travel through different paths to Durban. The pulses arriving in Durban would normally consist of the ground pulse and pulses reflected from various layers of the ionosphere. The heights of reflection will depend on the electron densities in the ionosphere between Grahamstown and Durban.

These pulses have different modes of propagation. The simplest of these is a one-hop which arrives after being reflected once in the ionosphere. The two-hop pulse leaves the transmitter, is reflected in the ionosphere and arrives on the ground at a point about midway between Grahamstown and Durban. Here it is reflected back to the ionosphere, and after a second reflection it arrives in Durban. The three-hop mode involves three reflections in the ionosphere and the four-hop pulse is reflected four times. Hence we may generalize to say that the n-hop pulse is reflected n times by the ionosphere.

In addition there are more complicated modes of propagation, for instance, the M-type and N-type. In the former type, the pulse leaves Grahamstown and is reflected by an upper layer of the ionosphere, say the F layer. While it is travelling down it is

reflected up again by a lower layer of high electron concentration, say the sporadic-E layer. It travels up again and after a second reflection by the F layer it arrives in Durban.

The N-type pulse travels up and is reflected by the F layer. On reaching the ground it is reflected back to the ionosphere but this time it is reflected by the E layer before arriving in Durban. Of course, in the N-type propagation there is a similar possibility that the E-region reflection can precede that by the F region.

All these modes of propagation have different path lengths from Grahamstown to Durban. Hence their times of propagation would differ. Therefore an observer in Durban would receive these pulses with different time delays. With the aid of these time delays it is possible to identify the paths followed by the various pulses, and information concerning the ionosphere could be obtained.

4.12 CALCULATION OF THE DISTANCE BETWEEN GRAHAMSTOWN AND DURBAN

The distance between Grahamstown and Durban was calculated using the well known theory of the spherical triangle which gives the following equation:

$$\cos\alpha = \cos\beta\cos\gamma + \sin\beta\sin\gamma\cos\lambda$$

where α is the angle between the two lines joining Durban and Grahamstown to the centre of the earth;

β and γ are the complements of the latitudes of Grahamstown and Durban respectively; and λ is the difference between the longitudes of Grahamstown and Durban.

The latitudes of Grahamstown and Durban are 33° 17'S and 29° 57'S, while the longitudes are 26° 31'E and 31° 12'E, respectively. Hence the value of α obtained is 5° 18'. The radius of curvature of the earth is 6371 kilometres. Using these data, the length of the arc of the great circle from Grahamstown to Durban is found to be 590 km.

4.13 THE GROUND PULSE

According to the records taken it seems highly improbable that the ground pulse was received in Durban. This is evident from the fact that pulses were received in Durban only during those times when propagation conditions were good. In addition, the time delays between the first pulse that arrives in Durban and the ensuing pulses do not fit into the calculations if the first pulse is assumed to be the ground pulse.

D.H. Menzel (55) gives the ground wave signal strength variation with distance of a wave produced by a 1 - KW transmitter. Here the ground wave intensity is plotted for certain distances against frequency of transmission. On extrapolating the curves for 500 km and 700 km distances, it is found that the intensity

for 590 km is about 50 dbs below 1 μvolt per meter for 4.73 Mc/s. The power correction for a 2-KW transmitter (which was used in this experiment) only increases the intensity by 3 dbs. This gives an intensity of 2×10^{-5} μvolt per meter at the antenna of the receiver, which is far too small to trigger the apparatus. This clearly indicates that the ground wave cannot be received in Durban.

4.14 METHODS FOR DETERMINING THE TIMES OF PROPAGATION FOR DIFFERENT MODES

Since the curvature of the earth is not very great between Grahamstown and Durban - the error

Fig. 16

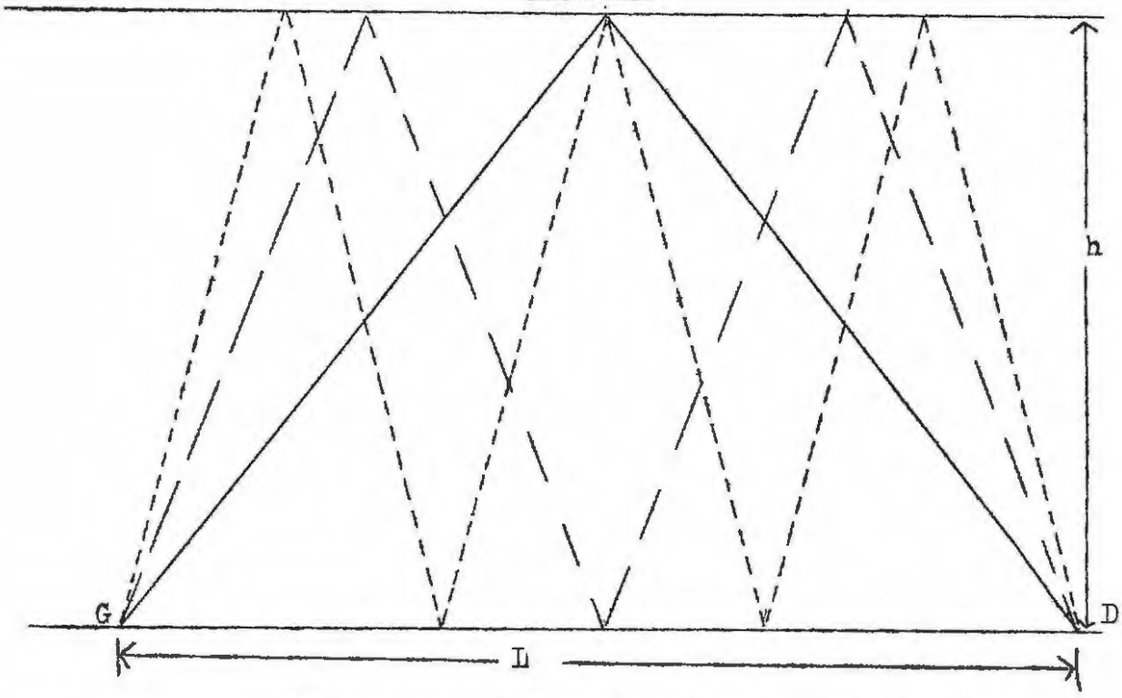

Height of reflection in km	TIMES OF PROPAGATION				
	1 - Hop	2 - Hop	3 - Hop	4 - Hop	5 - Hop
50	1995	2077	2206	2376	2578
80	2037	2236	2536	2901	3313
100	2076	2375	2806	3315	3870
120	2123	2535	3100	3755	4457
150	2207	2803	3588	4456	5373
180	2304	3103	4102	5180	
200	2376	3313	4458	5685	
250	2578	3871	5372		
300	2805	4456	6314		
350	3051	5065			
400	3313	5684			
450	3587				
500	3870				

TABLE I

introduced falls within the accuracy of the recordings taken (see section 3.4) - it may be assumed in the calculations for the times of propagation that the earth and the ionosphere are both flat.

The paths followed by the 1-hop, 2-hop and 3-hop propagations are shown in Fig. 16. It can be seen that the distance travelled by the one-hop pulse could be calculated from the formula

$$S = 2\sqrt{h^2 + (L/2)^2}$$

Similarly for the 2-hop and 3-hop pulses the formulae would respectively be

$$S = 4\sqrt{h^2 + (L/4)^2} \quad \text{and} \quad S = 6\sqrt{h^2 + (L/6)^2}$$

Hence a general formula for a N-hop mode is

$$S = 2N\sqrt{h^2 + (L/2N)^2}$$

Thus the times of propagation for 1-hop, 2-hop, 3-hop, 4-hop, etc. pulses could be calculated for different heights of reflection. These values are given in Table I. The curves relating times of propagation and heights of reflection are shown in Fig. 17 (see back cover).

4.15 SUNRISE TIME DELAYS

Ionograms for Grahamstown were used for comparison. These ionograms were extremely helpful for verification of hypotheses derived from the oblique incidence records.

Phenomena connected with sunrise would not be shown on the oblique incidence records and on the Grahamstown ionograms at the same instant. They would be delayed on the Grahamstown ionograms for a short period depending on the sunrise times at Grahamstown and Durban.

The times of sunrise for Grahamstown and Durban for a summer day were obtained in their L.M.T. using a computer program, and were found to be 04.91 (L.M.T.) and 05.04 (L.M.T.) respectively. The difference in longitude between Grahamstown and Durban is 4.7^{o}. Therefore the difference in L.M.T. is 0.31 hours.

When the sun rises in Grahamstown, the L.M.T. in Grahamstown is 04.91 hours. The L.M.T. at this instant in Durban is 04.91 + 0.31 = 05.22 hours. The sun rises in Durban at 05.04 hours L.M.T. Therefore the sun rises in Durban 0.18 hours (i.e. 11 mins.) earlier than in Grahamstown. Hence it is expected that a phenomenon seen on the oblique incidence records would appear on the Grahamstown ionograms within 11 minutes, the actual time delay depending on the mode of propagation. For example, a time delay of 5 or 6 minutes is expected for a 1-hop mode.

A similar calculation for winter showed that the sun rises in Durban 27 minutes earlier than in Grahamstown.

4.2 INTERPRETATION OF RECORDS

The whole experiment was conducted for a single pulse frequency. Pulses of 100 μsec duration at a carrier frequency of 4.73 Mc/s were transmitted. The repetition rate was 10 pulses per second. These were received in Durban and recorded on continuously running 35 mm positive film.

On the film there were about 20 time calibrating markers as well. The time interval between any two of these markers was 100 μsec. Therefore time differences between pulses up to 2000 μsec could be measured.

The first pulse coming through triggered the apparatus. This and the pulses that followed were recorded on the film. Therefore the time delay of any pulse w.r.t. the first pulse could be obtained with the aid of the time markers. In the discussions to follow the triggering pulse is often referred to as the "first pulse". The pulse that has a certain time delay, say 300 μsec for instance, after the first pulse is referred to as the "300 μsec pulse" or "the pulse at 300 μsec." All times are given in S.A.S.T.

Recordings were taken for summer as well as for winter. The summer recordings extend from 19th November, 1964 to 14th January, 1965. Winter recordings were taken for the periods 29th May, 1965 to 31st May, 1965 and 29th June, 1965 to 12th July, 1965.

Detailed analysis of all the recordings would make the discussion far too long. Therefore one summer day and one winter day were chosen for detailed

discussion. The rest of the recordings are given in Appendix I. Interesting phenomena from these recordings are discussed in section 4.23.

4.21 SUMMER DAY (29/12/1964)

Between 00.00 and 00.30 hours (Fig. 18a) three steady pulses appear on the record in addition to the triggering pulse. These pulses have the following time delays after the first pulse:-

600 μsec, 1200 μsec and 1600 μsec.

On following the pulses from the previous day, the 600 μsec pulse could straightaway be recognized as the F-layer reflection. It might be surprising to find that the F-layer reflection still exists long after the extraordinary Pedersen ray had joined the normal ray. However, it is clear from the record that the F-layer reflection does continue to exist. This is also verified by the Grahamstown ionograms. An F-plot drawn for the ionosphere over Grahamstown from 20.30 hours on 28/12/1964 to 01.45 hours on 29/12/1964 (Fig. 20) shows that the critical frequency remains essentially constant at 4.0 Mc/s from 23.00 hours on 28/12/1964 to 00.30 hours on 29/12/1964. Two points seem to be off by 0.05 Mc/s. However, this error is tolerable and falls within the limits of accuracy of the experiment. Therefore a smooth line is drawn through 4.0 Mc/s.

From this it is clear that the vertical incidence equivalent of 4.73 Mc/s must be below 4.0 Mc/s, if the

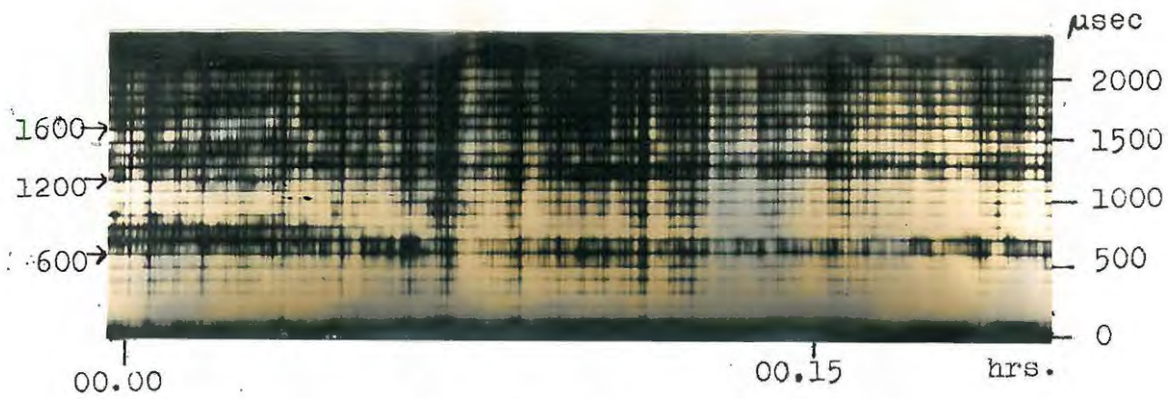

Fig.18(a)

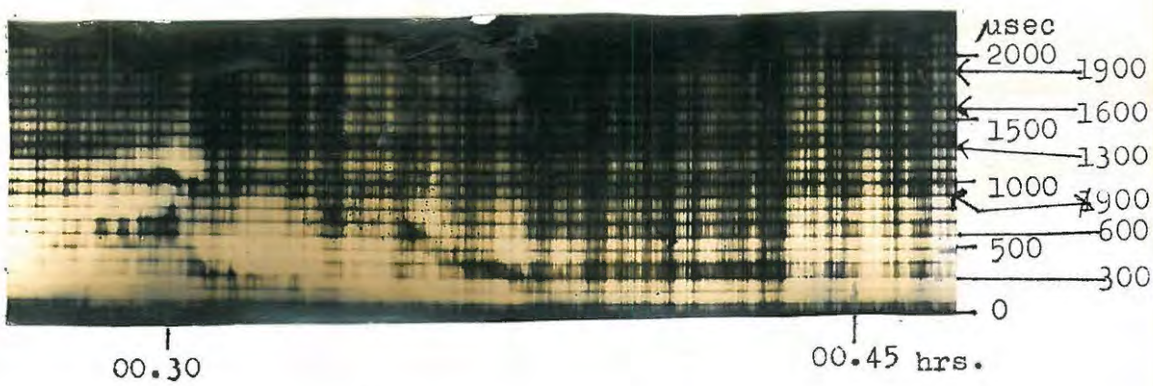

Fig.18(b)

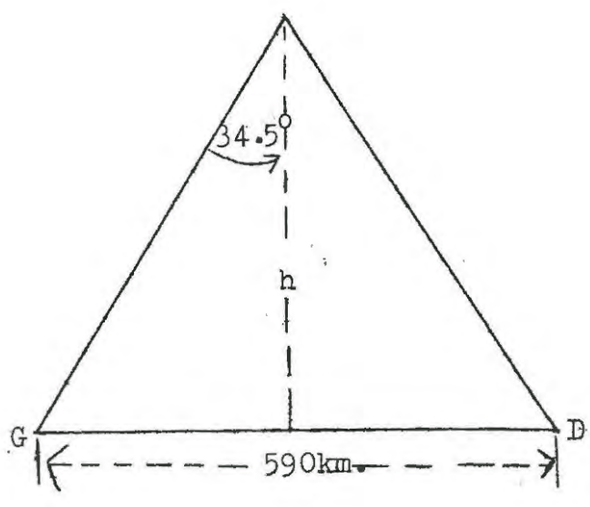

Fig.19

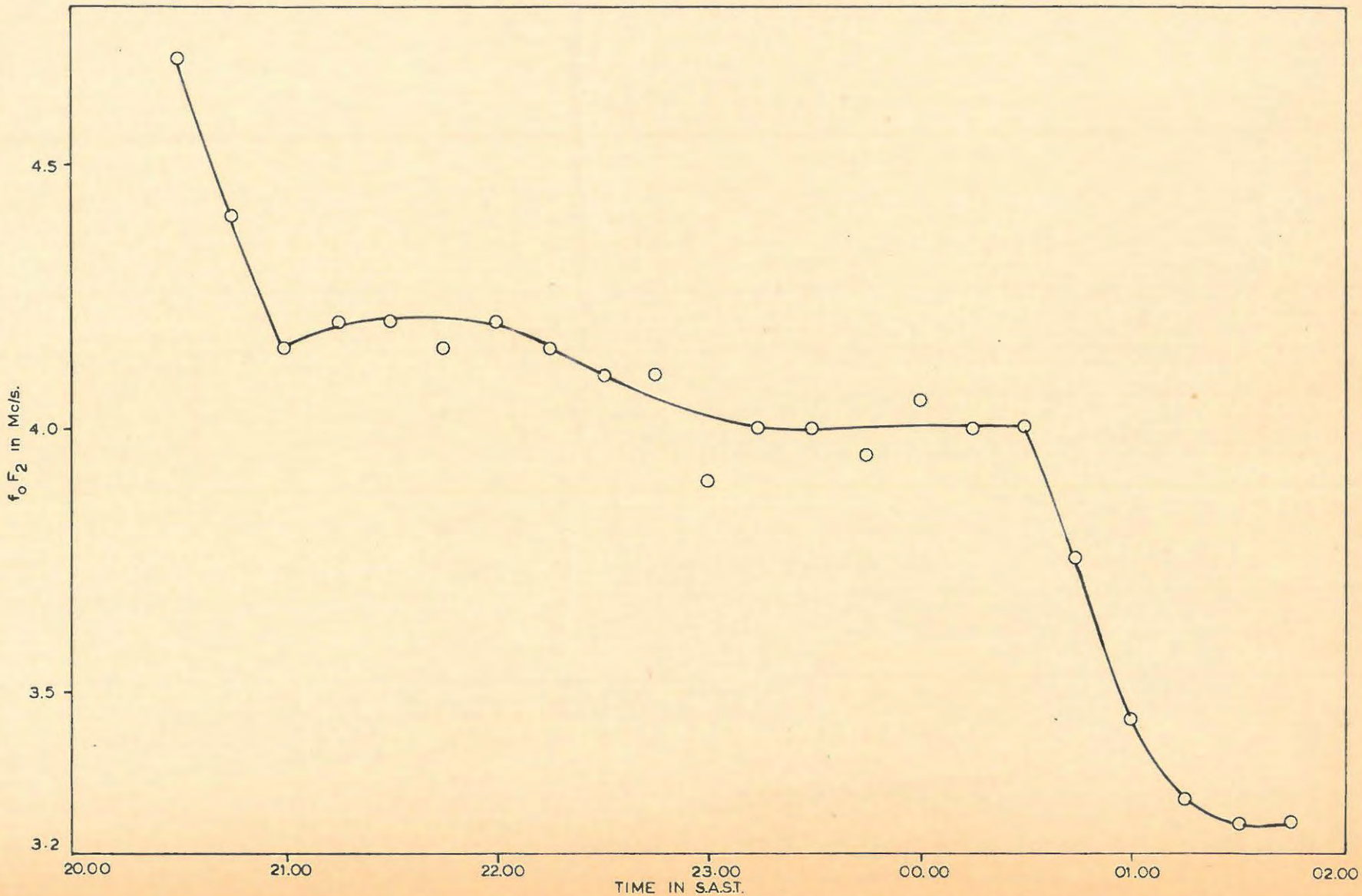

FIG. 20 F-PLOT FOR IONOSPHERE OVER GRAHAMSTOWN

600 μsec pulse is indeed an F-layer reflection. However, it could not be very far below 4.0 Mc/s because the extraordinary Pedersen ray had already joined the normal ray. Therefore it is guessed that the vertical incidence equivalent is 3.9 Mc/s.

If 3.9 Mc/s is the vertical incidence equivalent of the obliquely propagated 4.73 Mc/s, the angle of incidence, ϕ_o, of the latter on the ionosphere is calculated with the aid of the Secant Law as follows:

$$4.73 = 3.9 \sec \phi_o$$

$$\therefore \quad \phi_o = 34.5^\circ$$

The height of reflection of the pulse could easily be determined if Fig. 19 is considered. From the figure, it is clear that if h is the height of reflection,

$$\tan 34.5^\circ = \frac{295}{h}$$

$$\therefore \quad h = 430 \text{ km.}$$

However, on examining the Grahamstown ionogram for 00.15 hours, it is found that the virtual height of reflection for 3.9 Mc/s is 475 km. This disagrees with the value of 430 km obtained, thus violating Martyn's theorem. Therefore the guess of 3.9 Mc/s as the vertical incidence equivalent frequency is wrong.

It is therefore necessary to try another value. This time a figure of 3.8 Mc/s is taken as the vertical incidence equivalent frequency. Application of the Secant Law to this value gives the angle of incidence on the ionosphere as 37°. Hence the height of reflection is obtained as 400 km. On examining the Grahamstown

ionogram for 00.15 hours it is found that the height of reflection for 3.8 Mc/s is exactly 400 km.

If this did not agree another frequency would have to be assumed and the calculations repeated until the correct frequency and the correct height of reflection is obtained.

Now since it is known that the vertical incidence equivalent of 4.73 Mc/s is reflected from 400 km , it may be assumed that this is the height of reflection at the F layer and that the 600 μsec pulse is reflected from this level. Therefore the graph in Fig. 17 gives the time of propagation for the 600 μsec pulse as 3300 μsec. This helps to determine the time of propagation of the first pulse, which would be 3300-600 = 2700 μsec. Fig. 17 gives the only possibility for this time of propagation as a 2-hop from a sporadic-E layer at a height of 140 kilometres. This is given by the graph as having a time of propagation of exactly 2700 μsec. The Grahamstown ionograms give the height of the sporadic-E layer at this time as 135 kilometres which agrees reasonably well with the above calculations.

According to this assumption, the time of propagation of the 1600 μsec pulse would be 2700 + 1600 = 4300 μsec. An examination of Fig. 17 shows that this pulse could only be a 4-hop pulse from the sporadic-E layer at a height of 140 kilometres. It would (according to the graph) then have a propagation time of 4200 μsec. This agrees reasonably well with the time of 4300 μsec given by the record, which is, at best, not well-defined.

The 1200 μsec pulse could be explained if it is assumed that the apparatus is triggered sometimes by the one-hop and sometimes by the 2-hop pulses from the sporadic-E layer. The 1200 μsec pulse seems to appear only when the one-hop pulse triggers the apparatus. The time of propagation of the one-hop pulse is obtained from Fig. 17 as 2150 μsec. Then the 1200 μsec pulse would have a time of propagation of 2150 + 1200 = 3350 μsec. This would be the one-hop F-pulse whose time of propagation is given as 3300 μsec.

Further evidence that the one-hop E_s-pulse triggers the apparatus is given by the appearance of a faint streak at 500 μsec which would be the 2-hop having a propagation time of 2700 μsec, which normally triggers the sweep.

The 3-hop pulse from the E_s layer also seems to be coming through sometimes. This pulse, which has a propagation time of 3400 μsec, would have time delays of 1250 μsec when the one-hop pulse triggers the apparatus and 700 μsec when the 2-hop pulse does so. Faint impressions of this pulse are seen at the above times in the original record.

At 00.30 hours there is a sudden disappearance of the F-layer reflection pulse (see Fig. 18b). This is caused by the abrupt drop of the plasma frequency to below 3.8 Mc/s. The F-plot (Fig. 20) indicates that this happens at Grahamstown between 00.30 and 00.40 hours which agrees very well with the oblique incidence records.

Between 00.30 and 00.36 hours no measurements could be taken. There appear to be rapid changes in triggering pulses and a drop in the heights of reflection as shown in Fig. 18b.

The pulses settle down at 00.36 hours (Fig. 18b). In addition to the triggering pulse, pulses with the following time delays (in μsec) appear on the record:-

300, 600, 900, 1300, 1600, 1900.

The F-layer critical frequency is low now. Therefore only reflections from the sporadic-E layer are expected. The impression given by the record is that the E_s layer has dropped to 105 kilometres, since the time delays fit into the calculations if this height is assumed to be the height of reflection.

If it is assumed that the triggering pulse is a one-hop from the E_s layer at 105 kilometres, then it would have a time of propagation of 2100 μsec as given by Fig. 17. Therefore the 300 μsec pulse would have a propagation time of 2100 + 300 = 2400 μsec. The graph in Fig. 17 identifies this as a 2-hop from the same layer with a propagation time of 2400 μsec.

The 900 μsec pulse which has a propagation time of 2100 + 900 = 3000 μsec seems to fit reasonably well as a 3-hop from the same layer with a theoretical propagation time of 2900 μsec.

A 4-hop pulse, according to Fig. 17, would have a time of propagation of 3400 μsec. Calculation from the record gives this as the time of propagation for the 1300 μsec pulse (2100 + 1300 = 3400 μsec). Hence the

1300 μsec pulse could be identified as a 4-hop from the E_s layer at 105 kilometres.

The only possible identification for the 1900 μsec pulse is that it could be a 5-hop pulse from the E_s layer. Such a pulse would have a propagation time of 4000 μsec (see Fig. 17). This agrees very well with the time delay of 1900 μsec obtained which gives the time of propagation as exactly 4000 μsec.

The pulses still unidentified are the 600 and 1600 μsec pulses. They do not fit into the present pattern. However, if the recording is examined very closely, it could be noticed that they appear strongly but intermittently. This leads one to assume that at times the 300 μsec (2-hop E_s) pulse triggers the apparatus. During these times the 900 and 1900 μsec pulses drop to 600 and 1600 μsec respectively. Additional evidence of this is brought forward by the broad appearance of the 900 μsec pulse. What actually happens is that the 1300 μsec pulse drops to 1000 μsec, giving the impression that the 900 μsec pulse is broad. All pulses disappear after 01.30 hours.

Ionograms for Grahamstown indicate that there is a strong sporadic-E layer at this time and several multiple reflections from this layer are evident. Grahamstown ionogram for 01.45 hours is reproduced in Fig. 21. It indicates multiple sporadic-E reflections. However, this ionogram indicates that the sporadic-E layer reflects from a height of 130 km , but the pulses on the oblique incidence records could not be explained if this height is assumed.

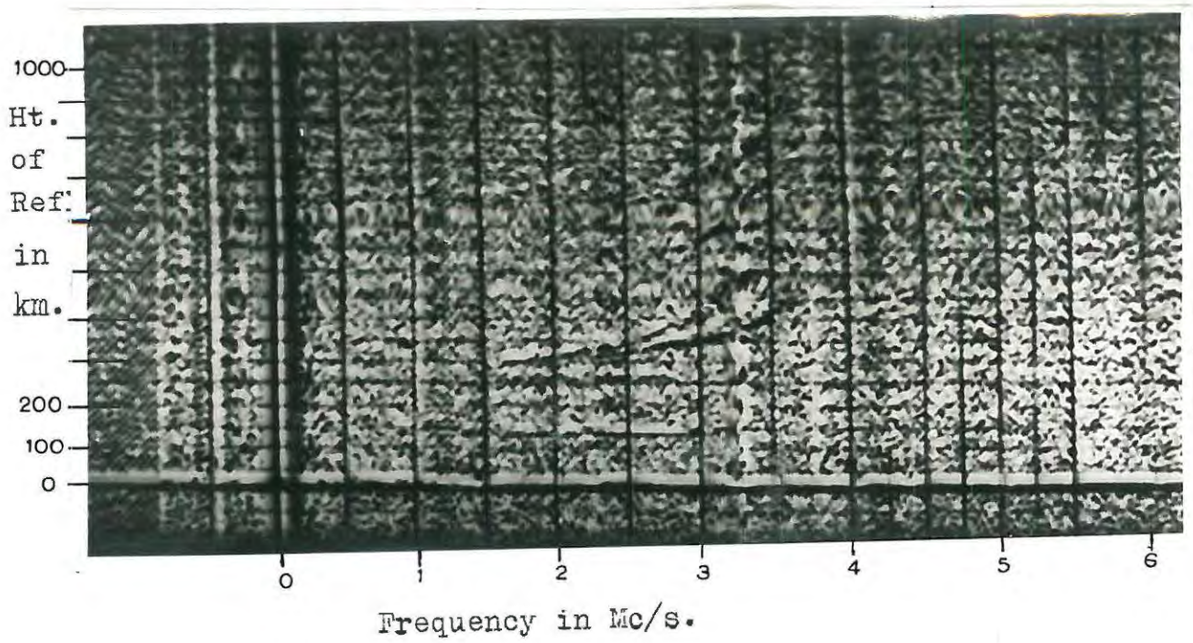

Fig.21

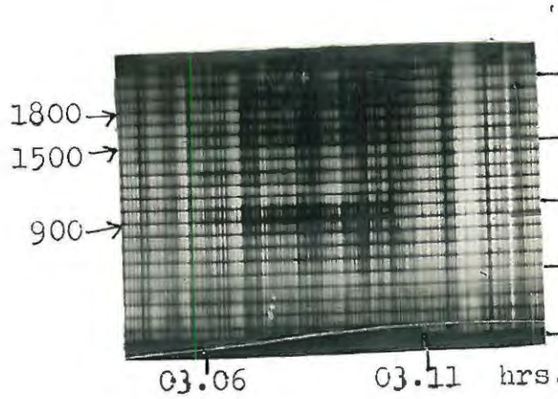

Fig.22

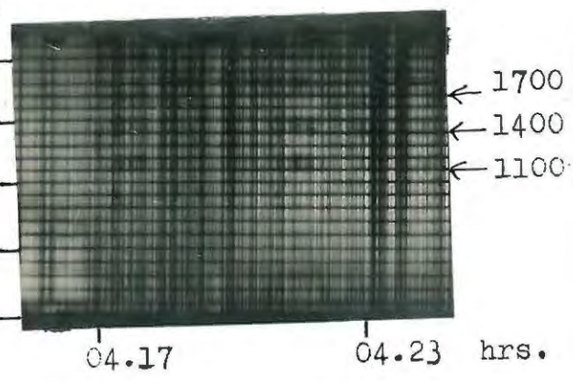

Fig.23

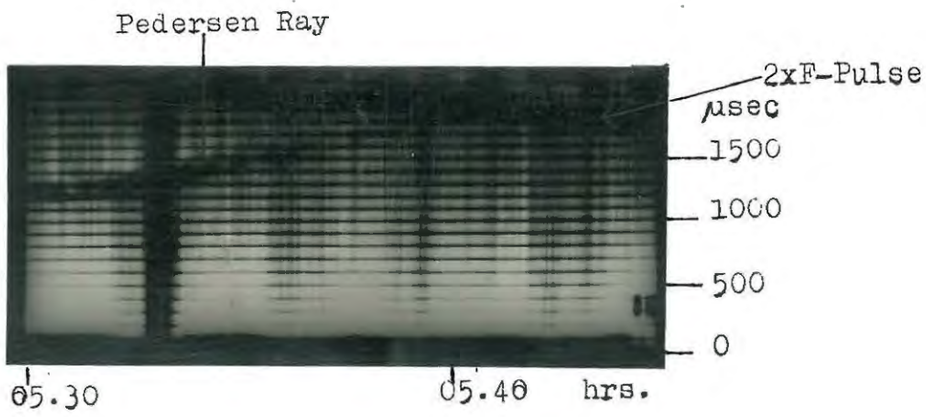

Fig. 25

The only height of reflection which could be used in explaining the pulses is 105 km. This discrepancy remains a puzzle. It is possible that the height may be different at the oblique incidence reflection areas.

At 03.06, three steady pulses are seen for a short period of 5 minutes (Fig. 22). Their respective time delays after the first pulse are 900, 1500 and 1800 μsec. In addition there are faint impressions of pulses at 300 and 1200 μsec.

Proof that there are no F-layer reflections is offered by the Grahamstown ionograms. The critical frequency for the F layer at Grahamstown at 03.15 hours is given as 3.1 Mc/s. The frequency of the oblique incidence transmission is 4.73 Mc/s. From the Secant Law, $f_{ob} = f_v \sec \phi_o$, it is seen that the minimum value sec ϕ_o could have is 1.5, where ϕ_o is the angle of incidence of the 4.73 Mc/s pulses on the ionosphere. Therefore the minimum value of ϕ_o is 49°. If the pulses are incident at angles smaller than this, they would penetrate the ionosphere. This sets an upper limit to the virtual height of reflection at about 250 km which is well below the value of $h'F_2$ (280 km) obtained from the Grahamstown ionograms for this time. Therefore it is impossible to get propagation via the F region. Hence it could be concluded that the pulses are reflected from the sporadic-E layer.

If it is assumed that the 2-hop from the E_s layer at a height of 100 km is the triggering pulse, then the 900 and 1500 μsec pulses would respectively be the 4-hop

and 5-hop pulses from the same layer. The times of propagation for the 2-hop, 4-hop and 5-hop pulses are respectively 2380, 3310 and 3870 μsec. This gives the time delays of the 4-hop and 5-hop pulses relative to the 2-hop as 930 and 1490 μsec respectively, which agree very well with the time delays shown on the record.

The one-hop pulse with a time of propagation of 2080 μsec seems to trigger the apparatus as well. This results in the 4-hop pulse appearing at 1200 μsec and the 5-hop at 1800 μsec. In addition, the fact that the one-hop does come through is substantiated by a faint line at 300 μsec. This would be the 2-hop when the one-hop triggers the apparatus.

The record shows from the intensities of the different pulses that the one-hop pulse is very weak and that the 2-hop triggers the apparatus much more often than one-hop.

Pulses very similar to the above appear on the record for 04.17 hours (Fig. 23). These last for 6 minutes. The time delays for the different pulses are 1100, 1400 and 1700 μsec. The height of reflection appears to be 110 km. If it is assumed that the 2-hop pulse reflected from this height triggers the apparatus most of the time, the 1100 and 1700 μsec pulses would respectively be the 4-hop and 5-hop pulses from the same layer. The time delays claculated from the graph in Fig. 17 agree very well for this hypothesis.

When the one-hop pulse triggers the apparatus, the

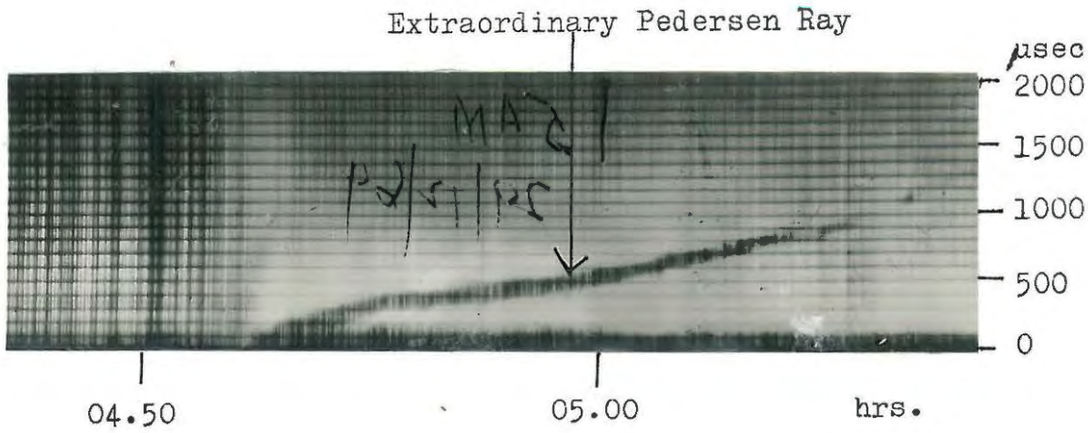

Fig.24(a)

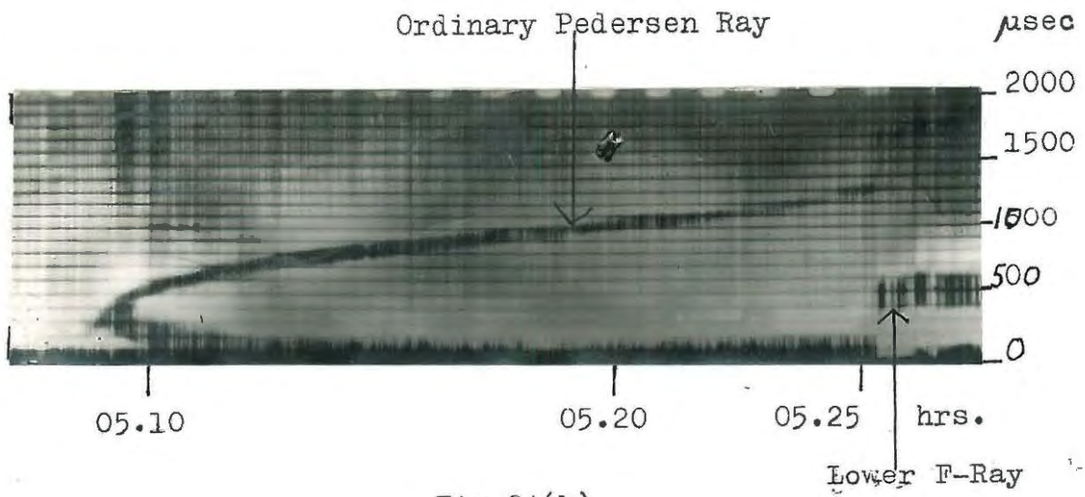

Fig.24(b)

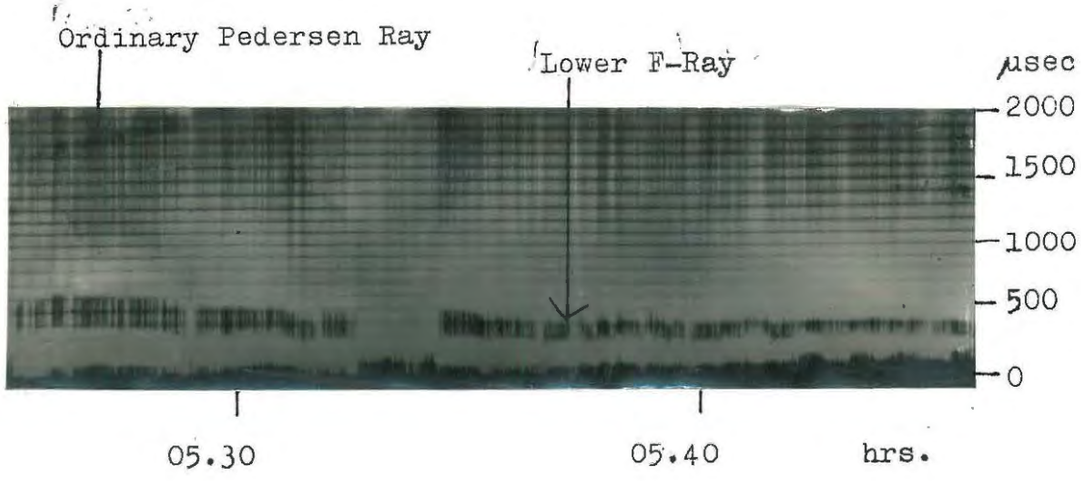

Fig.24(c)

5-hop pulse appears as a faint trace at 2000 μsec and the 4-hop appears at 1400 μsec. This again could be verified with the aid of Fig. 17. So in effect, two weak pulses, the one-hop and 2-hop, and two strong pulses, the 4-hop and the 5-hop, were received.

The above explanation, if true, indicates that the sporadic-E patch must have covered most of the region between Grahamstown and Durban. Since multiple reflections such as 4-hop and 5-hop pulses appear and disappear simultaneously it is presumably in the middle part of the region that the sporadic-E layer forms and controls the propagation.

At 04.52 hours the extraordinary ray of the F_2 layer makes its appearance (Fig. 24a). This is an indication that the electron density in the F_2 region is increasing due to the ultraviolet radiation of the sun being incident on it. When the electron density in the F_2 layer reaches a value such that 4.73 Mc/s is the MUF between Grahamstown and Durban for the extraordinary ray, pulses start arriving in Durban.

The Grahamstown ionogram for 05.00 hours indicates that the critical frequency for the extraordinary ray is 3.75 Mc/s. Therefore sec ϕ_o is given by

$$\sec \phi_o = \frac{4.73}{3.75} \qquad \text{(Secant Law)}$$

where ϕ_o is the angle of incidence of the oblique ray on the ionosphere. ϕ_o works out to be 37.5°. Assuming the pulse is a one-hop from the F_2 layer, the height of reflection is given by a diagram similar to Fig. 19 as

$$h = \frac{295}{\tan 37.5} = 385 \text{ km.}$$

The delay in diurnal variations between the point of reflection of the obliquely incident pulses (Umtata) and Grahamstown is 5 or 6 minutes (see section 4.15). This means that the height of reflection of the equivalent vertical frequency (3.75 Mc/s) should be 385 km at Grahamstown at 04.58 hours.

When the ionograms for Grahamstown are examined, it is found that 3.75 Mc/s is the critical frequency for the extraordinary ray at 05.00 hours. Thereafter the height of reflection of the extraordinary component drops rapidly to 330 km by 05.15 hours. It is therefore highly probable that the height of reflection was 385 km just after 05.00 hours. This is in good agreement with the oblique record. The error of a few minutes is negligible.

The extraordinary ray splits up and the lower ray triggers the apparatus while the Pedersen ray rises. The Pedersen ray is soon absorbed.

At 05.09, the ordinary ray begins to be reflected from the F region (Fig. 24b). The time delay of this ray relative to the extraordinary ray, which is now being reflected from 330 kilometres (as shown by Grahamstown ionograms), is 300 μsec. The time of propagation of the extraordinary ray, according to Fig. 17, is 2950 μsec. Therefore the time of propagation of the ordinary ray would be 2950 + 300 = 3250 μsec. The height of reflection would therefore be 390 kilometres, which agrees very well with the height of reflection obtained for the extraordinary ray at the MUF. The heights of reflection of

the extraordinary and ordinary rays at the MUF are generally the same, since both occur at the peak of the F_2 layer. Fig. 27a and Figs. 33a and 33b verify this.

If 390 km is assumed to be the height of reflection, the angle of incidence of the ordinary ray on the ionosphere is also given as 37.5°. The vertical incidence equivalent of 4.73 Mc/s at this angle of incidence is 3.75 Mc/s (by Secant Law).

If a vertical incidence ionogram were obtained at the point midway between Grahamstown and Durban (i.e. at Umtata) at 05.09 hours, the f_oF_2 would be expected to be 3.75 Mc/s. It is recalled that the time delay between Umtata and Grahamstown is 5 or 6 minutes. Therefore 3.75 Mc/s is expected to be the critical frequency for Grahamstown at 05.15 hours. The Grahamstown ionograms indicate that the f_oF_2 passes this value between 05.15 and 05.30 hours, which correlates very well with the oblique incidence records.

The ordinary ray also splits up and the lower ray joins the extraordinary ray while the Pedersen ray rises. At 05.25 hours the Pedersen ray has a time delay of 1250 μsec w.r.t. the lower ray (see Fig. 24b). At this instant the Pedersen ray jumps to 1650 μsec and a new pulse appears at 400 μsec.

It is clear from the record that another pulse is triggering the apparatus. The record shows that the time delay between the original triggering pulse (i.e. the lower F-ray) and the original position of the Pedersen ray on the record is exactly the same as the

time delay between the new 400 μsec pulse and the new position of the Pedersen ray (i.e. 1250 μsec). The apparatus is being triggered by a pulse with a shorter propagation time which could only be an E-layer pulse. The lower and upper rays are now the 400 and 1650 μsec pulses respectively. In other words all pulses have shifted up by 400 μsec and if the film is cut at 05.25 hours and shifted down by 400 μsec a true picture of the F-reflection pulses would be obtained.

The existence of the normal E layer is not shown in the Grahamstown ionograms until 05.45 hours. However, a sporadic-E layer comes up at 05.30 hours. If it is assumed that the triggering pulse is a 2-hop from the sporadic-E layer at a height of 100 km , its time of propagation would be 2375 μsec (see Fig. 17). Then the time of propagation of the lower F-ray would be 2375 + 400 = 2775 μsec. This gives the height of reflection from the graph in Fig. 17 as 290 km. The angle of incidence for this height of reflection is 45°. The vertical incidence equivalent of 4.73 Mc/s for an angle of incidence of 45° is found to be 3.3 Mc/s. The Grahamstown ionogram for 05.30 hours gives the height of reflection for 3.3 Mc/s as 300 kilometres which agrees very well with the height of reflection of the oblique rays.

At 05.33 hours the 400 μsec pulse disappears for 2 minutes and the triggering pulse is very broad (see Fig. 24c). This indicates that the sporadic-E layer pulse is weak and the apparatus is triggered for this

short period by the F-pulse.

The F-layer pulse has its time delay varying between 300 and 400 μsec up to 06.46 hours. Hence its time of propagation varies between 2675 and 2775 μsec. Therefore the height of reflection varies between 270 km and 295 km.

At 06.34 hours, when the height of reflection of the F-pulse appears to be 270 km, a new pulse is seen at 1800 μsec. This pulse is very weak and could be seen clearly only for about 4 minutes. However, there are indications that it has been dropping from a higher level before this.

There are two possibilities for this pulse. One is that it might be a Pedersen ray. If it was a Pedersen ray, then the electron density in the F_2 layer would be decreasing; otherwise the Pedersen ray would not drop. However, the ionograms for Grahamstown show a steady increase in the critical frequency until it reaches 8.7 Mc/s at 11.30 hours. Therefore it is impossible that this pulse is a Pedersen ray.

The other possibility is that it could be a 2-hop from the F_2 layer. It has a time delay of 1800 μsec after the triggering pulse. Therefore its time of propagation would be 2375 + 1800 = 4175 μsec. This gives the height of reflection for a 2-hop pulse as 280 km (see Fig. 17). The vertical incidence equivalent of a 2-hop pulse reflected at this height is 4.2 Mc/s. The Grahamstown ionogram for 06.45 hours gives the height of reflection for 4.2 Mc/s as 285 km which agrees very well

with the value obtained above. Hence it is highly probable that the new pulse is a 2-hop from the F_2 layer.

Further evidence that such a pulse is a 2-hop is given in the record taken on 23/12/64 at 05.30 hours (see Fig. 25). Here the Pedersen ray rises from 1200 μsec at 05.30 hours to 1500 μsec at 05.37 hours. In the meantime the 2 x F-pulse starts with a time delay of 2000 μsec at about 05.35 hours and drops to 1750 μsec by 05.45 hours. The existence of both these pulses simultaneously on the record simplifies the identification of the new pulse which could otherwise be mistaken to be a Pedersen ray.

After 06.46 hours the one-hop F-layer pulse appears intermittently until 07.44 hours when it disappears completely. No pulses were received for the rest of the day. This is expected from the high absorption that takes place during the summer months, considering that the transmitter gave only 2 KW output. With a more powerful transmitter, it might have been possible to get pulses in Durban during the day.

The pulses were again received late at night when the absorption was low. At 21.43 hours two pulses appear on the record with the following time delays relative to the first pulse:

600 and 1700 μsec.

On following these pulses, it is found that they merge at 22.20 hours (see Fig. 26a). This helps to identify them quite easily. The 600 μsec pulse would be the lower F-ray and the 1700 μsec pulse could be identified

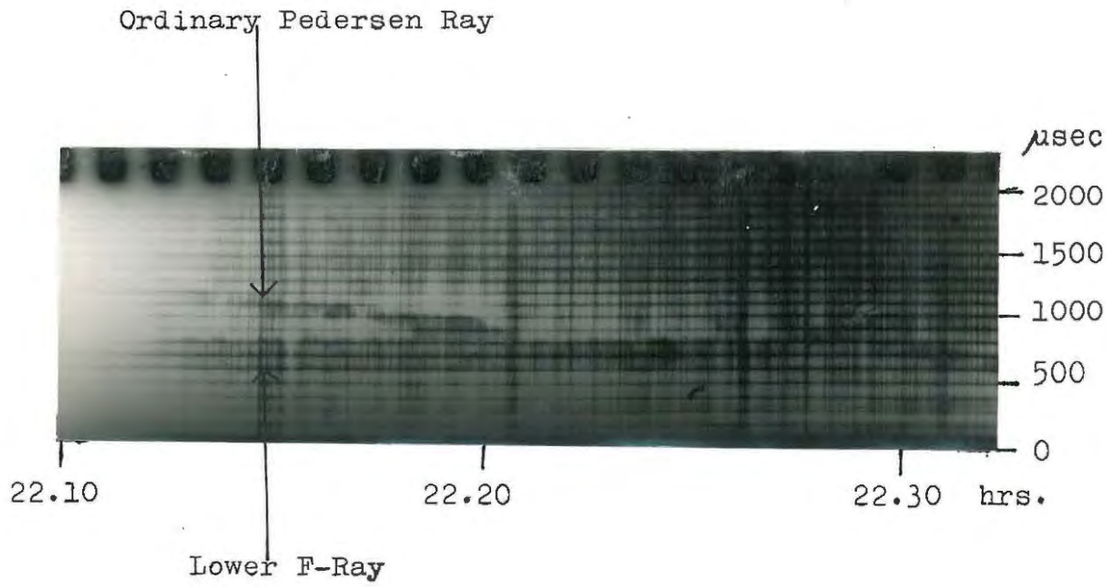

Fig.26(a)

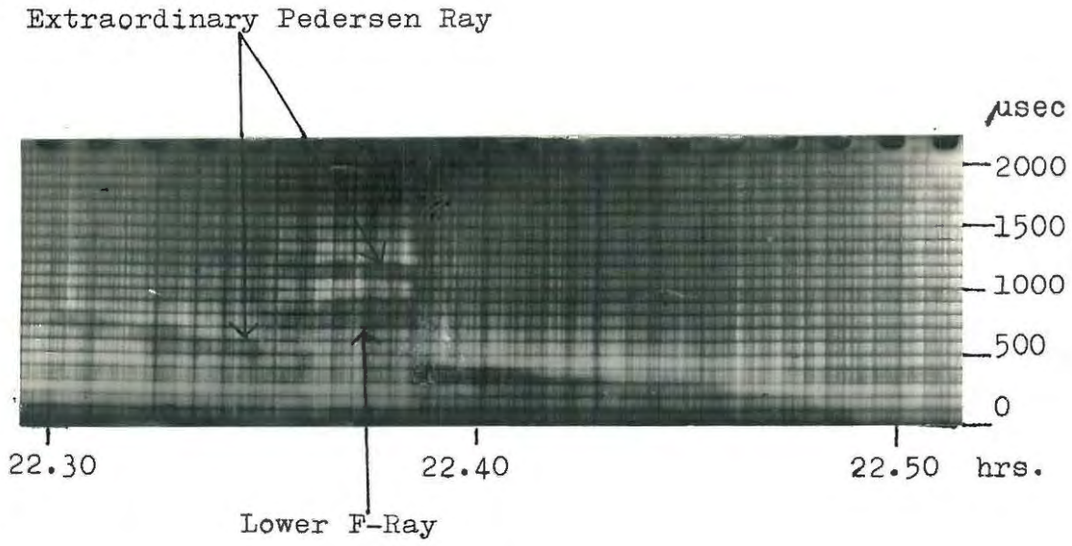

Fig.26(b)

as the ordinary Pedersen ray (the extraordinary Pedersen ray joins the lower ray later). These are both one-hop - if they are assumed to be 2-hop, the time delays do not fit into the calculation at the time when the ordinary critical frequency is reached.

The identification of the triggering pulse is made easy if the Grahamstown ionograms for this time are examined. They show clearly the existence of a steady sporadic-E layer at a height of 130 km. If it is assumed that the triggering pulse is a 2-hop from this layer, then its time of propagation is given by Fig. 17 as 2600 μsec. Therefore the propagation time for the lower F-ray would be 2600 + 600 = 3200 μsec. This gives the height of reflection as 380 km (see Fig. 17). The vertical incidence equivalent of 4.73 Mc/s reflected from this height is 3.73 Mc/s (by the Secant Law). Grahamstown ionograms give the height of reflection of 3.73 Mc/s at 21.45 hours as 390 km which agrees very well with the value obtained.

The lower F-ray continues to be reflected from 380 km while the Pedersen ray drops in height very gradually until both rays merge at 22.20 hours. This indicates that the critical frequency for the ordinary ray is reached. The vertical incidence equivalent of 4.73 Mc/s reflected from 380 km has already been found to be 3.73 Mc/s. When the Grahamstown ionograms are examined, it is found that the F-layer critical frequency passes through 3.73 Mc/s between 22.00 and 22.30 hours. The time of 22.20 is well within this range. As the

critical frequency drops very slowly, the ordinary F-layer reflections are received from the peak of the layer for a longer period than expected, rather as during the morning of the same day. It could be assumed that the extraordinary lower ray is together with the ordinary ray and both are having the same time delay. Grahamstown ionograms do verify that the f_oF_2 is dropping very slowly.

At 22.26 hours there is a sudden change (see Fig. 26a). The 600 μsec pulse disappears and only one pulse remains, which triggers the apparatus. It might have been mistaken that the F-pulse disappeared and the E_s-pulse remained had it not been for the appearance of the extraordinary Pedersen ray immediately after this. The Pedersen ray starts with a time delay of 800 μsec at 22.28 hours and drops in height to join the triggering pulse at 22.49 hours (Fig. 26b). It is known that at the MUF the height of reflection of the ordinary ray is the same as the height of reflection of the extraordinary ray. Therefore it would not be wrong to assume that the height of reflection now is 380 km. This gives the vertical incidence equivalent frequency as 3.73 Mc/s. From the delay in diurnal variations between Umtata and Grahamstown, 3.73 Mc/s would be expected to be the f_oF_x for Grahamstown at 22.49 + 00.06 = 22.55 hours which seems a possible time according to the ionograms for Grahamstown. (The ionograms give f_oF_x for 22.45 hours as 3.8 Mc/s and for 23.00 hours as 3.7 Mc/s).

In the meantime a sudden change had taken place at

22.35 hours for 4 minutes (see Fig. 26b). The original pulses which were identified as the lower and the Pedersen rays disappeared and the record showed two pulses with time delays of 700 and 1100 μsec w.r.t. the triggering pulse.

If the 700 μsec pulse were shifted down to where the triggering pulse is, then the 1100 μsec pulse would fit very well in that part of the film where the Pedersen ray is missing. Therefore it may be correct to say that the sporadic-E layer pulses have become strong enough to trigger the apparatus. The lower F-ray being reflected from a height of about 380 km has a time of propagation of 3200 μsec. Therefore the time of propagation of the triggering pulse would be 3200 - 700 = 2500 μsec. Fig. 17 shows that the only possibility for this pulse is a 2-hop from the E_s layer at a height of 115 km.

Although Grahamstown ionograms do not show any sign of sporadic-E at this time, nevertheless, it is possible that this short period of ionization in the E layer is caused by meteors and / or ionospheric wind-shear. The pulses disappear at 22.49 hours.

From 22.50 hours to midnight three more or less steady pulses appear on the record with the following time delays:-

300, 900 and 1700 μsec.

Though not as many, these pulses are very similar to those obtained the previous night at 00.36 hours. The conditions are almost identical too, i.e. the F-layer

critical frequency has dropped and no reflection from this layer is possible. Therefore they could be explained as the sporadic-E layer reflections. If it is assumed that the triggering pulse is a one-hop from the E_s layer at a height of 110 km, then the 300 and 900 μsec pulses fit reasonably well as the 2-hop and 3-hop pulses from the same layer. The possible identifications are given in Table II

Pulse	Time Delays	Propagation Times	
		From Record	From Fig. 17
1-hop	0	2100	2100
2-hop	300	2400	2450
3-hop	900	3000	2950
4-hop	1700	3800	3550

TABLE II

It is seen from Table 2 that if the fourth pulse is assumed to be a 4-hop, there is an error of 250 μsec which is far too high compared with the normal error of 50 μsec allowed in this experiment.

However, if it is assumed that the apparatus is sometimes triggered by the 2-hop pulse, the 1700 μsec pulse fits very well as a 5-hop pulse. If the 2-hop pulse is triggering the apparatus, then the time of propagation of the 1700 μsec pulse would be 2400 + 1700 = 4100 μsec. According to Fig. 17, the 5-hop pulse reflected from 110 km would have a propagation time of 4150 μsec. This agrees well with the value of 4100 μsec obtained above.

4.22. WINTER DAY (11/7/65)

There is no indication of any pulse on the records from midnight (00.00 hours) to 07.45 hours. Grahamstown ionograms for this period verify that it is impossible to get 4.73 Mc/s propagation between Grahamstown and Durban. The value of f_0F_2 remains below 2.7 Mc/s. (It is found to be between 2.4 and 2.6 Mc/s most of the time.) This gives the minimum value of sec ϕ_0 as 1.75; hence the minimum value of ϕ_0 is 55^o, where ϕ_0 is the angle of incidence of the oblique rays on the ionosphere. This sets an upper limit to the height of reflection to about 200 km, which is well below the $h'F_2$ values (the $h'F_2$ values vary between 230 and 270 km). In other words, Durban lies in the skip distance from Grahamstown. There is also no evidence of a sporadic-E layer on the ionograms.

From about 07.45 hours, a triggering pulse appears on the record. Since it is the only pulse, none of the usual measurements could be carried out. Nevertheless it would be correct to assume this to be an E-layer reflection because the record shows that the F-layer MUF between Grahamstown and Durban only reaches 4.73 Mc/s at 08.32 hours. In addition ionograms for Grahamstown indicate a sporadic-E layer at 07.00 hours and normal E layer at 07.30 hours. The pulse gets stronger and broader after 08.00 hours, attaining a pulse-width of over 200 μsec.

The second pulse makes its appearance at 08.32 hours when the electron density in the F region has increased

sufficiently such that the MUF for the extraordinary pulse propagated between Grahamstown and Durban attains the value of 4.73 Mc/s (see Fig. 27a).

The time delay between the triggering pulse and the F-layer reflection at 08.32 hours is 800 μsec. On examining the ionograms for Grahamstown it is seen that the height of reflection of the normal E and the sporadic-E layers is approximately 115 km. Since the time delay between the triggering pulse and the F-layer reflection is high (800 μsec), it may be assumed that the triggering pulse is a 1-hop reflected from a height of 115 km. Fig. 17 gives the time of propagation of this pulse as 2125 μsec. Therefore the time of propagation of the F-pulse would be 2125 + 800 = 2925 μsec. Hence the height of reflection is 325 km (see Fig 17). Calculation gives the angle of incidence of the pulses on the ionosphere to be 42°. Using this value in the Secant Law, the vertical incidence equivalent of 4.73 Mc/s is found to be 3.5 Mc/s. However, Grahamstown ionograms show that the f_xF_2 passes 3.5 Mc/s between 07.00 and 07.15 hours, whereas it would be expected to occur at 08.45 hours.

The noted difference in time of more than one hour (about 90 mins) appears throughout the winter records. This anomaly has not been explained with the facts so far known.

The Pedersen ray splits off from the normal ray and rises until it reaches a time delay of 1400 μsec at 08.38 hours, after which it disappears. Meanwhile

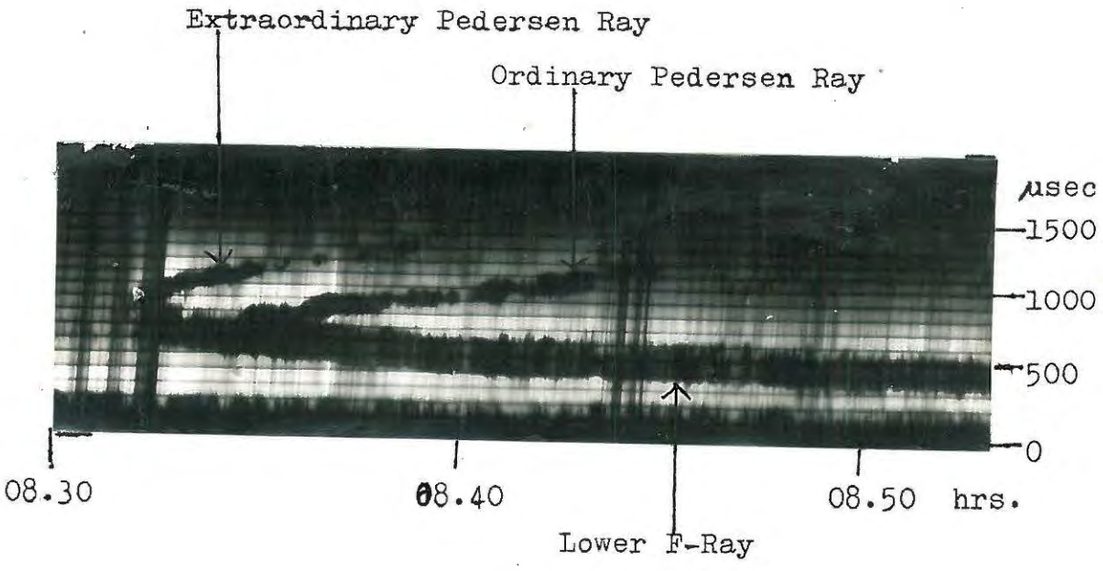

Fig.27(a)

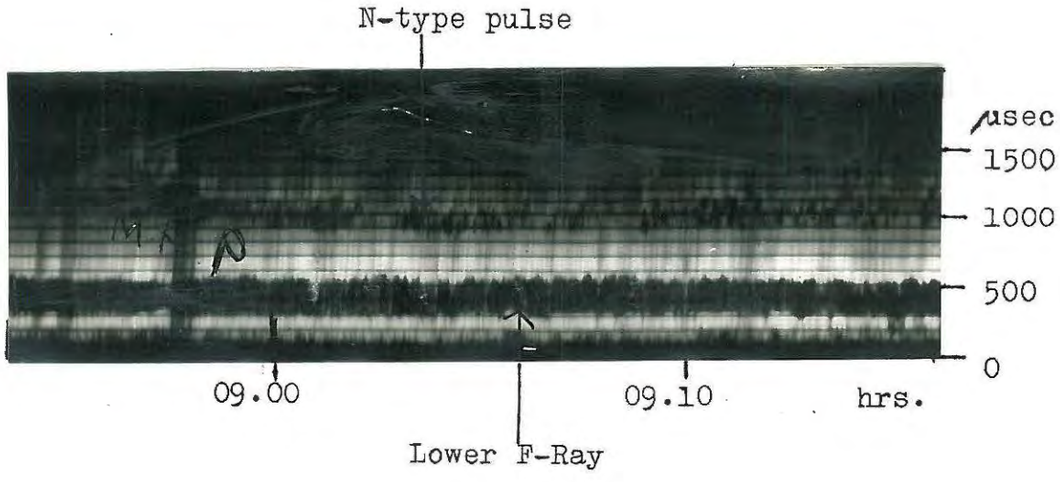

Fig.27(b)

at 08.34 hours, the ordinary Pedersen ray splits off from the normal ray (Fig. 27a). It is seen from the record that the heights of reflection for the ordinary and extraordinary rays at their respective MUFs are equal. Thus it may be concluded that the vertical incidence equivalent frequency of the ordinary 4.73 Mc/s is 3.5 Mc/s. Again whereas f_0F_2 is expected to pass 3.5 Mc/s at 08.47 hours, it does so about 90 minutes earlier.

The Pedersen ray rises and is completely absorbed at 08.45 hours. The height of reflection of the lower ray decreases and attains a steady value at 09.00 hours, when the time delay is 350 μsec. This gives the height of reflection as 230 km which is in good agreement with the Grahamstown ionograms. (These show that after 09.00 hours $h'F_2$ varies between 230 km and 250 km).

The normal F-layer pulse continues to be reflected from about 230 km until 11.00 hours. Of course there are fluctuations in time delays up to 100 μsec w.r.t. the first pulse. This could be attributed to the variation in the height of reflection of the F layer.

After 11.00 hours, the F-layer pulse is seen not as a continuous line but as broken lines developing into widely separated "spots". This is an indication that the pulse is weakening, presumably as a result of absorption in the ionosphere. These spots disappear after 12.35 hours.

In the meantime a poorly defined pulse starts at about 08.50 hours with a time delay of 1000 μsec (see Fig. 27b). The pulse drops rapidly to 900 μsec and

remains at this value until it disappears at 09.30 hours. When it has a time delay of 900 μsec, its time of propagation is 2125 + 900 = 3025 μsec. No mode of propagation shown in Fig. 17 seems to give a value anywhere near the time of 3025 μsec.

On calculating it is found that this pulse fits in as a N-type propagation with one hop on the F layer at a height of 230 km and the other hop on the E layer at a height of 115 km. This mode would have a path length of about 900 km. Hence the time of propagation is 3000 μsec, which is very close to the value of 3025 μsec given by the record. The weak nature of the pulse could be attributed to the partial penetration of the E layer.

Further examination of the record reveals that from about 11.00 hours to about 12.00 hours a fairly steady pulse with a large time delay occurs on the upper edge of the film. The pulse starts at 1700 μsec rises to 1800 μsec, remains at this value for a while, then drops to 1600 μsec before it disappears. It is seen to be a weak pulse. Grahamstown ionograms indicate that the E layer has dropped to 110 km after 10.30 hours. Hence the time of propagation for the E-pulse would be 2100 μsec. Therefore the time of propagation of the new pulse varies between 3700 and 3900 μsec. Fig. 17 identifies this pulse as a 2-hop from the F layer at a height varying between 235 and 250 km. Such a mode seems possible according to the Grahamstown ionograms, which give the $h' F_2$ values as varying between 230 and 240 km during this period.

Between 15.40 hours and 17.20 hours many pulses with rapidly varying time delays are seen (see. Figs. 28. a, b, c, d, e). This part of the film obviously requires very careful analysis. Nevertheless, if Grahamstown ionograms for this period are thoroughly investigated and a clear picture of the ionosphere over Grahamstown is obtained the analysis is considerably simplified.

Careful examination of the record indicates that in addition to the triggering pulse, there is a steady pulse which had started faintly at about 14.20 hours with a time delay of 475 μsec w.r.t. the first pulse. The height of reflection then very gradually decreases until the pulse is at 400 μsec at about 16.10 hours. Thereafter it remains at this value, disappearing at 17.20 hours.

Grahamstown ionograms indicate the existence of a sporadic-E layer which drops in height from 125 km at 13.15 hours to 115 km at 15.15 hours and remains at 115 km until it disappears at 16.15 hours. Taking into account the normal delays obtained between the oblique records and Grahamstown ionograms, it is found that this pulse could be identified as a sporadic-E layer reflection. Further corroboration is provided by the fact that this pulse does not follow the rapid variations that occur in the F region during this period.

An attempt to identify the triggering pulse as a 2-hop from the normal E layer meets with no success as

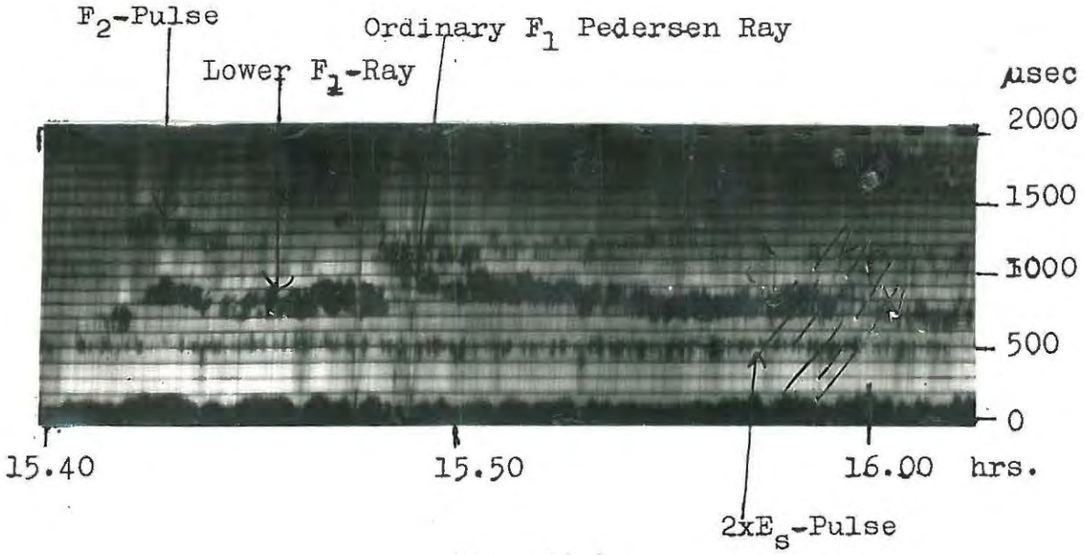

Fig.28(a)

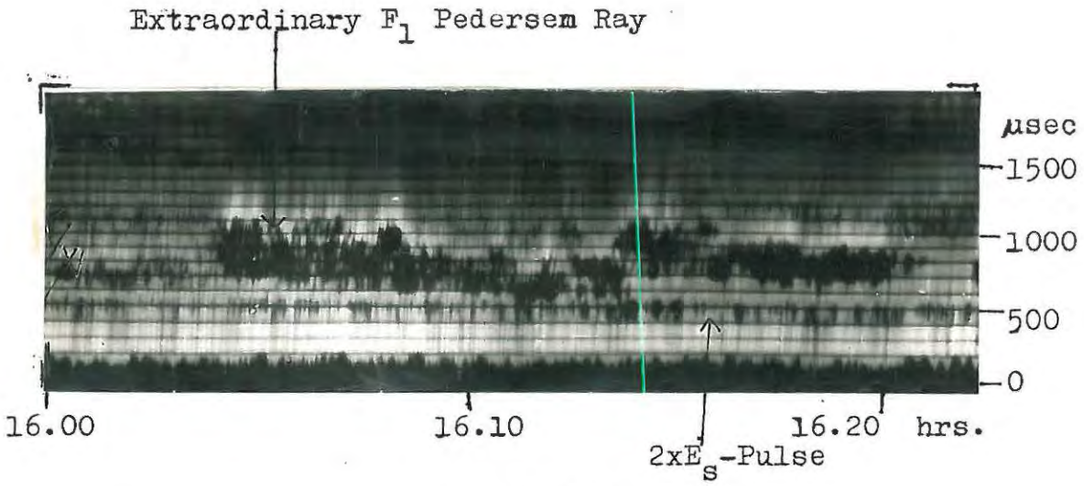

Fig.28(b)

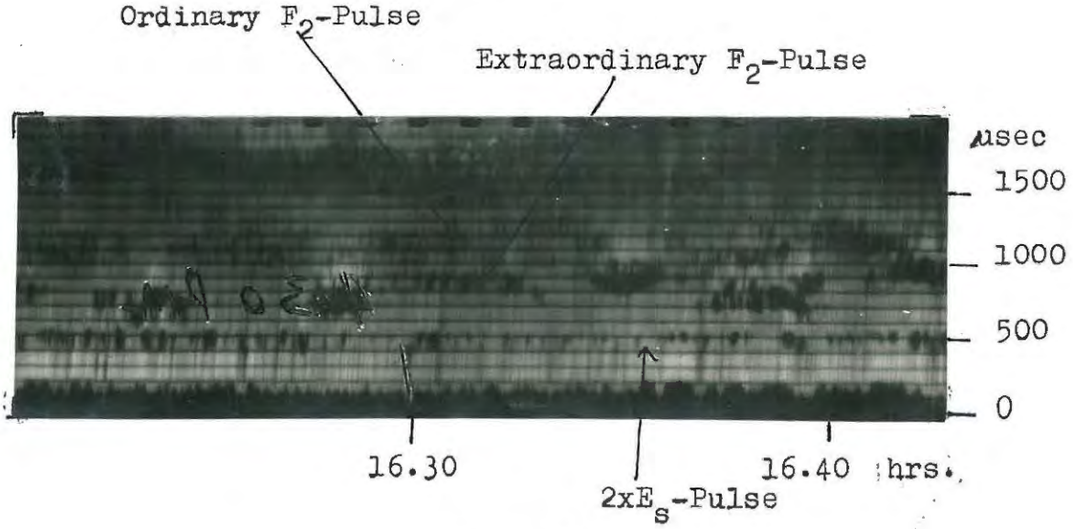

Fig.28(c)

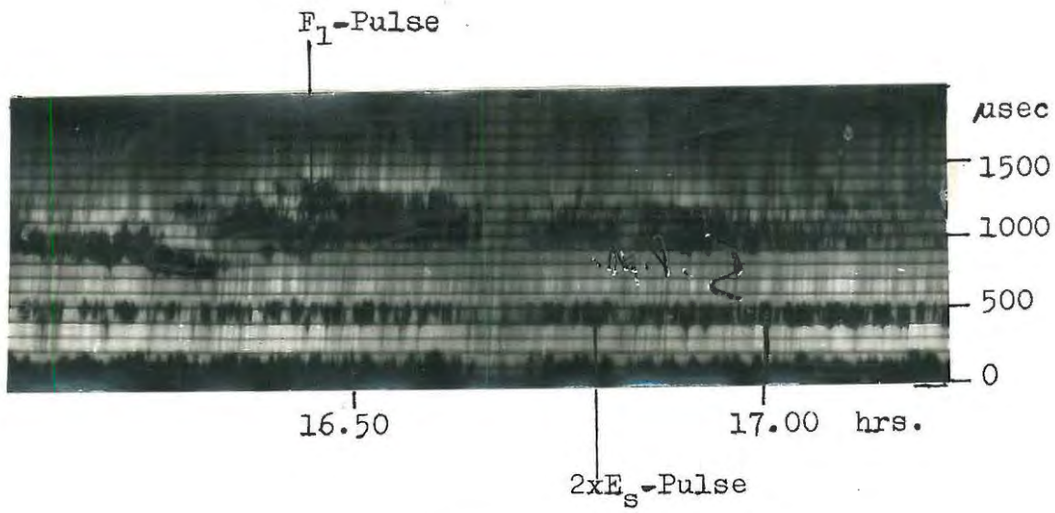

Fig.28(d)

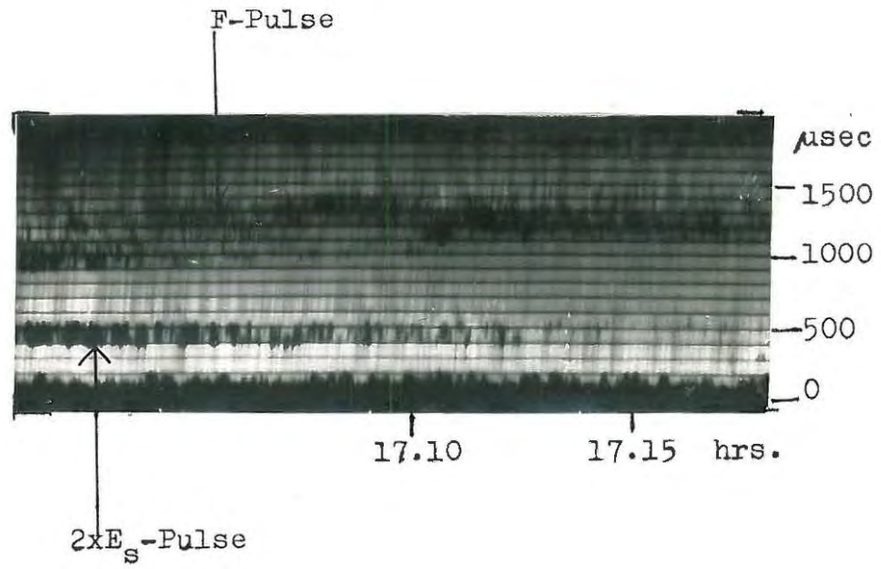

Fig.28(e)

shown by the following figures:- If the height of reflection is assumed to be 110 km (as given by Grahamstown ionograms) it is found that the vertical incidence equivalent frequency is 2.8 Mc/s which is well above the value of 2.5 Mc/s given by the Grahamstown ionograms for f_0E around this time.

Therefore a one-hop from the E layer seems more likely to be the triggering pulse. If a one-hop from the E layer at a height of 110 km is assumed to be the triggering pulse, its vertical incidence equivalent frequency works out to be 1.65 Mc/s which agrees with the f_0E values given by the Grahamstown ionograms.

The steady pulse that starts off at 475 μsec then fits in very well as a 2-hop from the sporadic-E layer. According to the time delays obtained, the propagation time decreases from 2575 μsec at 14.20 hours to 2500 μsec at 16.10 hours. This indicates that the height of reflection decreases from 125 km to 115 km, which is verified by the Grahamstown ionograms.

The pulses in the upper portion of the film show rapid variation in the heights of reflection. This itself leads one to believe these to be F-layer pulses since Grahamstown ionograms show similar characteristics for the F region. The 700 μsec pulse which starts at 15.43 hours (Fig. 28a) would have a time of propagation of 2800 μsec (2100 + 700). Fig. 17 gives its height of reflection as 300 km. From the Grahamstown ionograms the height of reflection of the equivalent frequency, 3.4 Mc/s, is found to be exactly 300 km, reflection

occurring at the peak of the F_1 layer. Hence this pulse could be identified as the lower F_1-ray. The 1200 μsec pulse which appears at 15.42 hours for 2 minutes is recognised, with the aid of Grahamstown ionograms, as an F_2-layer pulse reflected from a height of about 400 km.

The ordinary F_1 Pedersen ray appears at about 15.45 hours. It starts at 1500 μsec and drops rapidly in height to join the lower F_1-ray at 15.49 hours. The F_1-layer reflection continues at its peak. This is to be expected since Grahamstown ionograms indicate that f_oF_1 decreases very gradually. At about 16.00 hours, the extraordinary Pedersen ray makes its appearance as faint dots with a time delay of 1100 μsec. It joins the lower ray at 16.10 hours (Fig. 28b).

Thereafter the pulses become very broad and the heights of reflection vary widely. Grahamstown ionograms verify this since they themselves indicate rapid variation in heights of reflection. For pulses randomly chosen on the record, it is found that the heights of reflection obtained in the record agree within reasonable limits to heights of reflection of equivalent frequencies in Grahamstown ionograms (sometimes they agree with the ordinary components and at other times with the extraordinary components).

At 16.30 hours two pulses remain steady for a short period (Fig. 28c). Their time delays are 800 μsec and 1100 μsec, giving heights of reflection of 320 km and 380 km respectively. Again Grahamstown ionograms verify these

heights of reflection for the equivalent frequencies and identify them as the extraordinary and ordinary pulses from the F_2 layer respectively.

From 16.50 hours a single broad steady pulse with a more or less constant time delay of 900 μsec is seen (Fig. 28d). It remains at this value until 17.05 hours. Calculations give the height of reflection of this pulse as 340 km. Grahamstown ionograms give the heights of reflection for the equivalent frequency (3.6 Mc/s) for this period as varying between 340 and 360 km, which agrees reasonably well with the value obtained. Hence this pulse could be identified as a reflection from the peak of the F_2 layer. The broadness seems to be due to the Pedersen ray slowly joining it.

After 17.05 hours, the time delay increases to 1100 μsec (see Fig. 28e) which shows that the propagation time is now 3200 μsec (2100 + 1100), the corresponding height of reflection being 380 km. This is also verified by the Grahamstown ionograms which give the height of reflection of the equivalent frequency (3.7 Mc/s) as varying between 365 km and 380 km.

From about 17.20 hours a more normal pattern of behaviour of the pulses is observed. Here a strong steady pulse is seen varying between 400 and 500 μsec. In addition there is a weak pulse on the upper part of the film varying between 1600 μsec and 1800 μsec.

If it is assumed that the triggering pulse is still a one-hop from the E layer which has now risen to 120 km

(as shown by Grahamstown ionograms), then the 400 μsec pulse could be identified as a one-hop from the F layer at a height of 240 km, and the 1600 μsec pulse as a 2-hop from the same layer. The times of propagation of the three pulses would respectively be 2125, 2540, and 3750 μsec (according to Fig. 17). These values agree well with the times of propagation obtained from the record, viz., 2125, 2525, 3725 μsec respectively. Once again Grahamstown ionograms to a reasonable approximation validate the assumptions made.

The 2-hop pulse from the F layer becomes weak after 18.30 hours and soon disappears, whereas the one-hop pulse lasts till 19.30 hours.

No further pulses are observed on the record until midnight.

It may be interesting at this stage to comment on the relation of these results to selective fading. Thus, if there are two paths of propagation with a relative delay of 350 μsec, as in Fig. 27b, a sideband corresponding to a musical frequency of $\frac{10^6}{2 \times 350} = 1429$ c/s would just arrive in antiphase by the later path. Thus it is effectively lost, or very much weakened relatively to say 715 c.p.s., which has no second path delayed by half a cycle to affect it.

Time delays between pulses generally remain below 1000 μsec, which corresponds to a frequency of 500 c.p.s. Time delays up to 2000 μsec have very rarely been obtained. Thus most of the selective fading would affect the higher musical and speech frequencies over the Grahamstown-Durban path.

4.23 INTERESTING PHENOMENA

4.231 AN UNUSUAL TRAVELLING DISTURBANCE OBSERVED AT SUNRISE ON 30TH DECEMBER, 1964

The record for the morning of 30th December, 1964 shows the normal E- and F-layer reflections. At 06.33 hours the 2 x F-pulse makes its appearance at 1700 μsec and drops to 1200 μsec at 06.51 hours (see Fig. 29b). However, in the meantime, at 06.48 hours an unusual pulse appeared at about 1800 μsec time delay (Fig. 29b). This pulse only lasted 4 minutes and could not be explained by the usual assumptions.

Grahamstown ionograms for the period 06.45-08.00 hours indicate that there could have been a very large travelling disturbance during this period. The ionograms show an unusual sudden rise in the $h'F_1$ and $h'F_2$ values for a short interval around 07.30 hours. The $h'F_1$ and $h'F_2$ values for this period are given in Table III.

TIME	$h'F_1$	$h'F_2$
06.00	245	270
06.45	240	275
07.15	220	345
07.30	245	415
07.45	245	370
08.00	240	345
08.30	240	345

TABLE III

This sudden increase in the $h'F_1$ and $h'F_2$ values might be attributed to the passage over Grahamstown of an inverted trough of ionization of the type discussed by Munro (56) and McNicol, Webster and Bowman (57).

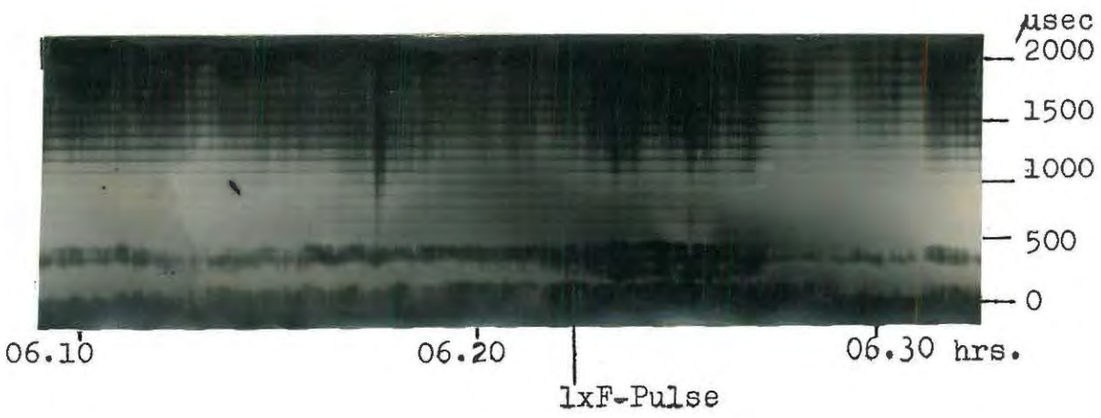

Fig.29(a)

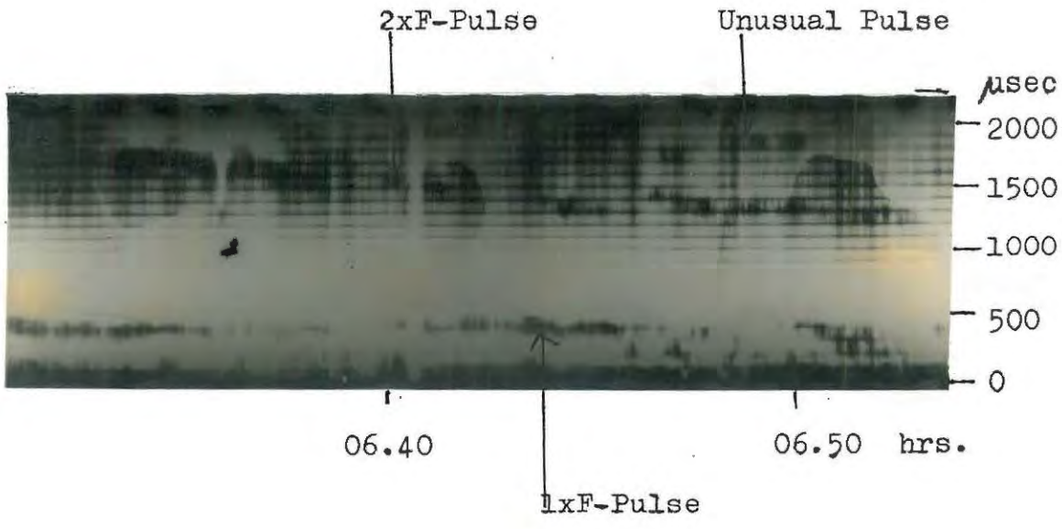

Fig.29(b)

It is possible that this effect is related to the unusual pulse seen at 06.48 hours on the oblique incidence record. The impression obtained from the record is that the 2-hop pulse from the F layer splits up and reflection takes place from two different heights. Therefore points at which the disturbance was likely to have affected the pulse would be $\frac{1}{4}$ of the way from Grahamstown to Durban or $\frac{3}{4}$ of the way. The latter is unlikely because if it was so, the disturbance would have been noticed again at a later time on the record, when it passed the first reflection point (i.e. $\frac{1}{4}$ of the way from Grahamstown). This is not indicated by the record. Therefore it could be assumed that the disturbance passes through the point 147 km from Grahamstown on the Durban-Grahamstown line at 06.48 hours.

It is interesting to note that the disturbance was observed at sunrise. A similar disturbance was observed in Grahamstown in August, 1960 also at sunrise (58). Therefore it might be suggested that sunrise contributes in some way to the formation of disturbances of this kind. There is a possibility that ripple effects caused by sunrise in the ionosphere could result in such unusual waves of ionization. The indications are that there is a massive motion of particles rather than just the increase and decrease of ionization in the F region.

It would be difficult to get the actual direction of travel of the disturbance or even its velocity.

Records at 3 points which are not in a straight line are necessary to determine this. Nevertheless, noting the disturbance at two definite points helps one to determine the component of its velocity along the Durban-Grahamstown line accurately. It is seen at a point 147 km from Grahamstown at 06.48 hours and at Grahamstown at 07.30 hours. Therefore it takes 42 minutes to travel 147 kilometres. Hence the component of the velocity along the Durban-Grahamstown line is 210 km/hour.

The Durban-Grahamstown line makes an angle 43° with the E-W line. Thus if it is assumed to be travelling from East to West its velocity would be,

$$V = 210 \text{ Cos } 43^{\circ} = 154 \text{ km/hour}$$

which compares well with the range of speeds recorded by Munro (59,60).

The disturbance takes 45 minutes to pass through Grahamstown. This information could be used to determine its width which is found to be 157 km.

From the Grahamstown ionograms virtual heights for a particular frequency for this period can be obtained. A knowledge of the velocity of the wave helps to convert the times to distances. That is, it is imagined that the disturbance is stationary and that the Grahamstown ionosonde is moving under it at 210 km/hour in the Durban direction and that recordings are taken at points separated by $\frac{210}{4} = 52.5$ km. It

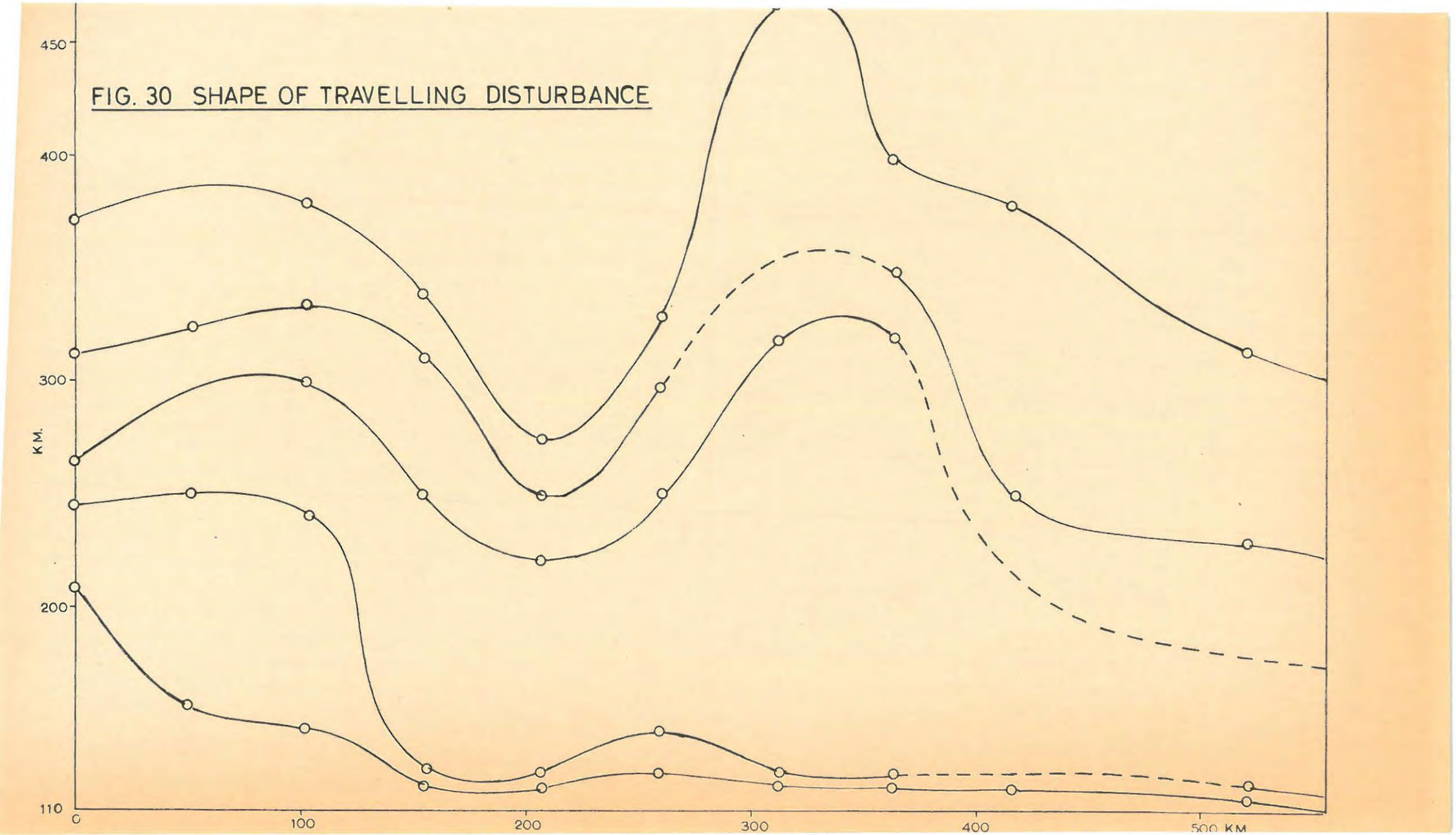
FIG. 30 SHAPE OF TRAVELLING DISTURBANCE
450
400
300
200
110
KM.
0
100
200
300
400
500 KM

is possible then to set up axes with heights as ordinates and distances travelled by the ionosonde as abscissae and plot the values of virtual heights. By repeating this for other frequencies a contour diagram of virtual heights is obtained. This is given in Fig. 30. These contours give the apparent shape of the disturbance as obtained from values of virtual height. Fig. 30 gives its amplitude as being in the order of magnitude of 200 km in the F_2 region and 25 km in the F_1 region.

Some of the apparent increase in virtual height could be due to retardation in the E region which is forming rapidly at this time. Thus the true shape of the disturbance might have been slightly different and the amplitude could have been smaller.

(a) Effect on 2-hop pulse

When the disturbance approaches the reflection point, the leading edge reflects the pulses. Soon the trailing edge joins in the reflection. However, the heights of reflection are more or less the same and this results in the propagation times being the same. Therefore only one pulse is seen on the record.

As the wave gets closer to Grahamstown, the height of reflection on the leading edge increases. Therefore the pulse is seen to split. The two components separate until a time difference of 500 μsec is reached when one of the pulses is reflected from the trough of the wave. This shows that there is a difference in height of reflection of about 100 km which seems possible according to Fig. 30.

Subsequently the pulse reflected from the trough disappears because the shape of the trough does not provide the correct inclination for the obliquely incident pulse to be returned to a point approximately midway between Grahamstown and Durban. The pulse reflected from the trailing edge soon disappears due to absorption.

(b) Effect on the One-hop pulse

According to calculations, the disturbance should pass through the midway point at 06.06 hours. Before 06.06 hours the reflection is expected to take place on the leading edge. On examining the shape of the disturbance it is seen that the change over of the point of reflection from the leading edge to the trailing edge would take place without much change in the time of propagation. However, the record shows a slight weakening of the pulse around this time.

Unlike the two-hop pulse, the reflection from the leading edge disappears very quickly because the angle of incidence on the ionosphere of the one-hop pulse is large and the walls of the trough are not inclined sufficiently to the vertical to return the pulses to Durban.

The inclination seems to be just right around 06.25 hours when the disturbance is 235 km from Grahamstown. The oblique incidence record shows that at this time the 1 x F-pulse gets very broad (300 μsec) and attains a high intensity (see Fig. 29a). A condition is possibly reached such that reflections from a number of points in the trough are focussed to Durban. Since the

reflection point is low, i.e. at a point where the trough is shallow, the pulse does not split.

A rough calculation may be made to test this hypothesis as follows: The distance of the actual point of reflection from Durban is 420 km and from Grahamstown is 320 km. Using the well-known formula for reflection from a curved surface, it is found that the radius of curvature of the reflecting surface is 90 km. On examining the disturbance it is found that the radius of curvature at the trough is 40 km and that it varies continuously until it reaches infinity near the edge. Since the Grahamstown -Durban line is inclined at an angle to the axis of the disturbance, the radius of curvature of 90 km obtained above seems to be of the right order of magnitude and the reflection (focussing) seen on the record appears to be reflected from near the trough of the disturbance.

4.232 ANOMALOUS PEAK IN THE F LAYER AT NIGHT

An interesting phenomenon in the F layer is shown after 01.00 hours on 25/12/64 (see Figs. 31 a, b, c, d, and e).

At 21.44 hours on 24/12/64 propagation through the F layer stopped because the MUF between Grahamstown and Durban had dropped to below 4.73 Mc/s. Now the plasma frequency should remain low or show a gradual decrease until the sun's ionizing radiations produce more electrons at sunrise. But that this is not the case is shown by the record for the period 01.00 hours to 03.00 hours.

From 01.22 hours a broad triggering pulse is seen (Fig. 31a). It continues to broaden until it splits at 01.34 hours. The wide variations in the time delay of this pulse rules out the possibility that it could be either a sporadic-E or a normal E reflection. Therefore it is apparently an F-layer pulse. This could be verified if one follows the pulses up to 03.00 hours and finds a new triggering pulse which may only be identified as a sporadic-E layer reflection.

Once it is established that these are the F-layer pulses, it is quite simple to identify the triggering pulse and the pulse that splits away from it, which are respectively the lower extraordinary F-layer pulse and the extraordinary Pedersen ray. The latter rises at first to reach 500 μsec time delay at 01.40 hours - denoting that the electron density in the F region is increasing. Thereafter the electron density seems to decrease as shown by the change in direction of the Pedersen ray which drops to 300 μsec and remains at this value until 01.50 hours. (Figs. 31 a and b).

Again between 01.50 and 02.10 hours there is a notable increase in the electron density in the F layer. This is made evident by the Pedersen ray rising until it reaches 800 μsec at 02.10 hours (Figs. 31 b and c). Two minutes later the ordinary Pedersen ray appears at a time delay of 100 μsec signifying a further rise in the plasma frequency. This ray is seen to disappear at 02.16 hours as the electron density falls again. Subsequently there is a gradual fall in

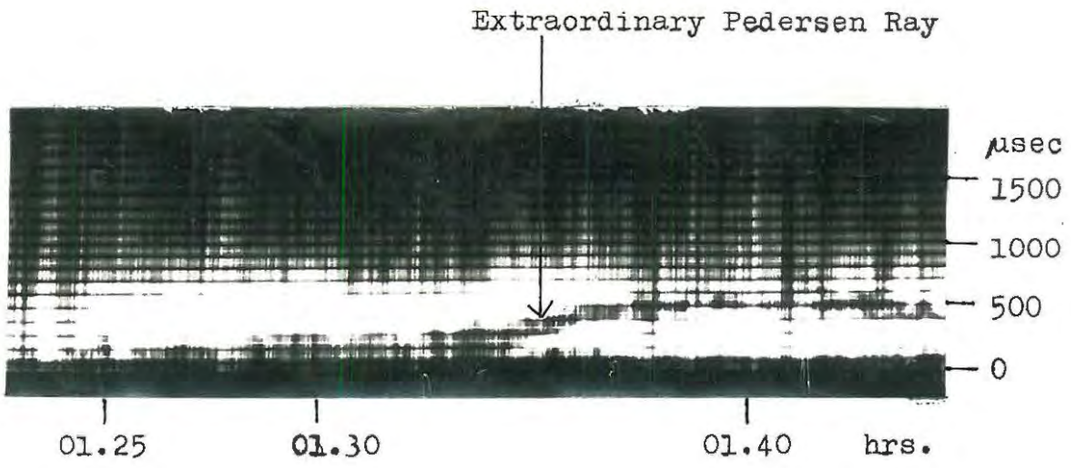

Fig.31(a)

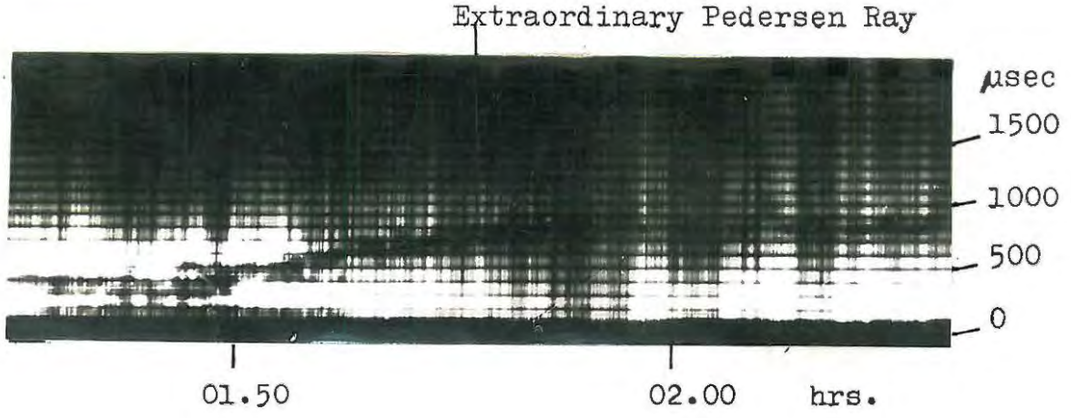

Fig.31(b)

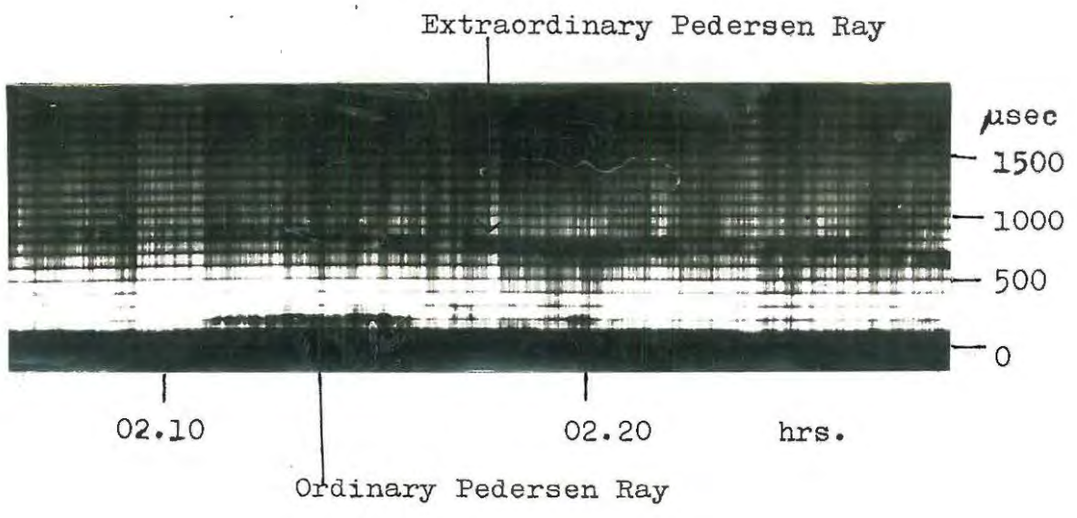

Fig.31(c)

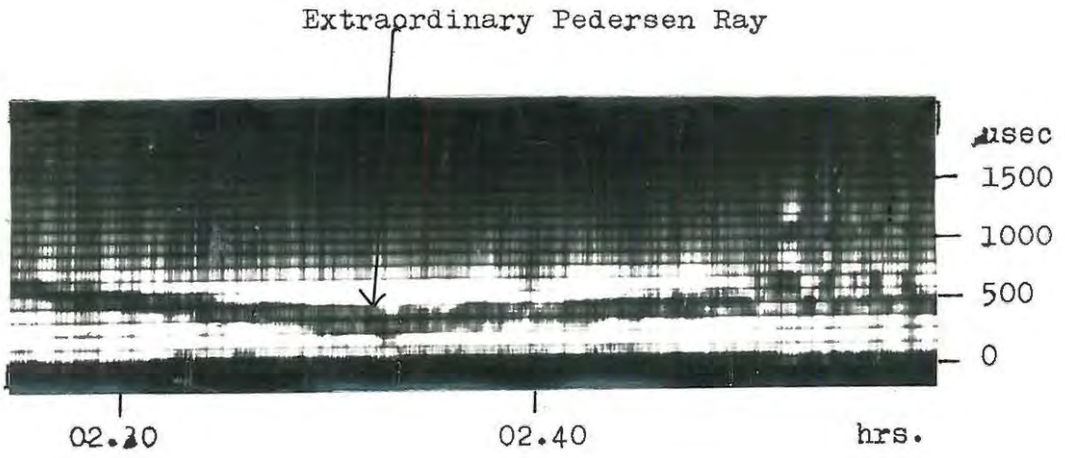

Fig.31(d)

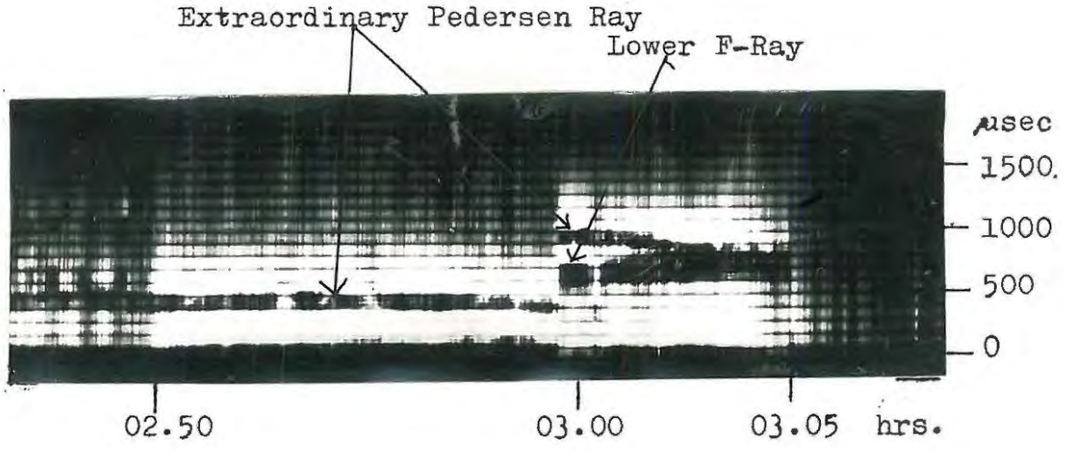

Fig.31(e)

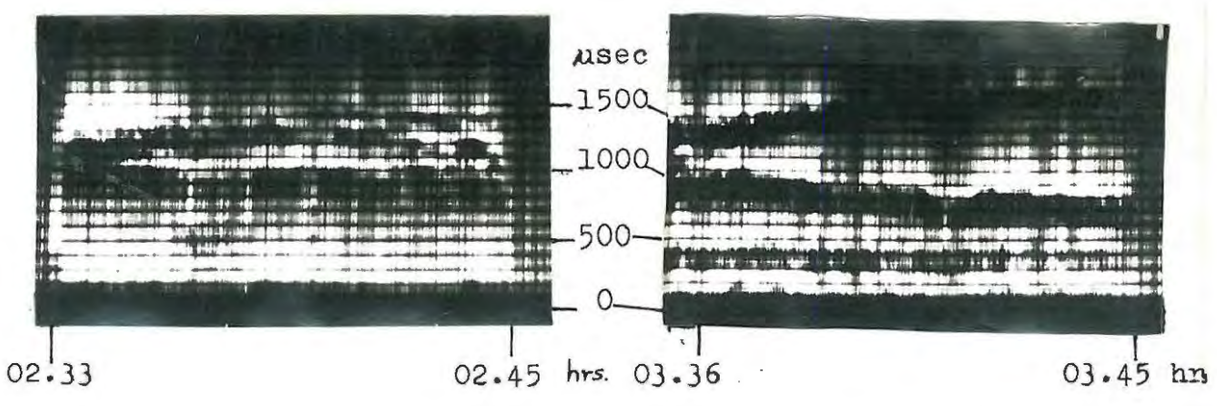

Fig.32(a)

Fig.32(b)

the extraordinary Pedersen ray until it reaches 300 μsec at 02.35 hours (see Fig. 31d) indicating a similar drop in the electron density. There seems to be still another change since the Pedersen ray again rises to 400 μsec.

At 02.59 hours there is an upward shift of all pulses corresponding to 500 μsec, which means that a new pulse is triggering the apparatus. The only possible identification for the triggering pulse is that it is a reflection from the E_s layer. If it is assumed that this pulse is a 2-hop reflected from a height of 120 km, the F-pulse would have a time of propagation of 2550 + 500 = 3050 μsec. This would give the height of reflection as being 350 km which falls within the normal range of values expected for an F-layer reflection near the peak. Finally the Pedersen ray joins the lower ray at 03.05 hours, after which all pulses disappear.

The behaviour of the ionosphere - as described above - is not unusual at all in summer. In fact, it is often found that f_oF_2 shows a peak at about 02.00 hours in summer. The peak is presumably not brought about by an increase in ionization, but rather by temperature changes. As the layer cools during the night, it contracts, leading to an increase in the electron concentration even though the loss process is tending to decrease the electron density.

If the rate at which the electron density increases due to the contraction of the layer is more rapid than the rate of loss (due to recombination, attachment, etc.),

the F-layer electron density increases to a maximum. Consequently the Pedersen ray rises. At times when the pulses remain at a constant level, e.g. 02.50 to 02.59 hours in Fig. 31e (i.e. the electron density is constant), the rates of the two processes are equal. On the other hand when there is a downward trend in the Pedersen ray, the rate of loss dominates.

Finally, when the layer has cooled sufficiently and is in a steady state there is little or no further contraction. Hence the loss process plays a major role in determining the electron density of the ionosphere. Therefore the plasma frequency decreases gradually, the MUF for the F layer dropping to below 4.73 Mc/s.

Similar features were noted on many other days. The record for 26/11/64 (see Figs. 32a and b) illustrates another example of such an occurrence.

4.233 E-LAYER CRITICAL FREQUENCY

When, at sunrise, the E layer is formed, there is no propagation via this layer until its MUF reaches 4.73 Mc/s. The starting of reflections from the E layer could be correlated with the critical frequency as was done for the f_xF_2 and f_0F_2.

The existence of a sporadic-E layer at the time when the normal-E MUF reaches 4.73 Mc/s makes these measurements impossible. Therefore it is necessary to choose a day when the sporadic-E is absent. Such conditions were found to prevail on 30/12/64.

On this day the extraordinary and ordinary MUFs of the F layer reached 4.73 Mc/s at 05.03 and 05.10 hours respectively. Subsequently the lower F-ray

triggers the apparatus until 05.40 hours. At 05.40 hours a new pulse is seen with a time delay of 400 μsec. This indicates a change in triggering. The first pulse is now an E-layer reflection while the F-pulse is at 400 μsec.

An examination of Grahamstown ionograms shows that the sporadic-E layer disappears at 05.00 hours and that the normal E layer makes its appearance at 05.30 hours. Therefore it would be correct to assume that it is the normal-E reflection that triggers the apparatus at 05.40 hours.

Grahamstown ionograms for 05.45 hours give the value of $h'E$ as 140 km and f_oE as 1.85 Mc/s. If it is assumed that the E-layer reflections take place at 140 km, then the angle of incidence (ϕ_o) of the pulses on the ionosphere works out to be 65^o. If on the other hand, 1.85 Mc/s is taken as the vertical incidence equivalent of 4.73 Mc/s and the Secant Law is applied to it, it is found that ϕ_o is 67^o. These two values of ϕ_o agree reasonably well and the error of 2^o involved is negligible.

It is shown from the above discussion that the E-layer propagation is observed to begin as expected when its MUF has reached 4.73 Mc/s. Therefore these propagations would ideally continue to exist throughout the day until the E-layer MUF drops after sunset. However, this is not so because of the high absorption that takes place during the day. Consequently the pulses soon disappear.

The night-time falling of the E layer is not observed because the absorption is still high at the time that its MUF drops to below 4.73 Mc/s. Pulses begin to reach Durban much later than this.

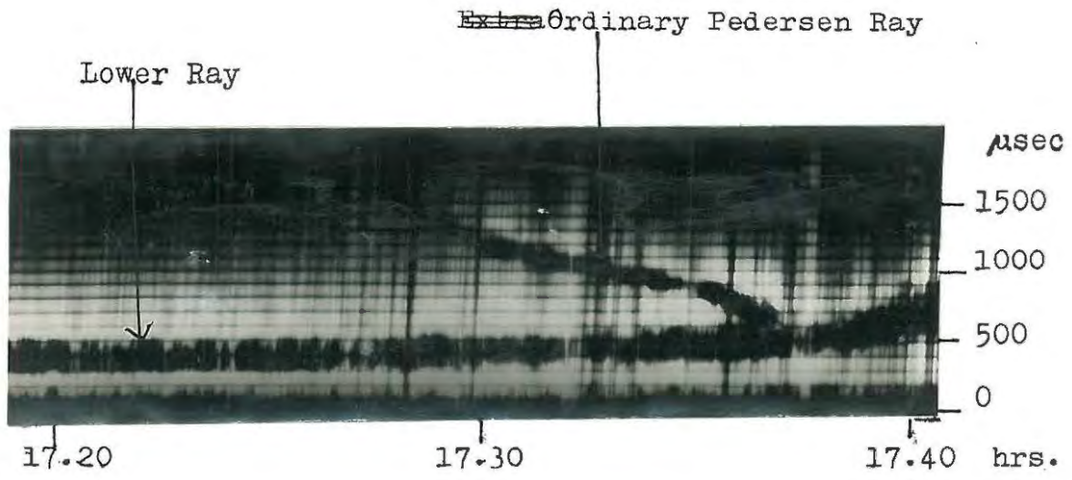

Fig.33(a)

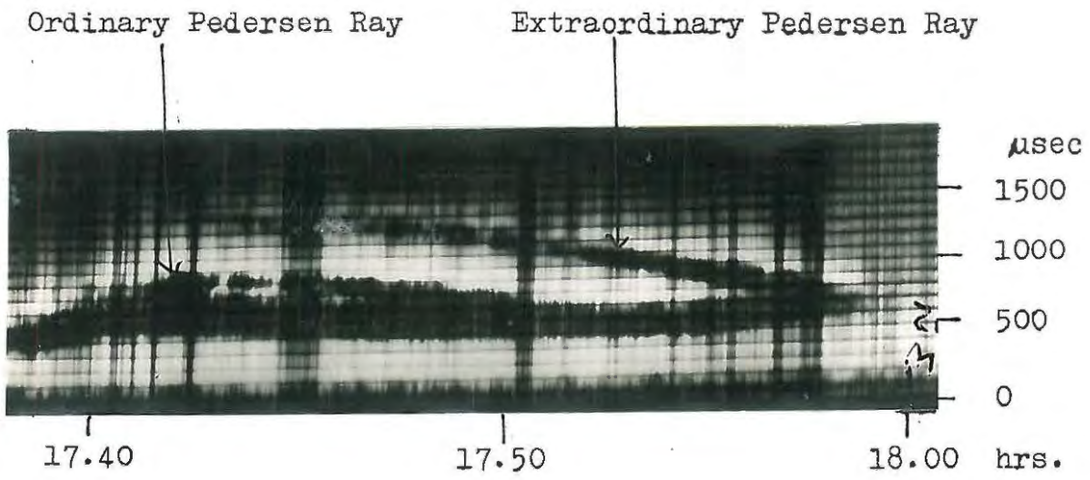

Fig.33(b)

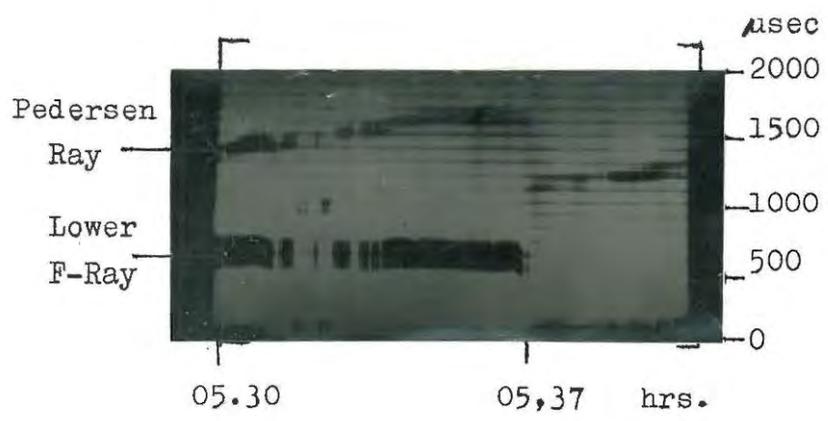

Fig.34

4.234 ELECTRON DENSITY IN THE F REGION AT SUNSET IN WINTER

An example of a very slow decrease of electron density in the F region during sunset in winter is shown by the record for 1/7/65 (Figs. 33 a and b). Here it is seen that from about 17.25 hours the F-layer pulse begins to rise from its time delay of 300 μsec, while the ordinary Pedersen ray appears at 1400 μseo just after 17.29 hours. At 17.38 hours the Pedersen ray joins the lower ray which has now reached a time delay of 400 μsec (see Fig. 33a).

Normally the next step would be the appearance of the extraordinary Pedersen ray which would then join the lower ray. However, this does not occur: the lower ray rises further (to 500 μsec) indicating that the reflection occurs at a much higher level. This is not unusual since the lower parts of the ionosphere are gradually disappearing into the shadow of the earth while the ultra-violet rays from the sun are only incident on the upper parts.

However, the splitting of the ordinary Pedersen ray again from the lower ray is an unusual occurrence. The former reaches a time delay of 900 μsec at 17.44 hours while the latter is at 500 μsec. This might be attributed to a drop in the rate of recombination due to rarefaction of the constituents of the upper atmosphere as well as contraction of the layer due to lowering of temperature.

After 17.44 hours a downward trend of the ordinary Pedersen ray is noted to a point where it merges

with the lower ray at 17.50 hours (Fig. 33b). Similarly the extraordinary Pedersen ray which had started at 17.36 hours with a time delay of 1600 μsec joins the lower ray at 17.59 hours, denoting that the extraordinary MUF for the F layer between Grahamstown and Durban passes 4.73 Mc/s. Thereafter the plasma frequency remains at a low level.

4.235 CHANGE IN TRIGGERING DUE TO DISAPPEARANCE OF THE SPORADIC-E REFLECTIONS

From the records taken it is seen that change of triggering is a general occurrence. A typical example will now be discussed.

On 30/11/64 (during a time when ¼ hour recordings were taken every hour) at 05.30 hours two pulses are seen - one at 500 μsec and the other at 1350 μsec (Fig. 34). The lower pulse remains at a more or less constant level while the upper one rises to 1600 μsec at 05.37 hours. This behaviour immediately indicates that the 500 μsec pulse is the lower F-ray while the upper one is a Pedersen ray. The triggering pulse would be an E-layer reflection since its time of propagation is lower.

At 05.37 a sudden change occurs. Both these pulses disappear and a single pulse appears at 1100 μsec which is exactly equal to the difference in time between the lower and upper F-rays. Thus it is clear that the E-layer pulse has disappeared and the triggering is taken over by the lower F-ray while it is the

Pedersen ray that appears at 1100 μsec.

This record serves also to identify the triggering pulse as a sporadic-E and not a normal-E reflection. A normal E layer would be in the process of forming at this time and would not disappear suddenly as has been seen to occur.

Careful examination of Fig. 34 shows that the change in triggering also takes place twice at about 05.32 hours.

4.24 RAY TRACING

Before ray tracing can be attempted, it is necessary to obtain an accurate N-H profile for the ionosphere. N-H profiles could be determined from Grahamstown ionograms. The ionograms must be distinct such that heights of reflection could be read off throughout the frequency range.

The ionogram taken at 07.45 hours on 11-7-1965 seems to fulfil the above requirements. (Although an ionogram taken at an earlier hour would, however, have been preferred, the earlier ionograms were found to be inadequate to obtain the N-H profile normally expected). For the ionogram chosen the equivalent time on the oblique incidence records would be about 09.05 hours (including the 90 min. unexplained winter delay). These records indicate that at this time the lower F-ray has a time delay of 350 μsec and the upper ray has already been absorbed. On extrapolation it is found that, if the upper ray were still received, it would have a time delay of approximately 1850 μsec.

From the ionogram for Grahamstown (for 07.45 hours) the virtual heights of reflection for 23 different frequencies were obtained, spaced 0.1 and 0.2 Mc/s apart. With the aid of a computer program based on Titheridge's method (61), the plasma frequency for various true heights in the ionosphere was obtained (see Table IV). From this a curve of plasma frequency versus height was plotted on a large graph paper. This is reproduced in Fig. 35.

It is assumed that the ionosphere between Grahamstown and Durban is horizontally stratified. Hence the plasma frequency for a particular height would be the same throughout the distance from Grahamstown to Durban. A large scale diagram of the vertical plane passing through Grahamstown and Durban was then drawn on graph paper. One inch was used to represent 10 km. The ionosphere on the scale diagram was then divided into many strata of 2 km at the lower parts and 1 km near the peak where the angle of incidence of the rays on the different strata would be large. For each of these strata, the mean plasma frequency was determined and the phase refractive index for a frequency of 4.73 Mc/s was calculated with the aid of equation 3.7. These values are given in Table V.

Next a certain angle of incidence on the ionosphere was assumed. A straight line was drawn at this angle from Grahamstown to the base of the ionosphere. The angle that this ray would make in the different strata was calculated using Snell's Law. Then the ray was traced through each stratum end to end, until the ray became horizontal.

The ray that reaches Durban would become horizontal at the midpoint between Grahamstown and Durban. Many angles of incidence were attempted and finally it was found that two rays, one incident at an angle of $28^{\circ}52'$ and one at $50^{\circ}52'$, became horizontal at the midpoint. These would be the Pedersen and lower rays, respectively. The other half of the ray diagram was completed by symmetry. The diagram was reduced and is shown in Fig. 36.

Plasma Freq. in Mc/s	Virtual Ht. in km	Real Ht. in km
1.100	112.00	112.000
1.200	112.00	112.000
1.400	112.00	112.000
1.500	113.00	112.108
1.600	115.00	112.400
1.700	130.00	114.139
1.800	175.00	119.880
1.900	175.00	124.397
2.000	178.00	128.455
2.100	260.00	139.231
2.200	245.00	146.611
2.300	240.00	152.572
2.400	235.00	157.403
2.500	230.00	161.314
2.600	230.00	164.855
2.800	235.00	171.286
3.000	240.00	177.232
3.200	250.00	183.359
3.400	255.00	189.016
3.600	258.00	194.101
3.800	260.00	198.640
3.900	272.00	201.486
4.000	290.00	205.121

TABLE IV N-H profile for Ionosphere over Grahamstown on 11/7/65 at 07.45 hours.

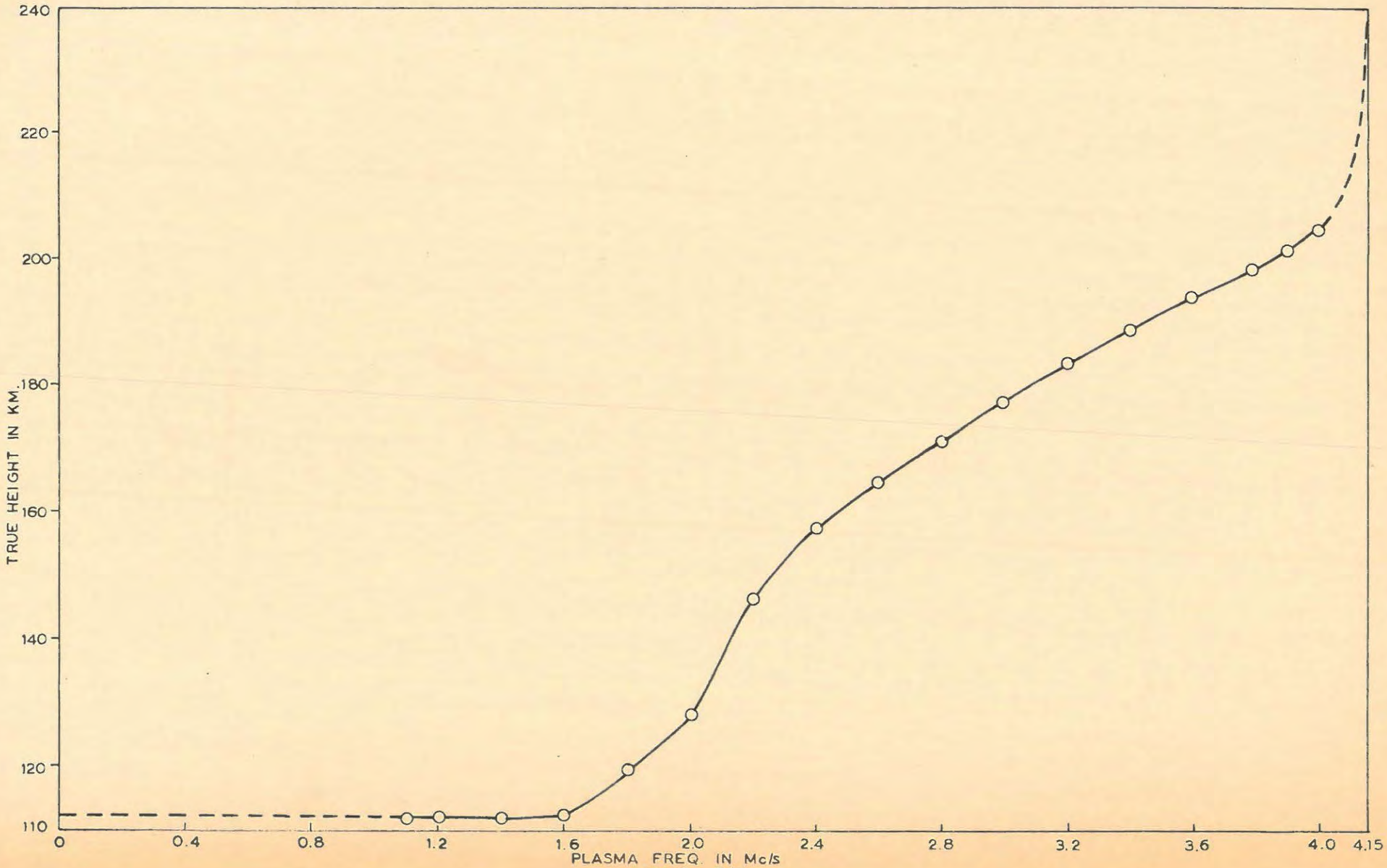
240
220
200
180
160
140
120
110
TRUE HEIGHT IN KM.
0
0.4
0.8
1.2
1.6
2.0
2.4
2.8
3.2
3.6
4.0
4.15
PLASMA FREQ. IN Mc/s

FIG. 35

T A B L E V

HEIGHT OF LOWER EDGE OF STRATUM IN KM	PLASMA FREQUENCY	REFR. INDEX FOR 4.73 MC/S (PHASE)	ANGLE PEDERSEN RAY MAKES WITH VERT.	ANGLE LOWER RAY MAKES WITH VERTICAL
110	0.000	1.0000	28°52'	50°52'
112	1.615	0.9400	30°54'	55°37'
114	1.715	0.9320	31°12'	56°20'
116	1.745	0.9295	31°18'	56°35'
118	1.780	0.9265	31°24'	56°51'
120	1.820	0.9230	31°32'	57°11'
122	1.860	0.9194	31°40'	57°32'
124	1.925	0.9134	31°54'	58° 7'
126	1.980	0.9081	32° 7'	58° 4'
128	2.005	0.9057	32°13'	58°56'
130	2.030	0.9032	32°18'	59°11'
132	2.046	0.9019	32°23'	59°22'
134	2.060	0.9002	32°26'	59°32'
136	2.080	0.8981	32°31'	59°45'
138	2.100	0.8960	32°36'	59°58'
140	2.125	0.8926	32°42'	60°15'
142	2.155	0.8902	32°50'	60°38'
144	2.180	0.8074	32°57'	60°57'
146	2.210	0.8841	33° 6'	61°20'
148	2.240	0.8807	33°15'	61°45'
150	2.275	0.8768	33°24'	62°13'
152	2.310	0.8727	33°36'	62°45'
154	2.350	0.8679	33°47'	63°21'
156	2.392	0.8627	34° 1'	64° 1'
158	2.440	0.8567	34°18'	64°51'
160	2.495	0.8508	34°37'	65°55'
162	2.545	0.8390	34°55'	66°58'
164	2.605	0.8347	35°20'	68°18'
166	2.665	0.8217	35°45'	69°52'
168	2.730	0.8119	36°15'	71°48'
170	2.792	0.8072	36°44'	73°57'
172	2.860	0.7965	37°18'	76°54'
174	2.925	0.7859	37°54'	80°42'
176	2.975	0.7775	38°23'	86°12'
177	3.008	0.7719	38°42'	— —

T A B L E V (continued)

HEIGHT OF LOWER EDGE OF STRATUM IN KM	PLASMA FREQUENCY	REFR. INDEX FOR 4.73 MC/S (PHASE)	ANGLE PEDERSEN RAY MAKES WITH VERT.
178	3.060	0.7626	39° 6'
180	3.126	0.7505	40° 1'
182	3.190	0.7384	40°50'
184	3.255	0.7256	41°42'
186	3.325	0.7114	42°44'
188	3.400	0.6953	43°58'
190	3.476	0.6782	45°24'
192	3.562	0.6582	47°11'
194	3.645	0.6374	49°14'
196	3.735	0.6137	51°52'
198	3.816	0.5911	54°33'
200	3.888	0.5697	57°56'
202	3.946	0.5514	61° 6'
204	3.986	0.5383	63°45'
205	4.008	0.5309	65°24'
206	4.024	0.5259	66°37'
207	4.038	0.5208	67°55'
208	4.052	0.5160	69°20'
209	4.064	0.5120	70°33'
210	4.074	0.5083	71°42'
211	4.083	0.5050	72°54'
212	4.091	0.5022	74° 0'
213	4.097	0.4998	75° 0'
214	4.099	0.4991	75°18'
215	4.103	0.4977	75°54'
216	4.107	0.4963	76°33'
217	4.112	0.4946	77°27'
218	4.115	0.4935	78° 4'
219	4.118	0.4924	78°36'
220	4.121	0.4909	79°30'
221	4.124	0.4899	80°12'
222	4.126	0.4892	80°40'
223	4.128	0.4885	81°12'
224	4.130	0.4873	82° 6'
225	4.132	0.4866	82°48'
226	4.134	0.4860	83°24'
227	4.136	0.4853	84° 6'
228	4.138	0.4845	85°12'
229	4.140	0.4837	86°30'
230	4.142	0.4830	88°18'

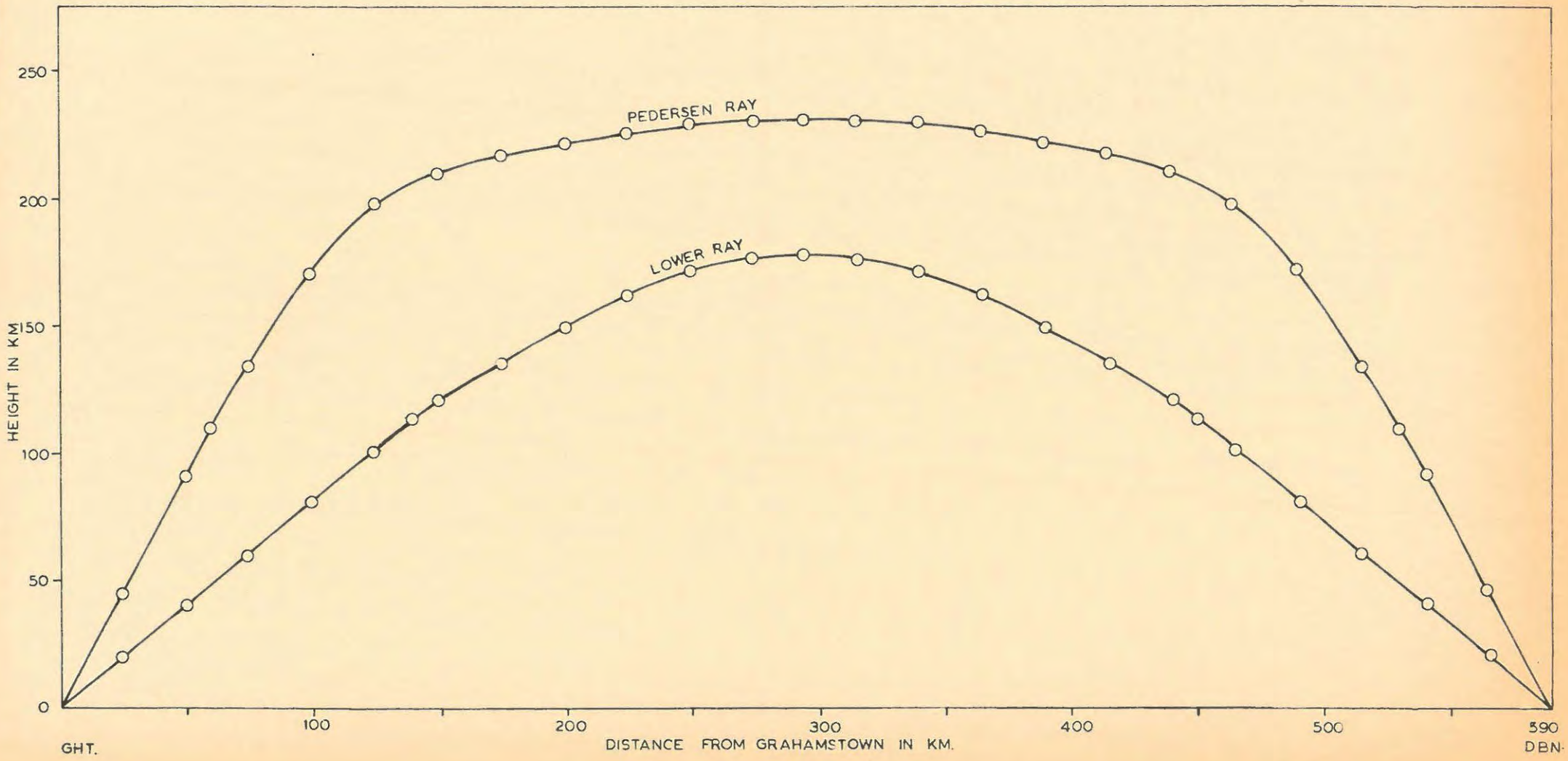
PEDERSEN RAY
LOWER RAY
HEIGHT IN KM
250
200
150
100
50
0
100
200
300
400
500
590
GHT.
DISTANCE FROM GRAHAMSTOWN IN KM.
DBN.

FIG. 36

The equivalent path-length could be obtained from the ray diagram. Using the phase refractive index, the group refractive index for each stratum was calculated with the aid of the equation $\mu\mu' = 1$, which assumes no dispersion due to magnetic field. The path-length for each stratum was read from the diagram. Hence the equivalent path length $\mu' ds$ was determined for each stratum. This gave $\sum \mu' ds$ for each ray. It was found that $\sum \mu' ds$ for the lower and Pedersen rays were 757 km and 1221 km, respectively. Therefore the times of propagation are 2523 and 4070 μsecs, respectively.

If specular reflections are assumed for these two angles of incidence the two rays would have path lengths of 760 km. and 1223 km, respectively, which agree very well with the values obtained above. The times of propagation of 2500 and 4000 μsecs, respectively, obtained from the records for 09.05 hours confirms the validity of the interpretations made of the pulses recorded.

5. CONCLUSION AND SUGGESTIONS FOR FURTHER RESEARCH

5.1 CONCLUSION

The research project resulted in a fair amount of success. Most of the pulses were identified with the aid of Grahamstown ionograms. The correct modes of propagation were obtained. Verification for this is offered by the trace made of the two F-rays which travelled from Grahamstown to Durban on 11-7-1965 (see section 4.24).

Detailed discussion of a summer and a winter day is helpful in the prediction of propagation conditions between Grahamstown and Durban. Further, the diagrams in Appendix II give an overall picture of propagation through various layers for each hour of the day both for summer and winter. Hence the probability of transmission of 4.73 Mc/s between Grahamstown and Durban could be predicted for each hour of the day.

Some interesting phenomena were noticed. These are discussed in section 4.23. The travelling disturbance on 30-12-1964, layer contraction and other unusual time delays noticed on the records merit further research.

This project provided the experience in analysing oblique incidence records. It is now possible to attempt an analysis of the pulses received from Sanae, Antarctica.

5.2 SUGGESTIONS FOR FURTHER RESEARCH

(a) Research on oblique incidence propagation should be carried out on a larger scale, particularly with three stations, which are not in a straight line, recording simultaneously. This would help to obtain more precise determination of such occurrences as travelling disturbances and layer movements.

(b) Sweep frequency oblique incidence propagation would most certainly derive useful data concerning the ionosphere. Here a receiver frequency should vary slowly while the transmitter sweeps rapidly. Then recordings are taken every time

the transmitter frequency passes the receiver frequency.

(c) A research on absorption in the ionosphere by recording the amplitude of the received pulses would undoubtedly yield valuable information on the ionosphere particularly the lower layers.

(d) Two-way propagation is another interesting project.

(e) It was found that at certain hours pulses were absorbed in the ionosphere and consequently did not reach Durban, due to the low power output of the transmitter. Therefore it is suggested that more powerful transmitters be used so that recordings could be taken throughout the day.

(f) Selective fading could also be used to derive information on the ionosphere. For this a transmitter with a central frequency, say 4.73 Mc/s, could be modulated with white noise say to a bandwidth of 10 kc/s.

A receiver tuned to 4.73 Mc/s and situated some distance away from the transmitter would pick up this white noise signal. Its output would consist of a broad range of frequencies (0-10 kc/s) with varying intensities.

By heterodyning the output of the receiver with an oscillator whose frequency can be varied from 0 to 10 kc/s, it is possible to select any frequency from the white noise range. Hence the intensity of the incoming signal on the entire frequency range can be measured. The minimum intensity would indicate a path difference of an odd multiple of half-wavelengths, while maximum intensity, multiple of a wavelength. Thus the delays on all propagation paths could be identified.

A P P E N D I X I

In the table below are given scaled values of all pulses recorded. It is apparent from the table that pulses were not received in Durban at certain times, due either to poor propagation conditions or to fault in the equipment. There is no need to differentiate between these two factors in this table. It is only necessary to interpret the pulses that have been received.

The following abbreviations are used in the table:-

P.R.(O). - Ordinary F Pedersen Ray.

P.R.(X). - Extraordinary F Pedersen Ray.

P.R.(F_1O). - Ordinary F_1 Pedersen Ray.

P.R.(F_2O). - Ordinary F_2 Pedersen Ray.

P.R.(F_1X). - Extraordinary F_1 Pedersen Ray.

P.R.(F_2X). - Extraordinary F_2 Pedersen Ray.

E_s($2E_s$) means both these pulses appear at the same time delay, either simultaneously or alternately.

DATE 1964	TIME IN SAST	TIME DELAYS IN USEC	INTERPRETATIONS	HEIGHT OF REFLECTION F	E
NOV. 19	18.30 - 18.45	0, 1050 - 1100	F, 2F	220	
	19.30 - 19.45	0, 1100 - 1200	F, 2F	240	
	20.30 - 20.45	0, 1550 - 1700	F, 2F	290	
	21.30 - 21.45	0, 475 - 0	F_x, P.R.(X).		
21	04.30 - 04.35	0, 300, 900, 1800	$2E_s$, F, $4E_s$, 2F	280	100
	05.30 - 05.45	0, 300, 1800	$2E_s$, F, 2F	280	100
23	18.30 - 18.45	0, 1200	F, 2F	240	
	19.30 - 19.45	0, 400, 1200 1600	E_s, F, 2F, 2F,	240	130
	20.30 - 20.45	0, 600, 1800 1450	E_s, F, P.R.(O)	290	130
	22.30 - 22.45	0, 400, 900, 1400 - 1300	E_s, $2E_s$, F_x, P.R.(X)	340	120
	23.30 - 23.45	0, 1100	E_s, F_x	380	
24	05.40 - 05.45	0, 450 - 0, 450 - 1000	F_x, F_o, P.R.(O)		
	06.30 - 06.45	0, 400, 600, 900	E_s, $2E_s$, F, $3E_s$	270	110
25	05.30 - 05.45	0, 1300	F, 2F	250	

DATE 1964	TIME IN SAST	TIME DELAYS IN USEC	INTERPRETATIONS	HEIGHT OF REFLECTION F	E
NOV.25	06.30 - 06.45	0, 300, 1700,	2E, F, 2F	265	100
	07.30 - 07.45	0, 300	2E, F	265	100
	17.30 - 17.45	0, 400	E_s, F	230	120
	18.30 - 18.45	0, 1150	F, 2F	230	
	19.30 - 19.45	0, 400, 1150, 1600	E_s, F, 2F, 2F,	230	120
	20.30 - 20.45	0, 400, 1600	E_s, F, 2F	240	120
	21.30 - 21.45	0, 600 - 400	F, P.R.(O)		
NOV.26	01.38 - 01.45	0, 900	E_s, F	340	100
(Fig.32)	02.34 - 02.45	0, 900 - 650 900 - 1200	E_s, F, P.R.(O)	310	100
	03.36 - 03.45	0, 300, 750-600, 1200-1500	E_s, $2E_s$, F, P.R.(X)	295	100
	04.30 - 04.45	0, 1200	F, 2F	240	
	05.30 - 05.45	0, 500, 1100	E_s, $2E_s$, $3E_s$		130
27	05.30 - 05.45	0, 500	E_s, F	250	100
	06.30 - 06.45	0, 150, 400	$2E_s$, F, $3E_s$	240	100
	07.30 - 07.45	0, 1400	F, 2F	265	
28	05.30 - 05.40	0, 1300	F, 2F	250	
	05.40 - 05.45	0, 400, 1700	E_s, F, 2F	250	130
	06.30 - 06.45	0, 200, 400,	$2E_s$, F, $3E_s$	250	100
29	15.30 - 15.45	0, 300, 800, 1800	$2E_s$, F, $4E_s$, 2F	280	100
	16.30 - 16.45	0, 300, 1800	$2E_s$, F, 2F	280	100
	20.30 - 20.45	0, 450, 1700	E_s, F, 2F	240	100
	22.30 - 22.45	0, 400	E_s, F	225	100
30 (Fig.34)	05.30 - 05.37	0, 500, 1350-1600	$2E_s$, F, P.R.(X)	310	100
	05.37 - 05.45	0, 1100-1200	F, P.R.(O)		
	06.30 - 06.45	0, 300	2E, F	270	100
	18.30 - 18.45	0, 1100	F, 2F	220	
	19.30 - 19.45	0, 1300	F, 2F	250	
	20.30 - 20.45	0, 1400	F, 2F	265	
DEC.1	05.30 - 05.45	0, 1700	F, 2F	305	
	06.30 - 06.45	0, 300, 1900	2E, F, 2F	295	110
2	05.30 - 05.45	0, 500	E_s, F	250	100
	06.30 - 06.45	0, 400	E, F	230	100

DATE 1964	TIME IN SAST	TIME DELAYS IN USEC	INTREPRETATIONS	HEIGHT OF REFLECTION F	HEIGHT OF REFLECTION E
DEC. 3	01.30-01.45	0, 800, 1200	F, $4E_s$, 2F	240	100
	04.40-04.45	0, 600	E_s, F	275	100
	05.30-05.45	0, 1500	F, 2F	275	
	06.30-06.45	0, 300, 1800	2E, F, 2F	275	100
	07.42-07.45	0, 500	E, F	275	135
	16.30-16.45	0, 300	$2E_s$, F	225	140
	17.30-17.45	0, 1100	F, 2F	225	
4	16.30-16.40	0, 800-300, 0-300	F_x, P.R.(0), F_o		
5	18.30-18.45	0, 300	$2E_s$, F	275	100
	20.30-20.45	0, 1200	F, 2F	240	
	21.30-21.45	0, 1200	F, 2F	240	
	22.30-22.45	0, 1300	F, 2F	250	
6	00.30-00.45	0, 500	E_s, F	250	100
	01.30-01.45	0, 600	E_s, F	275	100
	03.30-03.45	0, 600	E_s, F	275	100
	06.30-06.45	0, 300	2E, F	275	100
	07.30-07.45	0, 200	2E, F	250	100
7	17.30-17.45	0, 400	2E, F	300	100
11	22.30-22.36	0, 1700	F, 2F	305	
	23.30-23.36	0, 200	$2E_s$, F	305	125
12	03.30-03.36	0, 450	E_s, $2E_s$		125
	04.30-04.38	0, 200-500	F, P.R.		
	05.30-05.45	0, 1600-1500	F, 2F	285	
	06.30-06.45	0, 300	2E, F	275	100
	18.30-18.45	0, 1600	E_s, F	240	130
	19.30-19.45	0, 1200, 1600	E_s(F), 2F, 2F	240	130
	20.30-20.45	0, 400, 1300 1700	E_s(F), F, 2F, 2F	250	130
	21.30-21.45	0, 500	E_s, F	265	130
	22.30-22.40	0, 400-0	F, P.R.		
13	05.30-05.45	0, 1700	F, 2F	305	
	06.30-06.45	0, 300, 1600, 1900	2E(F), F, 2F, 2F	290	110
14	00.30-00.45	0, 500	$2E_s$, $3E_s$		110
	05.30-05.45	0, 600	$2E_s$, F	350	110
	06.30-06.45	0, 400	2E, F	310	110

DATE 1964	TIME IN SAST	TIME DELAYS IN USEC	INTERPRETATIONS	HEIGHT OF REFLECTION F	E
Dec.15	01.30-01.45	0, 1000	E_s, F	355	100
	16.30-16.45	0, 300	$2E_s$, F	280	105
	17.30-17.45	0, 400	$2E_s$, F	300	105
	18.30-18.45	0, 400	$2E_s$, F	300	105
	19.30-19.45	0, 400	$2E_s$, F	300	105
	20.30-20.45	0, 500	$2E_s$, F	320	105
	23.30-23.45	0, 800-500	F, P.R.		
16	02.30-02.40	0, 400-500	F, P.R.		
	04.30-04.45	0, 600	E_s, F	275	100
	05.30-05.45	0, 1500	F, 2F	275	
	06.30-06.45	0, 300	2E, F	280	100
	19.30-19.45	0, 1200	F, 2F	235	
	20.30-20 45	0, 1400	F, 2F	260	
	21 30-21.45	0, 1200-800	F, P.R.(O)		
	23.30-23.45	0, 1000-800	F, P.R.(X)		
17	05.30-05.45	0, 450, 1900	$2E_s$(F), F, 2F	340	120
	06.30-06.45	0, 1000, 2000	E(F), F, 2F	350	100
	07.30-07.45	0, 700	E, F	295	100
	18.30-18.45	0, 1500	F, 2F	280	
	19.30-19.45	0, 1300	F, 2F	250	
	20.30-20.45	0, 1500	F, 2F	280	
	21.30-21.45	0, 1700	F, 2F	305	
	22.30-22.45	0, 1100-200	F, P.R.(O)		
18	00.30-00.38	0, 600-0	F, P.R.(X)		
	01.30-01.45	0, 600-800	F, P.R.(X)		
	02.30-02.45	0, 600	F, P.R.(X)		
	05.30-05 45	0, 1300-2050, 2200-1900	F, P.R.(X), 2F	350	
	06.30-06.45	0, 300	2E, F	275	105
	19.30-19.45	0, 900, 1500	E_s, $3E_s$, $4E_s$		115
	20.30-20.45	0, 400, 900, 1500	E_s($2E_s$), $3E_s$, $4E_s$	230	115
	21.30-21.45	0, 500, 1200	E_s, $2E_s$, $3E_s$		135
	22.30-22.45	0, 500	E_s, $2E_s$		135
	23.30-23.45	0, 700, 1600	E_s, F, P.R.(O)	315	135
19	00.30-00.45	0, 400-0, 400-550-500	F_x, F_o, P.R.(O)		

DATE 1964	TIME IN SAST	TIME DELAYS IN USEC	INTERPRETATIONS	HEIGHT OF REFLECTION F	E
DEC.19	01.30-01.45	0, 500-600	F, P.R.		
	02.30-02.45	0, 700-800	F, P.R.		
	03.30-03.45	0, 700-600	F, P.R.		
	05.30-05.35	0, 1100	F, P.R.(O)		
	05.35-05.45	0, 400, 1500	2E, F, P.R.(O)	320	115
	06.30-06.45	0, 300	2E, F	300	115
	07.30-07.45	0, 700	E, F	300	115
	08.30-08.45	0, 400, 1500, 1900	2E(F), F, 2F, 2F	280	100
	14.30-14.35	0, 1300-0	F, P.R.		
	17.30-17.45	0, 400, 1500	E_s, F, 2F	230	115
	18.30-18.45	0, 400, 1100, 1500	E_s(F), F, 2F, 2F	230	115
	19.30-19.45	0, 1400	F, 2F	265	
	20.30-20.45	0, 500, 1500, 2000	E_s(F), F, 2F 2F	280	130
	22.30-22.45	0, 1800	F, 2F	320	
20	00.30-00.45	0, 1300	F, 2F	250	
	06.30-06.32	0, 400	$2E_s$, F	320	115
	07.30-07.40	0, 300, 650-900, 1100	$2E_s$, F, P.R., $4E_s$	300	115
	18.30-18.45	0, 300	$2E_s$, F	290	110
	19.30-19.45	0, 300	$2E_s$, F	290	110
21	18.30-18.45	0, 500	E_s, F	255	115
	19.30-19.45	0, 400	E_s, F	230	115
	20.30-20.45	0, 450	E_s, F	245	115
	21.30-21.45	0, 500	E_s, F	255	115
	22.30-22.45	0, 700	E_s, F	300	115
	23.30-23.40	0, 600	E_s, F	275	115
22	05.30-05.45	0, 500-300, 500-800	$2E_s$, F, P.R.	320	115
	06.30-06.45	0, 300-200	2E, F	300	115
	07.30-07.45	0, 700	E, F	300	115
	18.30-18.45	0, 1300	F, 2F	250	
	19.30-19.45	0, 1300	F, 2F	250	
	20.30-20.45	0, 1400	F, 2F	265	
	21.30-21.45	0, 1500	F, 2F	280	
	22.30-22.45	0, 600	E_s, F	280	115

DATE 1964	TIME IN SAST	TIME DELAYS IN USEC	INTERPRETATIONS	HEIGHT OF REFLECTION F	E
DEC.22	23.30-23.45	0, 700	E_s, F	300	115
23	00.30-00.45	0, 800	E_s, F	320	115
	01.30-01.45	0, 700	E_s, F	300	115
	02.37-02.45	0, 1200-900	F, P.R.		
(Fig.25)	05.30-05.45	0, 1200-1500, 2000-1800	F, P.R.(O), 2F	340	
	06.30-06.45	0, 300, 1900	2E, F, 2F	290	105
	17.30-18.10	0, 300	E_s, F	280	105
	18.10-23.25	0, 1500-1300-1400-2100	F, 2F	260	
24	00.50-02.20	0, 2000-1700-2000	F, 2F	320	
	02.31-02.48	0, 700-0	F, P.R.(O)		
	02.48-02.58	0, 700-0	F, P.R.(X)		
	04.22-04.35	0, 0-1200	F, P.R.(X)		
	04.29-04.55	0, 0-1700	F, P.R.(O)		
	04.50-05.10	0, 1900-1500	F, 2F	300	
	05.10-06.17	0, 350, 1800	2E, F, 2F	300	110
	06.54-06.55	0, 600	E, F	280	110
	18.20-21.04	0, 1250-1900	F, 2F	265	
	21.08-21.27	0, 1400-0	F, P.R.(X)		
	21.26-21.44	0, 1300-0	F, P.R.(O)		
25	01.22-02.59	0, 0-500-300-800-300-400	F, P.R.(X)		
(Fig.31)	02.25-02.31	0, 0-100	F, P.R.(O)		
	02.59-03.05	0, 500-600, 900-600	$2E_s$, F, P.R.(X)	350	120
	05.10-05.12	0, 750-900, 750-600	E_s, F, P.R.(X)	320	120
	05.12-05.25	0, 300-1100	F, P.R.(X)		
	05.18-05.35	0, 0-1300	F, P.R.(O)		
	05.35-0538	0	F		
	05.38-0600	0, 400	2E, F	300	105
	06.00-08.54	0, 400-300, 1900-1800	E, F, 2F	280	100
	16.15-16.39	0, 600	E, F	280	110
	17.10-17.20	0, 350	$2E_s$, F	280	100

DATE 1964	TIME IN SAST	TIME DELAYS IN USEC	INTERPRETATIONS	HEIGHT OF REFLECTION F	E
DEC.25	17.20-18.25	0, 350-300, 1600-1200, 1900-1600	$2E_s$(F), F, 2F, 2F	270	100
	18.25-23.30	0, 1200-1400-1600-2000	F, 2F	260	
26	01.05-0130	0, 1000-0	F, P.R.(O)		
	01.41-02.08	0, 600-0	F, P.R.(X)		
	02.13-02.28	0, 0-800	F, P.R.(X)		
	02.33-02.50	0, 0-350-0	F, P.R.(O)		
	02.48-03.00	0, 800-0	F, P.R.(X)		
	05.01-05.12	0, 0-1150	F, P.R.(X)		
	05.11-05.29	0, 0-1750	F, P.R.(O)		
	05.35-05.45	0, 1900-1700	F, 2F	320	
	05.45-07.48	0, 400-350-400	2E, F	280	105
	14.24-15.40	0, 1500-1300	F, 2F	260	
27	17.36-19.00	0, 300-400	2E, F	310	115
	20.10-20.24	0, 400	$2E_s$, F	320	115
	21.17-22.03	0, 400-500	$2E_s$, F	330	115
	22.03-22.22	0, 500-650, 1100-650	$2E_s$, F, P.R.(O)	360	115
	22.22-22.33	0, 650-700	$2E_s$, F	370	115
	22.33-22.50	0, 700, 1250-700	$2E_s$, F, P.R.(X)	380	115
28	05.09-05.21	0, 0-800	F, P.R.(X)		
	05.21-05.33	0, 450	$2E_s$, F	330	115
	05.33-05.40	0, 450-500, 1000-500	$2E_s$, F, P.R.(X)	340	115
	05.40-06.08	0, 500-350	$2E_s$, F	320	115
	06.08-06.10	0, 350, 350-900	$2E_s$, F, P.R.(X)	310	115
	06.10-06.25	0, 350, 900-350	$2E_s$, F, P.R.(X)	310	115
	06.25-06.44	0, 350-300, 350-800	$2E_s$, F, P.R.(X)	305	115
	06.44-07.40	0, 300, 800	$2E_s$, F, P.R.	300	115

DATE 1964	TIME IN SAST	TIME DELAYS IN USEC	INTERPRETATIONS	HEIGHT OF REFLECTION F	E
DEC.28	17.30-18.20	0, 300	$2E_s$, F	305	120
	19.20-20.20	0, 300-400	$2E_s$, F	335	130
	20.20-22.20	0, 400-700, 1700-1500-1600	$2E_s$, F, P.R.(0)	365	125
	22.20-22.37	0, 900	F, P.R.(0)	365	
	22.37-22.40	0, 700, 1600	$2E_s$, F, P.R.(0)	365	125
	22.40-23.31	0, 900-0	F, P.R.(0)		
	23.31-23.55	0, 600, 1200-600	$2E_s$, F, P.R.(X)	400	140
	23.55-24.00	0, 600, 1200, 1600	$2E_s(E_s)$, F, F, $4E_s$	400	140
29 (Fig18)	00.00-00.30	0, 600, 1200, 1600	$2E_s(E_s)$, F, F, $4E_s$	400	140
	00.36-01.30	0, 300, 600, 900, 1300, 1600, 1900	$E_s(2E_s)$, $2E_s$, $3E_s$ $3E_s$, $4E_s$, $5E_s$, $5E_s$.		105
(Fig22)	03.06-03.11	0, 900, 1500, 1800,	$2E_s(E_s)$, $4E_s$, $5E_s$, $5E_s$		100
(Fig23)	04.17-04.23	0, 1100, 1400, 1700	$2E_s(E_s)$, $4E_s$, $4E_s$, $5E_s$		110
(Fig24)	04.52-05.06	0, 0-1100	F, P.R.(X)		
	05.06-05.09	0,	F		
	05.09-05.25	0, 300-0, 300-1250	F_x, F_o, P.R.(0)		
	05.25-05.33	0, 400, 1650-2100	$2E_s$, F, P.R.(0)	290	100
	05.33-05.35	0,	F	290	
	05.35-06.34	0, 300-400-300	2E, F	285	100
	06.34-06.38	0, 300, 1850-1800	2E, F, 2F	280	100
	06.38-07.44	0, 300	2E, F	280	100
(Fig26)	21.43-22.20	0, 600, 1700-600	$2E_s$, F, P.R.(0)	380	130
	22.20-22.26	0, 600	$2E_s$, F	380	130

DATE 1964	TIME IN SAST	TIME DELAYS IN USEC	INTERPRETATIONS	HEIGHT OF REFLECTION F	HEIGHT OF REFLECTION E
DEC. 29 (Fig. 26)	22.26-22.35	0, 800	F, P.R.(X)		
	22.35-22.39	0, 700, 1100	$2E_s$, F, P.R.(X)	380	115
	22.39-22.49	0, 400-0	F, P.R.(X)		
	22.50-24.00	0, 300, 900, 1700	$E_s(2E_s)$, $2E_s$, $3E_s$, $5E_s$		110
30	00.00-02.00	0, 300, 600, 900, 1300	$E_s(2E_s)$, $2E_s$, $3E_s$, $3E_s$, $4E_s$		105
	02.15-04.40	0, 700	E_s, $3E_s$		100
	05.03-05.18	0, 0-1450	F, P.R.(X)		
	05.10-05.25	0, 0-1500	F, P.R.(O)		
	05.25-05.40	0,	F		
(Fig. 29)	05.40-06.22	0, 400-350	2E, F	300	110
	06.22-06.27	0, 250, 400	2E, F, F	300	110
	06.27-06.33	0, 350	2E, F	300	110
	06.33-06.51	0, 350, 1700-1200	2E,F, 2F	300	110
	06.51-07.30	0, 350	2E, F	300	110
31	15.30-19.00	0, 950-600	E, F	250	100
1965 JAN. 1	03.27-03.29	0, 1000	E_s, $3E_s$		120
	03.41-03.44	0, 600	$2E_s$, $3E_s$		120
	16.40-18.20	0, 1100-1000	E, F	360	100
2	15.00-17.00	0, 1250-600	E, F	340	100
7	00.30-00.45	0, 1200	F, 2F	240	
	05.30-05.40	0, 500-1000	F, P.R.		
	06.30-06.45	0, 400	2E, F	320	115
9	06.30-06.45	0, 700, 2000-1300	E, F, P.R.		
	07.30-07.45	0, 1500	F, 2F	280	

DATE 1965	TIME IN SAST	TIME DELAYS IN USEC	INTERPRETATIONS	HEIGHT OF REFLECTION F	HEIGHT OF REFLECTION E
JAN. 10	02.30-02.45	0, 600, 1300	$2E_s$, $3E_s$, $4E_s$		125
	03.30-03.45	0, 600	$2E_s$, $3E_s$		125
	04.30-04.45	0, 600	$2E_s$, $3E_s$		125
	05.30-05.45	0, 600	$2E_s$, $3E_s$		125
	06.30-06.45	0, 350	$2E_s$, F	320	125
	20.30-20.45	0, 600	$2E_s$, $3E_s$		125
	21.30-21.45	0, 600	$2E_s$, $3E_s$		125
	22.30-22.45	0, 600	$2E_s$, $3E_s$		125
	23.30-23.45	0, 600	$2E_s$, $3E_s$		125
11	00.30-00.45	0, 600	$2E_s$, $3E_s$		125
	03.30-03.45	0, 800, 1400	E_s, $3E_s$, $4E_s$		110
	05.30-05.45	0, 1400-1250	F, P.R.		
	06.30-06.45	0, 300, 500, 1900	E, 2E, F, 2F	260	110
	18.30-18.45	0, 1500	F, 2F	280	
	19.30-19.45	0, 1600	F, 2F	290	
	21.30-21.45	0, 600	E_s, F	290	125
12	04.30-04.45	0, 0-700	F, P.R.		
	05.30-05.45	0, 1300	F, 2F	250	
	06.30-06.45	0, 300, 1800	2E, F, 2F	280	105
	17.30-17.45	0, 300, 1100, 1400	E_s(F), F, 2F, 2F	225	140
	18.30-18.45	0, 300	E_s, F	225	140
	19.30-19.45	0, 300	E_s, F	225	140
	21.30-21.45	0, 650	E_s, F	290	110
	22.30-22.45	0, 750	E_s, F	310	110
13	05.30-05.45	0, 400	$2E_s$, F	310	110
	06.30-06.45	0, 350, 1100, 1700	$2E_s$, F($3E_s$), $4E_s$, 2F	300	110

DATE	TIME IN SAST	TIME DELAYS IN USEC	INTERPRETATIONS	HEIGHT OF REFLECTION F	HEIGHT OF REFLECTION E
1965 JAN.13	07.30-07.45	0, 300	$2E_s$, F	290	110
	16.30-16.45	0, 300	2E, F	290	110
	17.30-17.45	0, 300-350	2E, F	295	110
	20.30-20.45	0, 350	$2E_s$, F	300	110
	21.30-21.45	0, 300	$2E_s$, F	290	110
14	02.30-02.45	0, 700	E_s, $3E_s$		100
	05.30-05.45	0, 300	$2E_s$, F	290	110
	06.30-06.45	0, 300	$2E_s$, F	290	110
	07.30-07.45	0, 300	2E, F	290	110
1965 MAY 29	15.00-16.30	0, 350, 850, 1500	E_s, $2E_s$, $3E_s$, $4E_s$		110
30	08.24-10.00	0, 200, 1400	2E, F, 2F	240	110
	11.15-15.15	0, 1300-1200-1400-1800-1600-1700-1400-1300	F, 2F	285	
	15.15-17.30	0, 250, 1650-1600-1400-1500	2E, F, 2F	280	110
31	00.30-03.30	0, 1800	F, 2F	320	
	08.00-08.06	0, 0-650	F, P.R.(X)		
	08.04-08.13	0, 0-800	F, P.R.(0)		
	08.15-08.40	0, 1500-1100	F, 2F	250	
	08.40-09.15	0, 1100	F, 2F	220	
	09.15-10.15	0, 300-200, 1400-1500-1700	E, F, 2F	240	130
1965 JUN.29	13.00-13.07	0, 500	E, F	260	110
	13.24-13.25	0, 500	E, F	260	110
	13.35-16.20	0, 400	E, F	235	110
JULY 1	12.50-13.15	0, 350, 800	E_s, $2E_s$, $3E_s$		105
	15.00-16.32	0, 350, 800, 1300	E_s, $2E_s$, $3E_s$, $4E_s$		105
(Fig.33)	16.40-17.27	0, 400-300-350, 1600-1450-1600	E_s, F, 2F	230	120
	17.29-17.38	0, 350-400, 1400-400	E_s, F, P.R.(0)	255	120

DATE 1965	TIME IN SAST	TIME DELAYS IN USEC	INTERPRETATIONS	HEIGHT OF REFLECTION F	E
JULY 1 (Fig.33)	17.38-17.50	0, 400-550-500, 400-900-500, 1500-1300	E_s, F, P.R.(0), P.R.(X)	275	120
	17.50-17.59	0, 500-600, 1300-600	E_s, F, P.R.(X)	275	120
	17.59-18.40	0,	E_s		120
2	07.41-07.45	0, 0-700	F, P.R.(X)		
	07.44-07.49	0, 0-600	F, P.R.(0)		
	07.49-08.12	0	F		
	08.12-08.40	0, 1300	F, 2F	250	
	08.40-10.00	0, 200	2E, F	250	105
	14.30-17.45	0, 400	E, F	230	105
	18.55-1900	0, 500-0	F, P.R.(0)		
	19.03-19.08	0, 550-0	F, P.R.(X)		
3	08.23-08.31	0, 0-600	F, P.R.(X)		
	08.29-08.37	0, 0-500	F, P.R.(X)		
	08.37-09.20	0,	F,		
	09.20-11.00	0, 250	2E, F	260	100
	16.50-17.35	0, 300	2E, F	270	100
	17.35-17.49	0, 300-500-400, 1100-400, 1400-400	2E, F, P.R.(0), P.R.(X)	290	100
	17.49-17.53	0,	F,		
	20.58-21.13	0,	F,		
4	07.35-07.39	0, 0-700	F, P.R.(X)		
	07.39-07.48	0, 0-900	F, P.R.(0)		
	07.48-08.15	0, 1800-1150	F, 2F	230	
	08.15-10.15	0, 200-300-350, 1350-1550	E, F, 2F	230	130
	11.25-16.00	0, 600-500-400	E, F	250	110
	16.00-17.36	0, 400, 1800-1400	E, F, 2F	240	110
	17.36-17.46	0, 1000	F, 2F	210	
	17.46-17.54	0,	F,		
	17.54-18.08	0, 900-0	F, P.R.(0)		
	18.08-18.12	0, 600-0	F, P.R.(X)		
5	08.25-08.35	0, 0-750	F, P.R.(X)		

DATE 1965	TIME IN SAST	TIME DELAYS IN USEC	INTERPRETATIONS	HEIGHT OF REFLECTION F	E
JULY 5	08.35-08.52	0, 0-1000	F, P.R.(0)		
	08.52-09.00	0,	F,		
	09.00-10.30	0, 250	2E, F	280	110
	16.36-17.45	0, 300	2E, F	280	100
	17.45-18.50	0, 300, 900	2E, F, F&E(N-type)	280	100
	18.50-19.08	0, 300	2E, F	280	100
	19.08-19.11	0, 300, 700-300	2E, F, P.R.(0)	280	100
	19.10-19.13	0, 300, 1000-300	2E, F, P.R.(X)	280	100
	19.13-19.18	0, 300	2E, F	280	100
8	15.30-17.00	0, 350-300	2E, F	250	100
9	12.00-12.16	0, 600	E, F	280	110
	12.40-14.00	0, 400, 850	E, 2E, F	330	115
	14.00-14.20	0, 850-600	E, F	310	115
	14.20-14.30	0, 600, 1300-600	E, F, P.R.(0)	310	115
	14.30-15.00	0, 600, 1400-600	E, F, P.R.(X)	310	115
	15.14-18.16	0, 300, 800, 1500	E_s, $2E_s$, $3E_s$, $4E_s$		110
10	11.40-12.01	0, 400, 1800-1500	E, F, 2F	240	110
	12.05-12.09	0, 600	E, F	280	110
	12.35-12.36	0, 600	E, F	280	110
	12.26-13.02	0, 400, 1700	E, F, 2F	240	110
	13.13-13.15	0, 500	E, F,	260	110
	13.26-13.28	0, 500	E, F	260	110
	14.05-14.30	0, 600, 1400-600	E, F, P.R.(0)	280	110
	14.30-15.40	0, 600-400, 700-800-900-800-1200-900-1200-1100-400	E, F, P.R.	260	110
	15.54-16.06	0, 350, 700-350, 1200-950, 1700-1600	E, F, P.R.(0), P.R.(X), 2F	230	110

DATE 1965	TIME IN SAST	TIME DELAYS IN USEC	INTERPRETATIONS	HEIGHT OF REFLECTION F	E
JULY 10	16.20-16.32	0, 250, 1600	2E, F, 2F	250	100
	18.18-18.42	0, 1200-1300	F, 2F	240	
	18.50-18.56	0, 600-0	F, P.R.(0)		
	18.54-18.59	0, 500-0	F, P.R.(X)		
11	07.45-08.32	0,	E_s,		
(Fig.27)	08.32-08.34	0, 800-500, 800-1150	E_s, F, P.R.(X)	290	115
	08.34-08.38	0, 500-400, 500-850, 1150-1400	E_s, F, P.R.(0), P.R.(X)	240	115
	08.38-08.45	0, 400-350, 850-1300	E_s, F, P.R.(0)	235	115
	08.45-08.50	0, 350	E, F	235	115
	08.50-09.30	0, 350, 1000-900	E, F, F&E(N-type)	235	115
	09.30-11.00	0, 350	E, F	235	115
	11.00-12.00	0, 350, 1700-1800-1600	E, F, 2F	235	110
	12.00-12.35	0, 350	E, F	235	110
(Fig.28)	14.20-17.20	0, 475-400	E, $2E_s$		{110 {120
	15.43-15.45	0, 700	E, F_1	300	110
	15.42-15.44	0, 1200	E, F_2	400	110
	15.45-15.49	0, 700-800, 1500-800	E, F_1, P.R.(F_1)	300	110
	15.49-16.00	0, 800-700	E, F_1	300	110
	16.00-16.10	0, 700, 1100-700	E, F_1, P.R.(F_1X)	300	110
	16.10-16.21	0, 700	E, F	300	110
	16.21-16.30	0, 1600	E, F_2	450	110
	16.30-16.34	0, 800, 1100	E, F_o, F_x	{320 {380	110
	16.50-17.05	0, 900	E, F_2	340	110
	17.05-17.20	0, 900-1100	E, F_2	380	110
	17.20-18.30	0, 400-500-400, 1700-1800-1600	E, F, 2F	240	120
	18.30-19.30	0, 400	E, F	240	120
12	09.20-09.25	0,	F,		

DATE 1965	TIME IN SAST	TIME DELAYS IN USEC	INTERPRETATIONS	HEIGHT OF REFLECTION F	E/E_s	
JULY 12	09.25-09.32	0, 0-700	F, P.R.(X)			
	09.29-09.40	0, 0-800	F, P.R.(0)			
	09.40-09.46	0,	F,			
	09.46-10.10	0, 1600-1100-1300	F, 2F	240		
	10.10-10.20	0, 200, 1500	2E, F, 2F	250	100	
	10.20-11.55	0, 200-250	2E, F	240	110	
	11.16-11.20	0, 200, 600	2E, F, $3E_s$	240	110	115
	11.24-11.28	0, 200, 500	2E, F, $3E_s$	240	110	115
	11.38-11.48	0, 200, 700	2E, F, $3E_s$	240	110	115
	12.02-12.04	0, 600	2E, $3E_s$		110	115
	12.11-12.12	0, 300	E, 2E		110	
	12.32-12.35	0, 900	2E, $3E_s$		110	135
	12.45-14.07	0, 500	E, F	250	115	
	14.07-14.16	0, 500, 700	E, F, $3E_s$	250	115	
	14.16-14.35	0, 500, 700-1200	E, F, $3E_s$	250	115	135
	14.35-15.02	0, 500, 1200-700, 1900-1500	E, F, $3E_s$, 2F	250	120	
	15.02-17.50	0, 300, 1500-1800-1500-1700 1500-1600-1400	2E, F, 2F	250	100	
	17.30-17.40	0, 1100	F, 2F	230		
	17.40-17.48	0,	F			
	17.48-17.56	0, 600-0	F, P.R.(0)			
	17.52-18.02	0, 800-0	F, P.R.(X)			

A P P E N D I X II

In the tables below are given types of propagation observed between Grahamstown and Durban for each hour of the day, Table A for summer and Table B for winter. The first column gives the total time for which recordings were scaled. Here only those records that were clearly discernible were taken into account. Thus positive identification could be made, as to whether pulses came through or not. The other three columns, give the percentage of the time when propagation was obtained through the different layers. The propagation through the various layers occurred at different times as well as concurrently. Therefore it would be wrong to add up the propagations through the various layers to obtain the percentage of the overall propagation. Figs. 37 and 38 give an illustration of the percentage of each pulse received for each hour of the day for summer and for winter.

TABLE A : SUMMER RECORDINGS

P E R I O D	Total time Recordings were scaled in mins.	Percentage of Time F-Layer Prop. obtained	Percentage of Time E_s-Layer Prop. obtained	Percentage of Time E-Layer Prop obtained
00.00-01.00	624	19	28	0
01.00-02.00	690	36	24	0
02.00-03.00	750	29	12	0
03.00-04.00	735	6	18	0
04.00-05.00	705	16	13	0
05.00-06.00	840	80	26	17
06.00-07.00	780	89	21	70
07.00-08.00	735	50	9	37
08.00-09.00	690	10	0	0
09.00-10.00	660	0	0	0
10.00-11.00	705	0	0	0
11.00-12.00	585	0	0	0
12.00-13.00	600	0	0	0
13.00-14.00	540	0	0	0
14.00-15.00	640	6	0	0
15.00-16.00	690	24	2	16
16.00-17,00	690	42	9	32
17.00-18.00	840	43	20	21

TABLE A : SUMMER RECORDINGS (continued)

P E R I O D	Total Time Recordings were scaled in mins.	Percentage of Time F-Layer Prop. obtained	Percentage of Time E_s-Layer Prop. obtained	Percentage of Time E-Layer Prop. obtained
18.00-19.00	895	59	16	18
19.00-20.00	850	51	15	0
20.00-21.00	840	55	26	0
21.00-22.00	660	70	34	0
22.00-23.00	615	67	35	0
23.00-24.00	525	40	32	0

TABLE B : WINTER RECORDINGS

P E R I O D	Total Time Recordings were scaled in mins.	Percentage of Time F-Layer Prop. obtained	Percentage of Time E_s-Layer Prop. obtained	Percentage of Time E-Layer Prop. obtained.
00.00-01.00	480	6	0	0
01.00-02.00	480	13	0	0
02.00-03.00	480	13	0	0
03.00-04.00	480	6	0	0
04.00-05.00	420	0	0	0
05.00-06.00	420	0	0	0
06.00-07.00	420	0	0	0
07.00-08.00	420	10	4	0
08.00-09.00	493	70	9	24
09.00-10.00	540	85	0	71
10.00-11.00	480	50	0	48
11.00-12.00	405	53	6	42
12.00-13.00	470	50	3	39
13.00-14.00	540	52	3	41
14.00-15.00	600	64	16	61
15.00-16.00	676	58	34	62
16.00-17.00	603	70	34	69
17.00-18.00	570	67	25	50
18.00-19.00	520	33	11	23
19.00-20.00	488	12	0	10
20.00-21.00	420	0	0	0
21.00-22.00	420	3	0	0
22.00-23.00	420	0	0	0
23.00-24.00	420	0	0	0

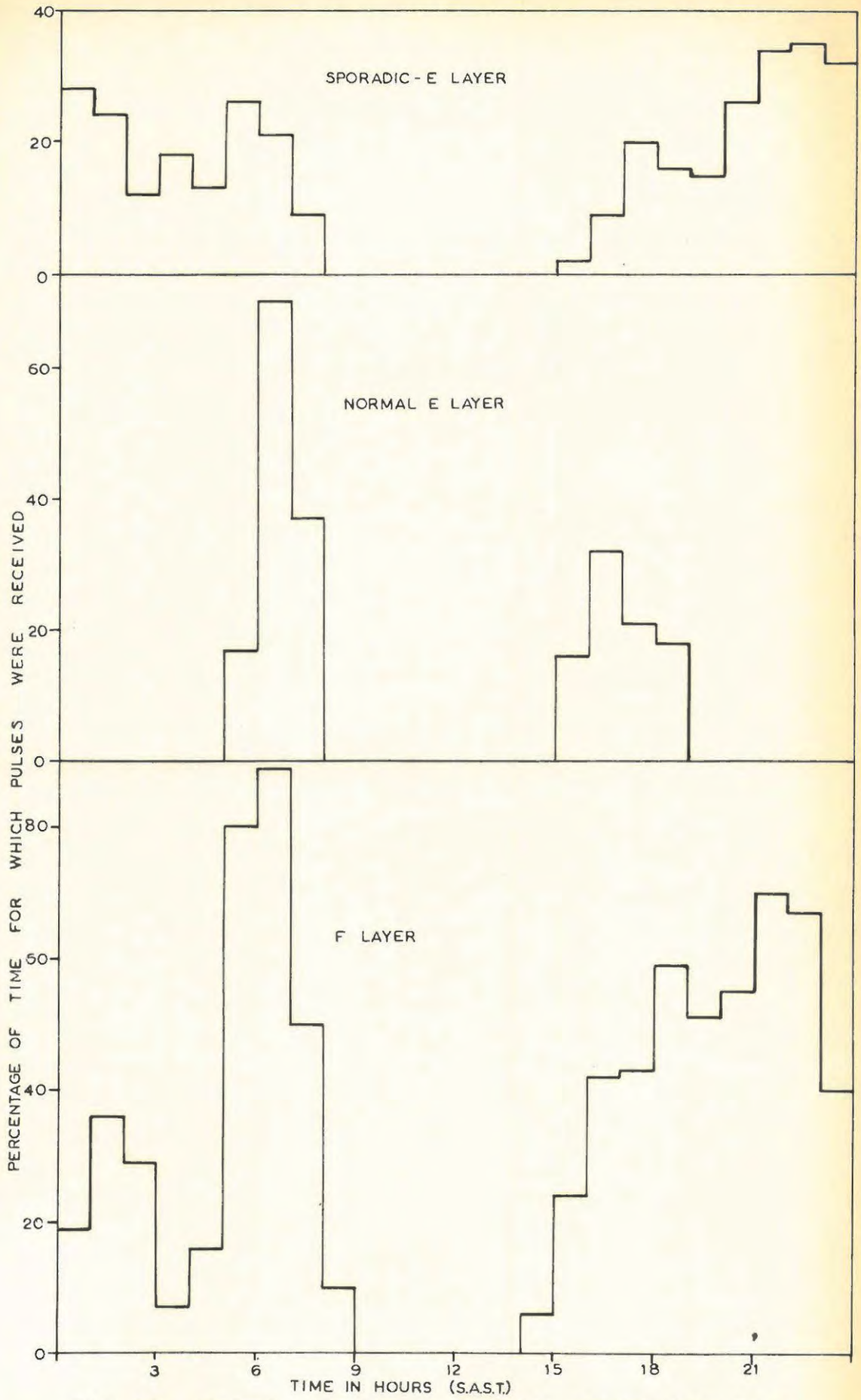

FIG. 37 TYPES OF PROPAGATION OBSERVED FOR EACH HOUR OF THE DAY DURING SUMMER

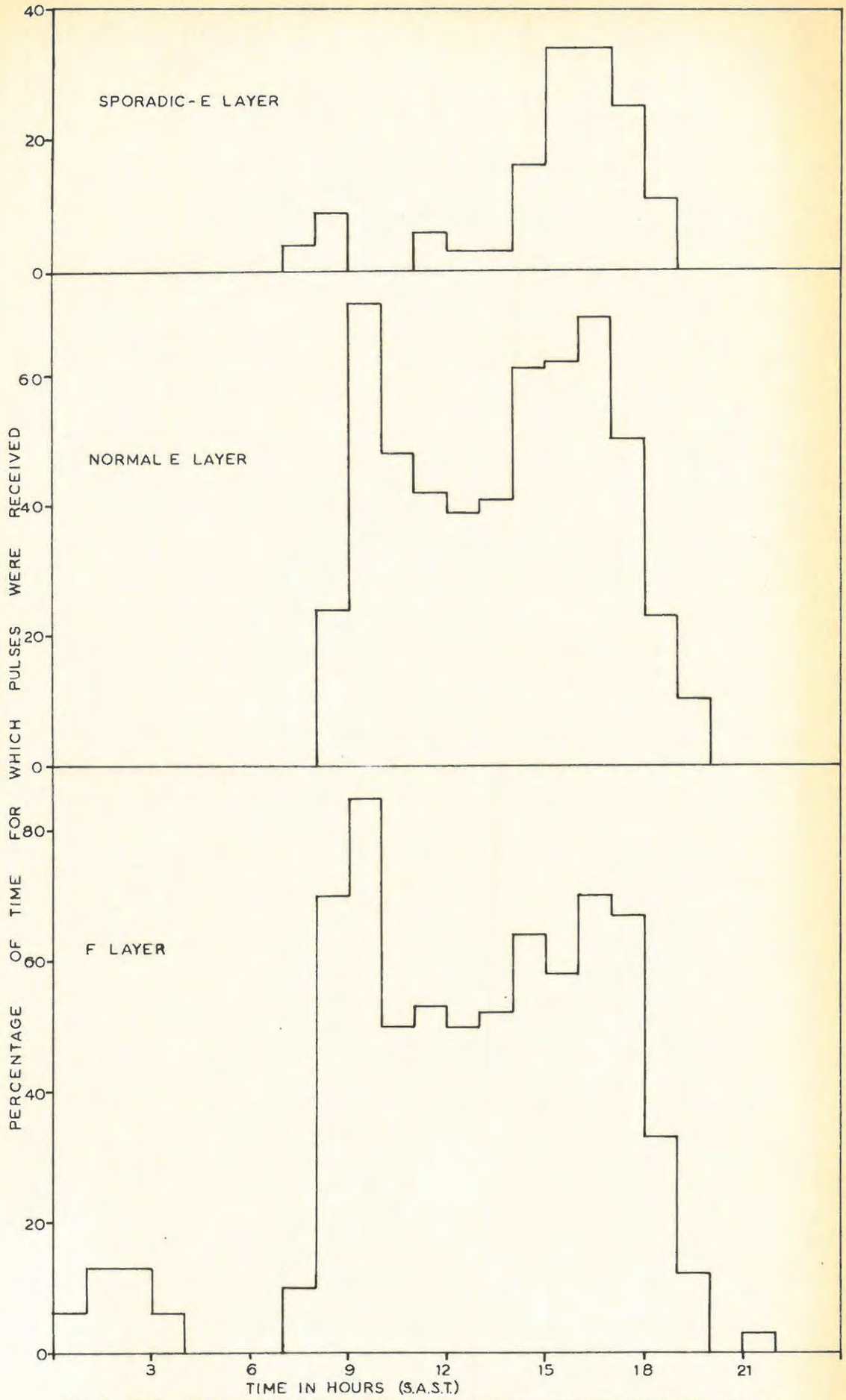

FIG. 38 TYPES OF PROPAGATION OBSERVED FOR EACH HOUR OF THE DAY DURING WINTER

BIBLIOGRAPHY

(1) S. Chapman in "Physics of the Upper Atmosphere", (J.A. Ratcliffe ed.), p. 5, Academic Press, (1960).

(2) G. Marconi, Proc. Roy. Soc., Series A, 70, 344, (1902).

(3) A.T. Story, "The Story of Wireless Telegraphy", p. 91, Hodder and Stoughton, London.

(4) A.E. Kennelly, Electrical World, 39, 473, (1902).

(5) O. Heaviside, "Encyclopaedia Britannica," 13, 215, (1902).

(6) E.V. Appleton and M.A.F. Barnett, Proc. Roy. Soc., Series A, 109, 621, (1925).

(7) G. Breit and M.A. Tuve, Phys. Rev. 28, 554, (1925).

(8) Annals of the I.G.Y., Vol. III, Part 1, p. 4, Pergamon Press, (1957).

(9) Standards on Wave Propagation, Defin. of Terms, Proc. I.R.E., 38, 11, 1264, (1950).

(10) J.C. Seddon in "Ionospheric Sporadic-E", (E.K. Smith and S. Matsushita ed.), p. 78, Pergamon Press, (1962).

(11) S. Chapman, Proc. Phys. Soc., 43, 26, (1931).

(12) K.G. Budden, Radio Waves in the Ionosphere, p. 5, Cambridge University Press, (1961).

(13) S. Chapman, Proc. Phys. Soc., 43, 483, (1931)

(14) N.E. Bradbury, Terr. Mag., 43, 55, (1938).

(15) F.L. Mohler, J. Res. N.B.S. Washington, p. 507, (1940).

(16) S. Chapman, Proc. Phys. Soc., 51, 93, (1939)

(17) M. Nicolet, J. Atmos. & Terr. Phys., 1, 3, 141, (1951).

(18) J.C. Seddon, A.D. Pickar, and J.E. Jackson, J. Geophys. Res., 56, 487, (1951).

(19) T. Shimazaki, J. Radio Res. Lab. (Tokyo), 6,109 (1950).

(20) F. Hoyle and D.R. Bates, J. Geophys. Res., 53, 51, (1948).

(21) L. Vegard, Phil. Mag., 46, No. 271, Series 6, 193, (1923).

(22) E.O. Hulburt, Phys. Rev., 53, 344, (1938).

(23) L. Vegard, Geophys. Publ. (Oslo), 12, No. 14, (1938).

(24) R. Penndorf, J. Geophys. Res., 54, 7, (1949).

(25) M. Nicolet and P. Mange, J. Geophys. Res., 59, 15, (1954).

(26) E.T. Byram, T.A. Chubb, and H. Friedman, "The Threshold of Space" (M. Zelikoff ed.) p. 211, Pergamon Press, (1957).

(27) H. Friedman, S.W. Lichtman, and E.T. Byram, Phys. Rev., 83, 1025, (1951).

(28) R.J. Havens, H. Friedman, and E.O. Hulburt, "Physics of the Ionosphere", Phys. Soc. London, p. 237, (1954).

(29) K. Watanabe, F. Marmo, and J. Pressman, J. Geophys. Res., 60, 513, (1955).

(30) R.E. Houston, Jr., Scientific Report No. 95, Pennsylvania State University, State College, (1957).

(31) M. Nicolet, Mem. Inst. Roy. Met. Belg., 19, (1945).

(32) M. Nicolet and A.C. Aiken, J. Geophys. Res., 65, 1469, (1960).

(33) H.E. Hinteregger and K. Watanabe, J. Geophys. Res., 67, 3, p. 999, (1962).

(34) H.E. Hinteregger and K. Watanabe, J. Geophys. Res., 67, 9, p. 3373, (1962).

(35) D. Layzer in "Ionospheric Sporadic-E", (E.K. Smith and S. Matsushita ed.) p. 260, Pergamon Press, (1962).

(36) S. Matsushita in "Ionospheric Sporadic-E", (E.K. Smith and S. Matsushita ed.), p. 344, (1962).

(37) W.H. Pfister and J.C. Ulwick, J. Geophys. Res., 63, 2, 315, (1958).

(38) P.M. Millman, J. Geophys. Res., 64, 12, 2122 (1959).

(39) E. Manring, J.F. Bedinger, H. Knaflich, and R. Lynch, Geophys. Corp. of America (Bedford, Mass.) Tech. Rept. 61-1-N. (1961).

(40) W.H. Eccles, Nature, 89, 191, (1912).

(41) F.T. Farmer and J.A. Ratcliffe, Proc. Phys. Soc., 48, 839, (1936).

(42) D.F. Martyn, R.O. Cherry, and A.L. Green, Proc. Phys. Soc., 47, 340, (1935).

(43) Crone, Kruger, Goubou, and Zenneck, Hochfrequenztech u Electroakust, 48, 1, (1936).

(44) J.A. Pierce, Nature, 164, 512, (1949).

(45) F.E. Terman, Radio Engineer's Handbook, p. 788, McGraw-Hill Book Co, (1943).

(46) W.H. Evans, Introduction to Electronics, p.475, (1962).

(47) E.N. Lurch, Fundamentals of Electronics, John Wiley & Sons, p. 492, (1960).

(48) R.C. Kloeffler, M.W. Horrell, & E. Hargrave. Basic Electronics, p. 371, J. Wiley & Sons, (1949).

(49) R.C.A. Receiving Tube Manual p. 106, (1960).

(50) S. Seely, Electron Tube Circuits, p. 458, McGraw-Hill Co. Inc. (1958).

(51) J.A. Gledhill & M.E. Szendrei Ph.D. Thesis, Vol. I, Rhodes University, (1947).

(52) K.G. Budden, Radio Waves In the Ionosphere, p. 25, Cambridge University Press, (1961).

(53) Ibid. p.226, (1961)

(54) Annals of the I.G.Y., v.III, part 1, "The Ionosphere", p. 54, Pergamon Press, (1957).

(55) D.H. Menzel, "The Elementary Manual of Radio Propagation", p. 123, Prentice-Hall, (1948).

(56) G.H. Munro, Proc. Roy. Soc., A 219, 447 (1953).

(57) R.W.E. McNicol, H.C. Webster, and G.G. Bowman, Aust. J. Phys., 9, 247, (1956).

(58) D.C. Baker, and J.A. Gledhill, J. Atmos. Terr. Phys., 27, 1223, (1965).

(59) G.H. Munro, Proc. Roy. Soc., A 202, 208, (1950).

(60) G.H. Munro, Aust. J. Phys., 11, 91, (1958).

(61) J.E. Titheridge, J. Atmos. Terr. Phys., 17, 96, (1959).

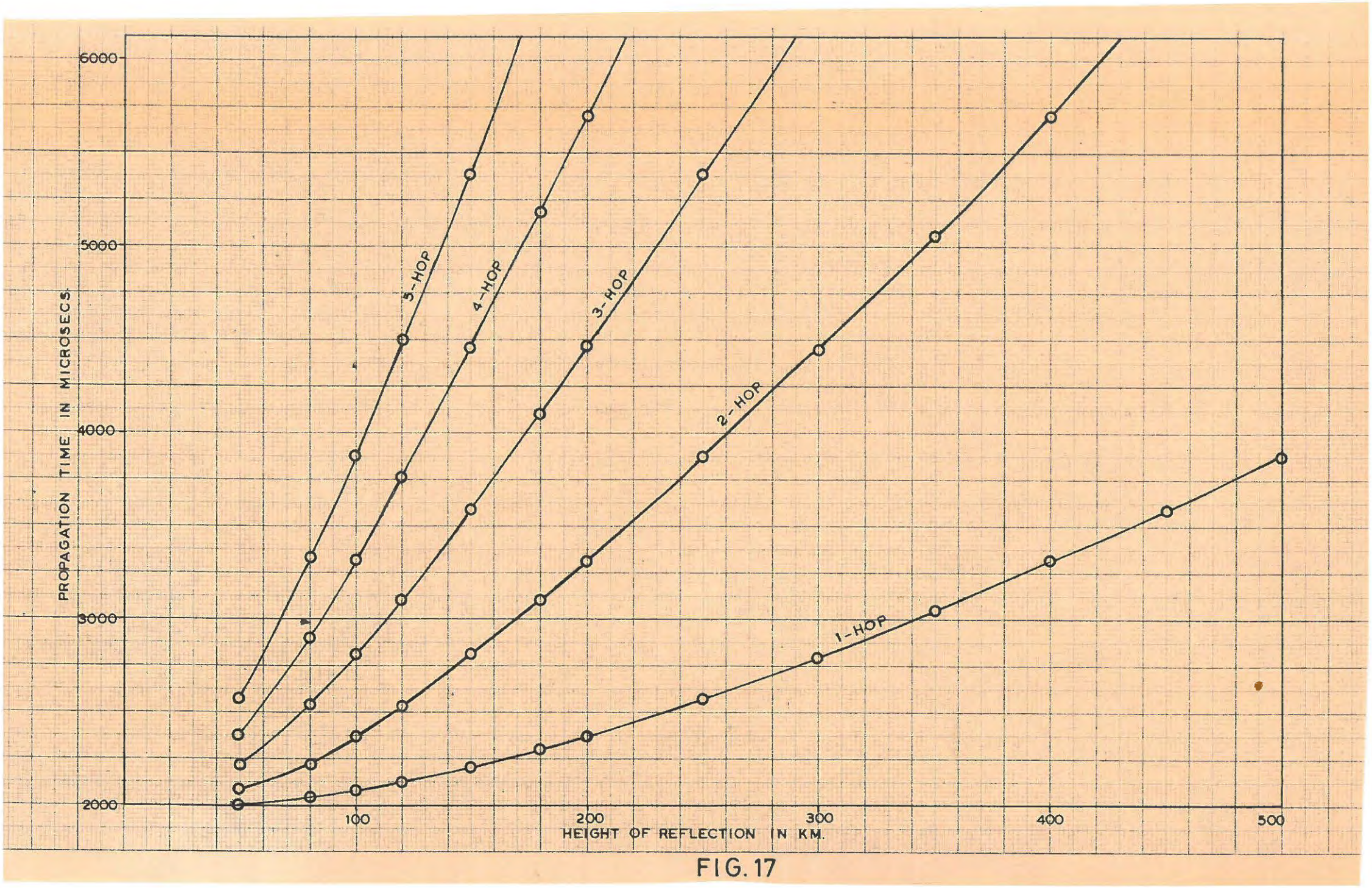
6000
5000
4000
3000
2000
PROPAGATION TIME IN MICROSECS.
5-HOP
4-HOP
3-HOP
2-HOP
1-HOP
100
200
300
400
500
HEIGHT OF REFLECTION IN KM.

FIG. 17